Petrofacies Evolution of Upper Siwalik-equivalent (?) Pliocene-Pleistocene Dupi Tila Formation, Bengal Basin, Bangladesh

by

Mustuque Ahmed Munim

A thesis submitted to the Graduate Faculty of
Auburn University
in partial fulfillment of the
requirements for the Degree of
Master of Science

Auburn, Alabama
August 5, 2017

Keywords: Dupi Tila, Upper Siwalik, Provenance, Pliocene-Pleistocene, Bengal basin, Bangladesh

Copyright 2017 by Mustuque Ahmed Munim

Approved by

Ashraf Uddin (Chair), Professor of Geosciences
Charles E. Savrda, Professor of Geosciences
David T. King, Jr., Professor of Geosciences
Willis E. Hames, Professor of Geosciences

TO THE MEMORIES
*OF **MY MOTHER***

ABSTRACT

Nearly 2.5-km-thick Pliocene-Pleistocene Dupi Tila Formation of the Bengal basin is composed of yellow, light brown, and pink, coarse- to very fine-grained, moderately to loosely indurated sandstone, siltstone, silty clay, mudstone and shale with some pebble beds. These synorogenic sediments crop out in northern (foothills of Garo hills and Shillong Plateau), eastern (Sylhet Trough and Chittagong Hills), and central Bangladesh (Comilla and vicinity) and occur in the subsurface in most other areas of Bangladesh, including the northwest Indian Platform area. Detrital history from this area provides data pertaining to uplift and erosional history of the hinterland areas (i.e., Himalayas, Indo-Burma Ranges and Shillong Plateau).

A systematic study of available detrital modes of sandstones from the Sylhet Trough, Lalmai hills, Garo hills, Stable Platform, and Sitapahar anticline in Chittagong hills include an array of sublithic to subfeldspathic quartz arenites. Modal analyses of the sandstones of the Dupi Tila Formation from Sitapahar anticline ($Qt_{64}F_{10}L_{27}$), Garo hills ($Qt_{88}F_{2}L_{10}$), Northwest Stable Platform ($Qt_{87}F_{6}L_{7}$), Sylhet Trough ($Qt_{66}F_{9}L_{25}$) and Lalmai hills ($Qt_{64}F_{6}L_{30}$) suggest that the sandstones have orogenic provenance signatures. Only samples from the Garo hills, which contain higher amounts of mono- and polycrystalline quartz, differ from the other area samples. The abundance of low- to intermediate-grade lithic fragments (Lm_{2}) in all samples suggest unroofing of deep crustal levels of the orogens.

The Dupi Tila Formation samples contain an average 0.8% heavy minerals, comprising opaque minerals, garnets, sillimanite, tourmaline, kyanite, andalusite, epidote group minerals, chloritoid & chlorite, staurolite, etc., in order of decreasing in abundance. The opaque fraction includes magnetite, hematite, ilmenite, pyrrhotite, and rarely pyrite. The heavy mineral data suggest an orogenic provenance for the Dupi Tila Formation. The relative abundance of aluminosilicates and related heavy minerals in the Dupi Tila

Formation throughout the Bengal basin reflect systematic unroofing of deeper crustal levels in the eastern Himalaya. Sillimanites (fibrolites) indicate the sediments were sourced from protoliths of high-grade regional metamorphic rocks.

Garnet chemistry data for the Dupi Tila Formation indicate a substantial amount of almandine suggesting provenance from amphibolite and granulite facies rocks. The presence of Mn-rich garnets (spessartine) in the Stable platform samples indicates provenance from pegmatite and low-grade metamorphic facies rocks. Tourmaline chemistry suggests derivation from Al-bearing metapelites, metasammites, calc-silicate rocks, Li-bearing pegmatites, granitoid pegmatites, and aplites. Epidote chemistry reveals sediment derivation from relatively high-grade metamorphic rocks of epidote-amphibolite facies. Chloritoid chemistry suggests that sediments originated from high-pressure blueschist metamorphic facies.

Whole rock geochemical data suggest that the majority of the sediments were derived from felsic igneous source terranes. Based on the chemical index of alteration, the intensity of weathering in the source area was moderate to high.

Sediments of the Upper Siwalik sequences in the Himalayan foreland basin are similar to the Dupi Tila Formation in terms of sandstone petrography and heavy mineral character. Hence, the Dupi Tila Formation of the eastern Himalayas may serve as the Upper Siwalik-equivalent extension of the western Himalayas. Future research projects employing detrital geochronology should provide additional information on the provenance history of the Dupi Tila Formation.

ACKNOWLEDGMENTS

I would like to express my gratefulness to almighty God who has been with me all the way and gave me the scope to study about the mystery of the Earth. It is my pleasure to thank all those who assisted directly and indirectly with my thesis research. It is my utmost pleasure to express my humble gratitude to Dr. Ashraf Uddin, my thesis advisor. I appreciate all his help and support that he provided to me for last two years. Dr. Uddin helped me not only as the principal advisor but also as a guardian to get the best outcome of this research.

I would also like to express my heartfelt thanks to Dr. Charles E. Savrda, David T. King, Jr., and Willis E. Hames for their contributions to this research as my thesis committee members. Dr. Savrda helped with significant editing in this thesis. I am grateful to Dr. King, for giving me a better handle on stratigraphy. Also, I would like to thank all other faculty members of Geosciences at Auburn University.

Auburn University and the Geological Society of America provided financial assistance without which this research would not have been possible. I would like to express my heartfelt gratitude to Dr. M. K. Roy from Rajshahi University, Bangladesh, Dr. Humayun Ahkter and Dr. Chowdhury Qumruzzam, the University of Dhaka for their help with logistics in collecting samples from the different parts of the Bengal basin. I would like to thank Mr. Ershadul Haque, Director of Geological Survey of Bangladesh, who helped me tremendously in collecting sediment core samples from northwest part of the Bengal basin.

I want to thank Dr. David Nikles and Mr. Robert Holler of the Central Analytical Facilities at the University of Alabama for giving me permission and assistance during electron microprobe analysis. I am also grateful to Ms. Sheila Arington for her support with administrative work. I thank Dr. Zeki Billor for his guidance in magnetic mineral

separation. I would also like to thank all graduate students and my colleagues, for their help and support.

Finally, I would like to thank my mother, who prior to her passing, gave me everything that she had. I also like to thank Mrs. Jasmine Ashraf for her care and support during my 2-year period in Auburn. I would like to thank my wife, Shakura Jahan, former AU student, for support and motivation, and my siblings for all their continuous support and encouragement.

Table of Contents

List of Tables

List of Illustrations

List of Acronyms

BSE Back Scattered Electron

CAF Central Analytical Facilities

CIA Chemical Index of Alteration

EDS Energy Dispersive Spectroscopy

EPMA Electron Probe Microanalyzer

GAB Geosciences Advisory Board

GDH Geological Drill Hole

GSA Geological Society of America

GSB Geological Survey of Bangladesh

HRL Himalayan Research Lab

UA University of Alabama

USNM United States National Museum

WDS Wavelength Dispersive Spectroscopy

Chapter 1: INTRODUCTION

1.1 INTRODUCTION

Continental collision represents an extreme end-member in compressional tectonic history. Associated crustal thickening produces dramatic surface relief and subsidence of flanking basins, resulting in rapid erosion and accumulation of clastic detritus. Sedimentary basins associated with mountain belts provide important repositories that record evidence of orogenic processes, including the interrelationship of tectonic, climatic, and erosion events. Petrofacies evolution of sedimentary sequences that are deposited on the flanks of mountain belts provides rudimentary constraints on mountain-building processes and the history of exhumation of mountain belts (Uddin and Lundberg, 1998a).

Compositional analysis of detrital sediments is a very important part in tracing sediment provenance (Dickinson, 1970, 1982; Dickinson and Suczek, 1979; Ingersoll and Suczek, 1979; Dickinson 1985; Garzanti et al., 1996). It focuses on key attributes of detrital mineralogy, providing important constraints on basin evolution and unroofing history of the mountain belts (Graham et al., 1976; Uddin and Lundberg, 1998b; Rahman, 2008). For sandstone compositional analyses, in which proportions of detrital framework grains within sand (stone) samples are plotted on different ternary diagrams (such as QtFL, QmFLt, and QmPK), can help distinguish various tectonic settings of source areas (Ingersoll et al., 1984; Ingersoll and Busby, 1995). Various factors other than source rock may have significant control on the composition of detrital sediments. Petrofacies studies to evaluate tectonic histories are based on the assumption that modes of transportation, depositional environments, climates, and diagenesis have not significantly altered detrital grain composition (Suttner, 1974; Mack, 1984; Kumar 2004; Sitaula, 2009).

During the transport of sediments from source areas to a distant basin, feldspar grains and lithic fragments become separated from relict quartz and are chemically broken down. This results in quartz-rich sandstones that are characteristic of continental interiors and passive-margin platform settings, and massive, mud-rich deltas characteristic of passive continental margin slope settings.

The Miocene-Pliocene Siwalik Group of the sub-Himalayan range of the northern Indian subcontinent, representing ancient Gangetic floodplain deposits, are subdivided into three subgroups- Lower Siwalik, Middle Siwalik, and Upper Siwalik. The Pliocene-Pleistocene Upper Siwalik (700-2300 m) deposits of the western Himalayan basins show similarity in petrological and sedimentological characters with the Dupi Tila Formation (300-2500 m) of the Bengal basin, which exhibits typical freshwater molassic deposits laid down mostly by the ancestral paleo-Brahmaputra.

1.2 LOCATION

The Bengal basin is a large prograding delta-dominated basin. Formed by crustal loading during the Indian-Asian-Burmese collision, the basin is over 20 km deep, extends over an area of 200,000 km^2, and is filled with synorogenic sequences derived from both the Himalayas and the Indo-Burman ranges (Uddin and Lundberg, 1998a). The basin is bounded by the Indian craton to the west, the Shillong Plateau and the Himalayan belt to the north, and the Indo-Burman ranges to the east (Fig. 1.1). The Bengal basin lies roughly between N $20^0$34' to N $26^0$38' and E $88^0$01' to E $92^0$41'. The basin is located primarily in Bangladesh, with a smaller part extending into the West Bengal state of India. It is open towards the south and extends into the Bay of Bengal. It has one of the world's largest deltaic plains, associated with the flow of three giant rivers: the Ganges, Brahmaputra, and Meghna. These giant rivers have carried huge volumes of sediment to the proto-Bengal basin, concomitant with subsidence of the Bengal basin. The sedimentation rate in the basin was particularly high during Eocene through Pliocene (Johnson and Nur Alam, 1991). Seismic-reflection studies (Curray, 1991) show that sedimentary and metasedimentary rocks in the Bengal basin are at least 22 km thick; 16 km are inferred to be collisional deposits. The latter sediments overlie 6 km of pre-collisional strata, interpreted as buried continental rise and pelagic deposits. Cenozoic

sequences within the basin increase in thickness from west to east and from north to south (Uddin, 1987).

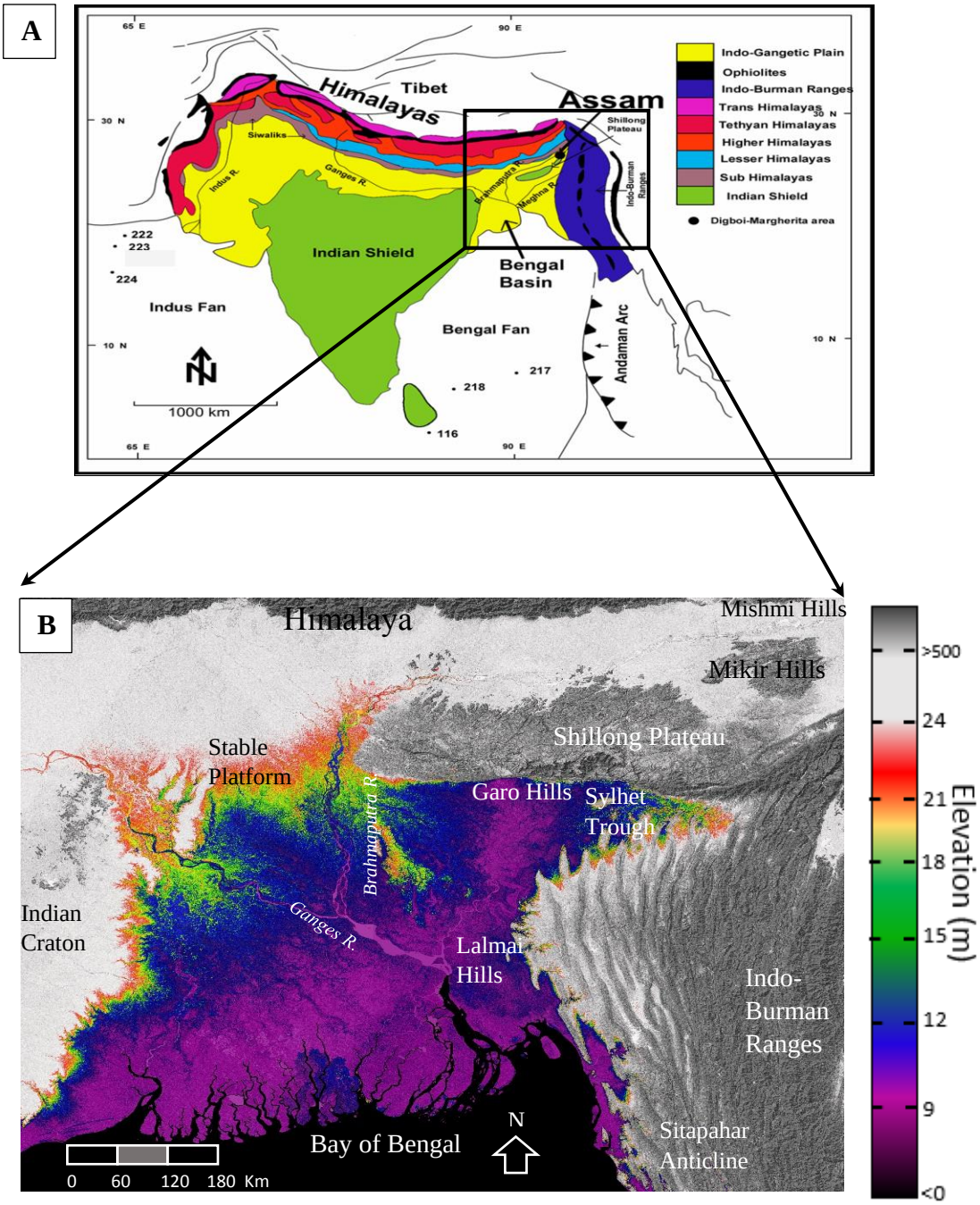

Fig.1.1 Location maps of the Study area. (A) Lithotectonic belts of Himalayan and Indo-Burman orogens (Uddin and Lundberg, 1998a). (B) Bengal basin and adjacent regions (modified after Pickering et al., 2017).

1.3 PREVIOUS WORKS

1.3.1 DEPOSITIONAL ENVIRONMENTS

Hiller and Elahi (1988) suggest that the Dupi Tila Formation was deposited synchronously with folding in the Sylhet Trough. The depositional environment of the Dupi Tila Formation has been interpreted by Johnson and Nur Alam (1991) as alternating channel and flood-plain deposits that are organized into fining-upward cycles of probable meandering stream origin. The abundance of coarse sediments, prevalence of pebbly beds, presence of carbonaceous material, common occurrence of cross bedding, and lack of fossils strongly suggest a fluviatile environment of deposition for the Dupi Tila Formation (Johnson and Nur Alam, 1991; Khan, 1991). The Upper Dupi Tila Formation of the Sylhet Trough has been interpreted as having been deposited by small-scale, mud-rich meandering river systems with the dominance of single fluvial channels characterized by simple bank-attached bars (Reimann, 1993; Gani and Alam, 2002). Recent reports of glauconite in the Upper Dupi Tila (Roy et al., 2012) indicate possible marine depositional environments during Pliocene-Pleistocene. Roy et al. (2012) suggest that the depositional environment changed from subaerial alluvial fans with heavily loaded braided rivers to shallow marine and estuarine environments.

1.3.2 PETROGRAPHIC STUDIES

Miocene and younger sandstones show an orogenic provenance (Uddin and Lundberg, 1998a); lithic sediments of the Dupi Tila Formation indicate progressive unroofing of the Himalayas through time. The abundance of potassium feldspar in the younger (Pliocene-Pleistocene) sand, compared to plagioclase-rich sands in the underlying Miocene Surma Group, indicates a granitic source, probably Miocene leucogranites of the High Himalayan Crystalline terrane (Uddin and Lundberg, 1998a). Kumar (2004) focused on the provenance history of the Cenozoic sediments of the north Assam area, near the eastern syntaxis, and suggested that sediments of the Assam basin were derived from the Himalayan orogen. Coeval (?) Siwalik sediments have been well studied along the strike of the Himalayas; i.e., in the western Himalayan foreland basin (i.e., Opdyke et al., 1982; Johnson et al., 1985; Critelli and Ingersoll, 1994), in Nepal (Tamrakar and Syangbo, 2014), in Darjeeling (Kundu et al., 2011), and near the eastern

syntaxis of the Himalayas (i.e., Chirouze et al., 2011). These studies suggest that detrital modes reflect a collision-orogen provenance. Petrological parameters described by Critelli et al. (1994) indicate sediment derivation from mid-crustal rocks and overlying sedimentary strata within various tectonostratigraphic units of the High Himalaya and Tibetan zone. Tamrakar and Syangbo (2014) inferred that the provenance of the Siwalik Group was mainly a recycled orogen and that the source rocks through time shifted from the low-grade metamorphic rocks of the Lesser Himalaya to the high-grade rocks of the Higher Himalaya.

1.3.3 AGE

Sediments of the Dupi Tila Formation are devoid of fossils and thus, present a great problem in accurate age determination. Available literature assigns a Mio-Pliocene age to the Dupi Tila Formation based mostly on lithostratigraphy (Khan, 1991). Since age-diagnostic fossils are not yet known, Reimann (1993) suggested that the age assignments ranging from middle Miocene to middle Pliocene are unreliable. During the last 7 to 3 Ma, there have been two orogenic events in the Himalaya (Amano and Taira, 1992; Harrison, et al., 1997; Catlos et al., 2002) that are related to movement along the Main Central Thrust (MCT). During these events, extensive erosion from the Himalayas resulted in deposition along the Himalayan foothills and adjacent basins (Catlos et al., 2002). The only Pleistocene representatives identified to date are scattered occurrences of the Dihing Formation, within the Bengal basin. It is likely, therefore, that the Dupi Tila Formation was deposited during Pliocene-Pleistocene time in response to orogenesis (Reimann, 1993). Notably, magnetostratigraphic studies by Worm et al. (1998) indicate that age of the topmost Dupi Tila deposits is between 4.9 and 1.4 Ma.

1.4 OBJECTIVES

This study focuses on petrofacies evolution of the Dupi Tila Formation in the Bengal basin, in order to evaluate and reconstruct the regional tectonic and detrital histories of the basin during the Pliocene-Pleistocene.

The main objective of the thesis research is *to infer the provenance of the Dupi Tila Formation based on sandstone petrography, heavy minerals, mineral chemistry and whole rock geochemistry of detrital grains.*

Based on overall lithology and sediment thickness, the Upper Siwalik sediments resemble those of the Dupi Tila Formation. The second objective of this research is to compare the Dupi Tila Formation with well-documented Upper Siwalik sediments from Pakistan, India, Nepal, and with the Upper Irrawaddy Formation of Myanmar, in an attempt to develop an orogenic scale unroofing history from the western to the eastern syntaxes of the Himalayas and the Indo-Burman ranges.

Chapter 2: TECTONIC SETTING AND REGIONAL GEOLOGY

2.1 INTRODUCTION

The tectonic history of the Bengal basin is related to the evolution of Himalayan orogenic belts, which were formed in response to the collision of India and Eurasia. The collision was brought by the migration of the Indian plate as the intervening Tethyan Ocean was subducted beneath southern margin of the Eurasian plate (Kearey and Vine, 1990). Magnetic anomalies in the Indian Ocean and paleomagnetic measurements on the subcontinent confirm the northward drift of India and allow the reconstruction of its path.

Basin development began in the Early Cretaceous (about 127 Ma) when the Indian plate rifted away from Antarctica along an inferred northeast-southwest-trending ridge system (Sclater and Fisher, 1974). After plate reorganization at about 90 Ma, the Indian plate began migrating rapidly northward, leading to its collision with Asia, which probably initiated during the Eocene between 55 to 40 Ma (Curray et al., 1979; Molnar, 1984; Rowley, 1996). Owing to the counter-clockwise rotation of the Indian plate (Lee and Lawver, 1995) sometime after the initial convergence with Asia, the basin in the east gradually started to close from north to south (oblique subduction). In the eastern part of the basin, the subduction complex of the Indo-Burman arc emerged above sea level, although major uplift of Himalayas may not have begun until the Miocene (Gansser, 1964). The intensity and pattern of plate-to-plate interaction varied with time, affecting the basin architecture and sedimentation style throughout the basin.

2.2 TECTONIC SETTING

The Bengal basin is bordered by two young orogenic belts; the east-west trending Himalayas and north-south trending Indo-Burma Range (Fig. 2.1). The basin is gradually

closing due to oblique subduction and orogeny along the eastern and northern margins (Rowley, 1996). The Bengal basin has two broad tectonic provinces: (1) the stable shelf, where thin sedimentary successions overlie the rocks of the Indian craton in the northwestern part of Bangladesh; and (2) thick basin fill that overlies the basement of undetermined origin in the south and east (Bakhtine, 1966; Khandoker, 1989). These two provinces are separated by a northeast–southwest trending hinge zone. Compared to those in the fold belt area to the east, strata in the deeper basin have experienced limited tectonic deformation. A few deep basement faults and very gentle low angle folds with narrow closure have been recognized from seismic data (Salt et al., 1986; Murphy, 1988; Imam and Hussain, 2002). Sedimentation within the Bengal basin took place in five distinct phases (Alam et al., 2003): (1) Permo-Carboniferous to early Cretaceous; (2) Cretaceous–Mid-Eocene; (3) Mid-Eocene–Early Miocene; (4) Early Miocene–Mid-Pliocene; and (5) Mid-Pliocene–Pleistocene. Each of these phases of sedimentation was controlled by the tectonic cycles, which involved the interaction and collision pattern of the major plates. Sedimentation in the basin has been divided into several stages: (1) syn-rift stage; (2) drifting stage; (3) early collision stage; and (4) late collision stage (Johnson and Alam, 1991; Alam et al., 2003). East-west and north-south cross-sections through the Bengal basin are shown in figures 2.2 and 2.3.

The local and regional tectonics of northwestern Stable Platform, Sylhet Trough, Garo hills, Sitapahar anticline, and Lalmai hills, where samples were collected for current research, are described below and highlighted in figure 2.1.

i) The data derived from seismic surveys and exploratory wells revealed that the northwestern Stable Platform flank is underlain by the Indian Shield consisting of an Archean gneissic complex at varying depths over which the Gondwana sediments have been deposited in intracratonic basins. The Late Cretaceous Rajmahal basaltic trap flows and Cretaceous-Cenozoic sediments, in turn, have been deposited over Gondwana sediments. The Stable Platform is also known as Indian Platform or Stable Shelf.

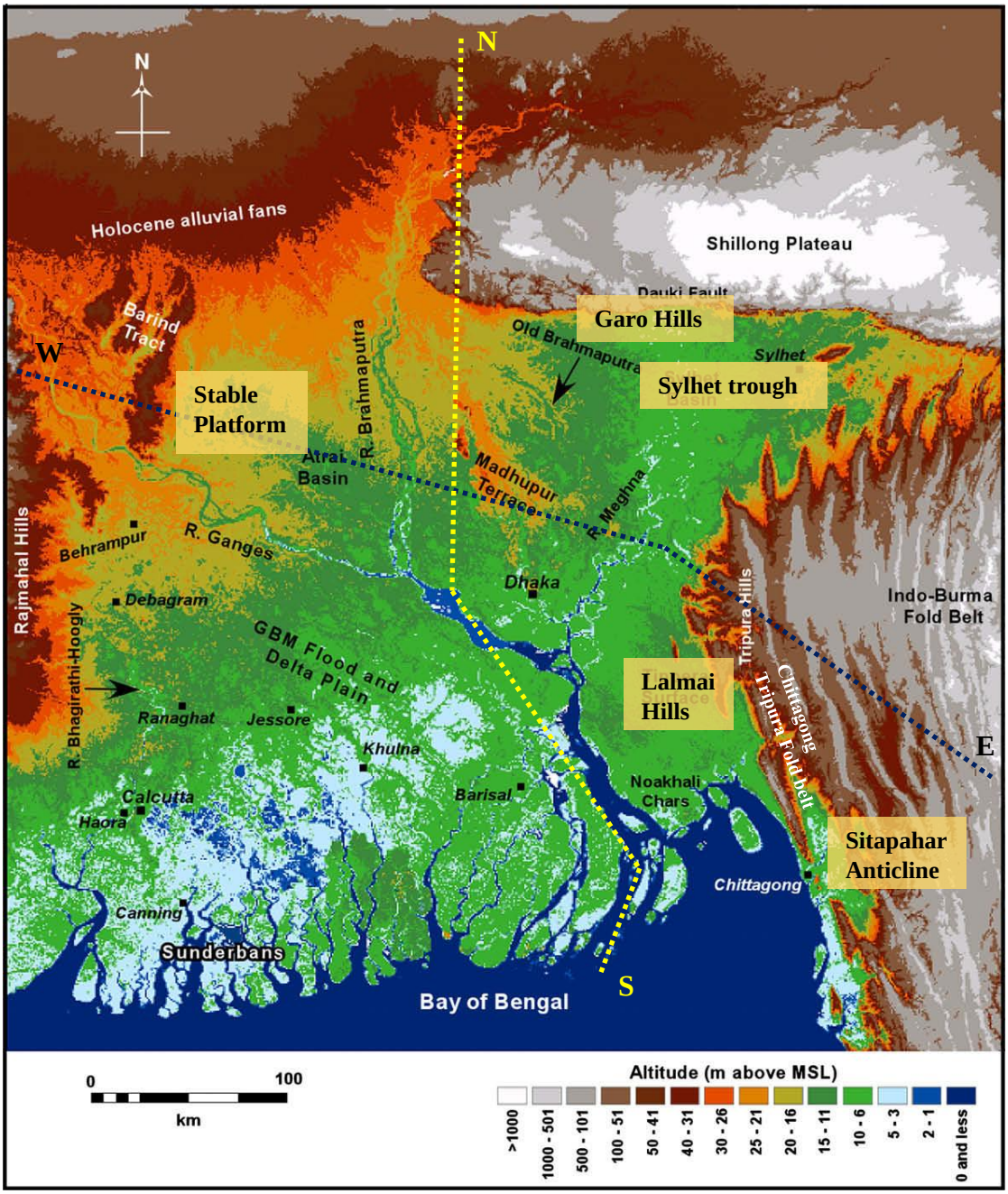

Fig. 2.1 Tectonic Map of the Bengal basin showing different tectonic elements of the basin. The N-S and E-W cross-sections are shown in the figure 2.2 and 2.3, respectively. Tectonic regions are Stable Platform, Sylhet Trough, Garo hills, Lalmai hills, and Sitapahar anticline.

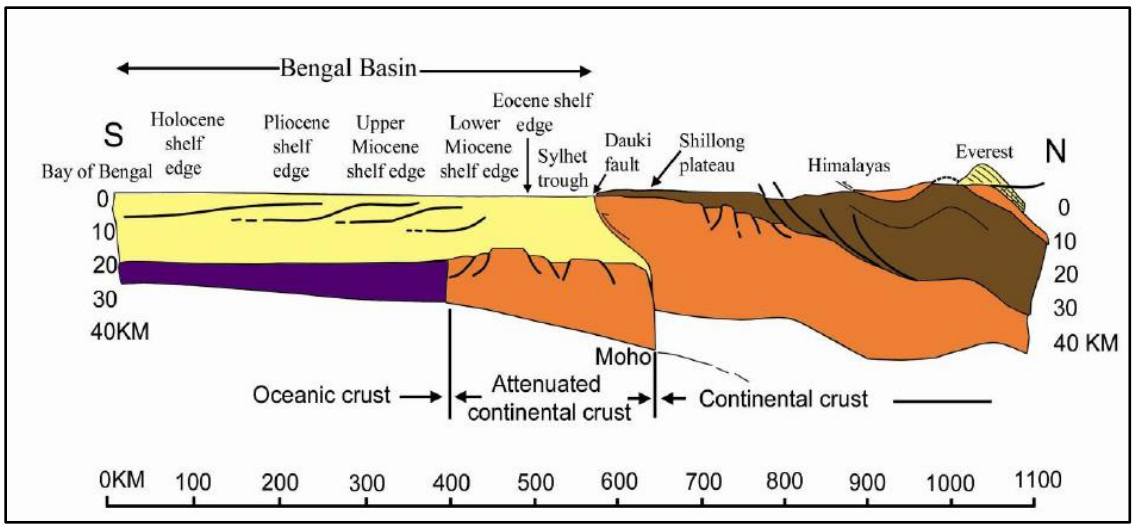

Fig. 2.2 North-south cross section through the Bengal basin (after Uddin and Lundberg, 2004).

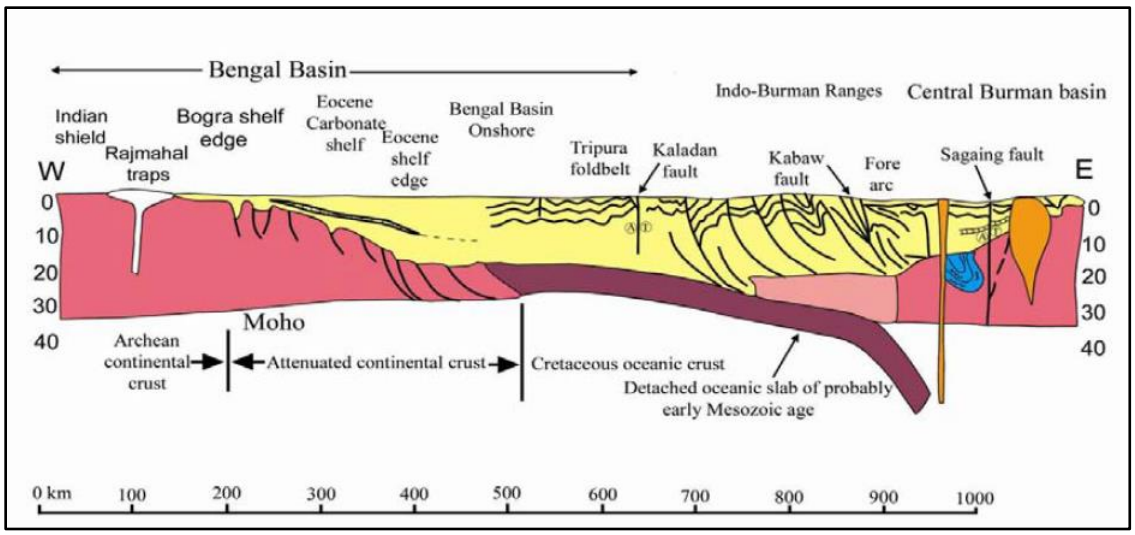

Fig. 2.3 East-west cross section of the Bengal basin (after Uddin and Lundberg, 2004).

ii) The Sylhet Trough (Fig. 2.1) is bounded to the north by the Shillong Plateau and to the east and south by the Chittagong Tripura fold belt (Johnson and Nur Alam, 1991). It is mostly underlain by continental crust, has accumulated more than 13 to 17 km of sedimentary strata (Evans, 1964; Hiller and Elahi, 1984). It has been mainly controlled by two tectonic events: increased movement along the Dauki Fault (upthrust); and westward advancement of the Indo-Burman Ranges due to continued

oblique subduction of the Indian Plate beneath the Burmese Plate after Paleogene (Gani and Alam, 2002).

iii) The Garo hills (Fig. 2.1) of the north-central part of the basin are part of the Garo-Khasi range in Shillong, India, the tectonic history of which has to be explained in relation to the total structure of the Shillong Plateau. The Shillong Plateau is considered to be a basement pop-up structure, uplifted along steep and seismically active reverse faults; i.e., the E-W trending Dauki fault in the south, and the inferred WNW-ESE trending Oldham Fault in the north (Bilham and England, 2001; Rajendran et al., 2004; Kayal et al., 2006; Clark and Bilham, 2008). An Archean gneissic complex with acid and basic intrusives, Lower Gondwana rocks, and Cretaceous-Cenozoic sediments are found in Garo hills stratigraphic sequence. During the Miocene, sedimentation continued over the southern and western part of the Garo hills and the southern fringe of the Khasi Hills. The major uplift of the plateau as a whole started at the end of the Miocene, resulting into the formation of the Khasi and Garo hills. The Pliocene (Dupi Tila) sediments were deposited in nearby basins as the uplift of the Shillong Plateau continued.

iv) The Sitapahar anticline (Fig. 2.1) is located in the southeastern part of the basin. This anticline was formed by compressive forces exerted by convergence of the Indian and Burmese plates. The evolution of the Indo-Burman range and Arakan-Yoma range is related to this anticline. In the late Pliocene, when the Chittagong Tripura Fold Belt was uplifted at the eastern margin of the Trough, a huge volume of clastic sediments was shed off, resulting in the deposition of Pliocene-Pleistocene Dupi Tila sediments in the resulting foreland basin. The axis of the anticline trends NNW-SSE along with the main structures of the Chittagong Tripura Folded Belt (CTFB). This doubly plunging anticlinal structure is approximately 400 km long and 12-15 km wide, and a major part of the western flank is steeper than the eastern one. Both Lower and Upper Dupi Tila sequences are well exposed here.

v) The Lalmai hills (Fig. 2.1) are located in the south-central part of the Bengal basin. These hills are bounded on the east and west by faults; the entire structural unit can be considered a horst (Khan, 1991). Morgan and McIntire (1959) described the Lalmai hills as an uplifted block of highly oxidized, red Pleistocene sediments. The average elevation is about 22 meters above sea level, although some of the individual peaks of the hills are more than 45 meters high. Alluvium, Madhupur clay, and Dupi Tila Formation are well exposed in the core of the anticlines of the Lalmai hills.

2.3 REGIONAL GEOLOGY

The Bengal basin is asymmetric; sediment thickness increases toward the south and the east (Bakhtine, 1966; Curray and Moore, 1974; Murphy, 1988; Khandoker, 1989; Uddin and Lundberg, 2004). The basin contains approximately 16 km (Fig. 2.2 and 2.3) of Cenozoic siliciclastic sediments (Uddin and Lundberg, 1998a). The basement of the Indian platform slopes to the northwest and southeast from a central ridge, which is underlain by the shallowest occurrence (~140 m) of Precambrian rocks in Bangladesh. These basement rocks are the eastward subsurface continuation of the Indian shield. The width of the basin ranges from 200 km in the north to more than 500 km in the south where it extends into the Bay of Bengal.

Stratigraphic nomenclature of the Bengal basin has been established based on type sections in the Assam basin (northeast India; Khan and Muminullah, 1980; Uddin et al., 2010). Pre–Tertiary stratigraphic units of the Bengal basin are known only from the northwestern part of the basin. A Precambrian basement complex composed of diorite, gneiss, schist, amphibolite, diabase, migmatite, granite, granodiorite, and quartz-diorite makes up part of the Indian craton (Zaher and Rahman, 1980; Uddin and Lundberg, 1999; Hossain, 2009). Basement rocks are overlain by a ~1–km–thick bituminous coal–bearing sequence formed during the Permo–Carboniferous in intracratonic, fault–bounded basins (Zaher and Rahman, 1980). This coal–bearing sequence is overlain by ~500 m of Cretaceous volcanic rocks, the Rajmahal/Sylhet Traps, which are older than the Late Cretaceous Deccan Traps of western India. These are composed of hornblende

basalt, olivine basalt, and andesite (Khan and Muminullah, 1980; Uddin and Lundberg, 1999).

The generalized post–Mesozoic stratigraphy of the Bengal basin is shown in Table 1. The Paleocene–Eocene units of Tura/Cherra Sandstone have been recovered in drill holes in the northwest platform region (Khan and Muminullah, 1980) and are exposed at a single locality, in a south–dipping block near the Shillong Plateau in the northwestern part of the Sylhet trough (Uddin and Lundberg, 1999). This unit is overlain by Middle Eocene open–marine Sylhet Limestone and late Eocene marine Kopili Shale (Reimann, 1993; Jahan et al., 2017). The Kopili Shale is overlain by the Oligocene Barail Group. This group, deposited in tide–dominated shelf environments (Khan, 1991; Jahan et al., 2017), ranges from 800-1600 m thick and is exposed along the northern fringe of the Sylhet trough near the Dauki fault (Johnson and Nur Alam, 1991). In platform areas, Barail equivalent rock units are less than 200 meters thick and are known as the Bogra Formation (Khan and Muminullah, 1988; Imam, 2005). The Miocene Surma Group is subdivided into two units: 1) The Bhuban; and 2) Boka Bil formations (Holtrop and Keizer, 1970; Hiller and Elahi, 1984; Khan, 1991), both of which extend throughout the Bengal basin. The Surma Group was deposited in transitional delta–front settings and comprises progradational sequences. The Surma Group is unconformably overlain by the upper Miocene to Pliocene Tipam Group. The Tipam Group consists of the Tipam Sandstone and Girujan Clay units, which were deposited in bed–load dominated, braided–fluvial and lacustrine environments (Johnson and Nur Alam, 1991; Reimann, 1993). The overlying Dupi Tila Formation was deposited in meandering river environments (Johnson and Nur Alam, 1991).

Table 1. Generalized Cenozoic stratigraphic succession of the Bengal basin (based on Johnson and Nur Alam, 1991; Uddin and Lundberg, 1998a, 1999; Imam, 2005).

Age	Group	Formation	Thickness (m)	Lithology
Holocene	Alluvium			
Pleistocene	Dihing	Dihing	129	Yellow and gray, medium–grained, occasionally pebbly sandstone
Pliocene	Dupi Tila	Dupi Tila Claystone		Claystone with subordinate sandstones and pebbles
		Dupi Tila Sandstone	2393	Medium–to coarse–grained, gray to yellow sandstone with clay balls
	Tipam	Girujan Clay		Red, brown, and purple mottled clay with sand lenses
		Tipam Sandstone	1450	Gray to brown, coarse–grained, cross-bedded, massive sandstone
Miocene	Surma	Boka Bil	1500	Alternating shale, siltstone and sandstone
		Bhuban	3100	Sandstone, siltstone, clayey sandstone, clays and lenticular conglomerate
Oligocene	Barail	Renji	800-1000	Coarse–grained sandstone, carbonaceous shale and lenses of coal
		Jenum		Dark gray silty and sandy shale
Eocene to Paleocene	Jaintia	Kopili Shale	15-150	Alternating dark gray calcareous shale and thin limestones
		Sylhet Limestone	148	Gray to dark gray, highly fossiliferous limestone
		Tura/Cherra Sandstone	240	White, pink to brown, coarse–grained, cross–bedded, carbonaceous sandstone
Pre–Paleocene	Undifferentiated sedimentary rock			

2.4 SIWALIKS OF INDIAN SUBCONTINENT

The term ‘Siwalik hills’ was introduced by Cautley to designate the sub-Himalayan ranges occurring between the Ganges and Yamuna rivers. Studies of vertebrate fossils and detailed magnetic stratigraphy were done in the area (Opdyke et al., 1982; Johnson et al., 1985 and many others). Hugh Falconer, a Scottish paleontologist, designated it as the “nearly continuous series of Tertiary formations stretching from Punjab down to Irrawaddy” (Tripathi, 1986). The Siwalis hills are relatively low, ranging in height from 1000-1200 m above mean sea level with variable trends running parallel to the Himalayas.

Genetically, the Siwaliks represent clastic freshwater molasse that accumulated in a long narrow foredeep formed to the south of the rising Himalaya, which had its inception in the most intense uplift during the middle Miocene (Tripathi, 1986). Clastic sediments accumulated in four different environments; lacustrine, channel and floodplains, outwash plains, and piedmont. The age of the Siwalik Group ranges from middle Miocene to middle Pleistocene. The Siwalik Group is subdivided into three subgroups- Lower Siwalik, Middle Siwalik, and Upper Siwalik (Table 2).

The Lower Siwaliks (Chinji and Kamlal formations) constitute gray and green, carbonate-cemented, fine- to medium-grained greywackes interbedded with well-developed chocolate brown and maroon sandy clays (Pilgrim, 1913; Tripathi, 1986; Carveny, 1986). The Lower Siwaliks are also characterized by alterations of sandstones and clays. The Lower Siwalik Formation is underlained by the pre-Siwalik Murree Formation.

Table 2. Summary of Siwalik Stratigraphy (ages from Johnson et al 1985, modified from Cerveny, 1986).

Age		Lithostratigraphy			Lithology	Thickness (m)	Boundary Age (m.y.)
		Group		Formation			
Quaternary	Pleistocene	Siwalik	Upper	Soan	Compact, massive conglomerates with interbeds of varicolored sandstones, siltstones, and claystones; numerous volcanic ashes, several of which are very widespread.	2000	3.0
Neogene	Pliocene						
	Miocene		Middle	Dhok Pathan	Dominantly light gray to reddish brown sandstones with orange to brown siltstones and claystones, no known volcanic ash beds.	400	8.5
				Nagri	Massive gray to grayish brown sandstone with subordinate dark red to dark brown siltstones and claystones, at least 1 known volcanic ash.	750	10.8
			Lower	Chinji	Mostly bright red siltstones and claystones with subordinate light gray sandstones, 1 suspected volcanic ash.	700	14.0
				Kamlal	Gray to dark gray sandstones with interbedss of reddish purple siltstones and claystones, 2 known volcanic ash beds.	600	18.3
Paleogene	Oligocene	Rawalpindi		Murree	Dominantly reddish gray to maroon sandstones with interbeds of dark red and purple siltstones and claystone, no known volcanic ash beds.	Up to 2000	

The Middle Siwaliks (Nagri and Dhok Pathan formations) consist predominately of coarse-grained sandstones (Pilgrim, 1913; Cerveny, 1986; Tripathi 1986). They grade from greywacke in the lower portions to arkose in the higher portions. They are soft and friable owing to limited carbonate cementation. They are less well sorted compared to the Lower Siwalik and contain unweathered feldspars and abundant woody material. Pebbles are common towards the top. The clays are arenaceous. The thickness of the Middle Siwalik, which conformably overly the Lower Siwalik, is 1390 m (Table 2).

The Upper Siwalik sediments (Soan Formation) comprise variegated, soft, and massive pebbly sandstone with gray and brown clay beds, although conglomerates predominate in the upper portions (Pilgrim, 1913; Tripathi 1986). The sandstones and the conglomerates friable and contain streaks of lignite in places. The thickness of the Upper Siwalik Formation is 2350 m.

Primary sedimentary structures observed in the Siwalik sediments include large-scale tabular and trough cross beds and cut-and-fill structures. Small-scale cross beds, wavy and parallel lamination, lunate and linguoid ripple marks, flute and load casts, horizontal bedding, and mud cracks are also common (Johnson et al., 1985; Cerveny, 1986).

2.5 DUPI TILA FORMATION

2.5.1 DISTRIBUTION

The Dupi Tila Formation is widespread throughout the Bengal basin. It crops out in most areas in the hilly regions of Sylhet, Comilla, Chittagong, and Hill Tract districts where it commonly is overlain by a thin mantle of younger alluvium. On the flood plains of the Ganges, Jamuna, and Meghna rivers, in the central table-land, and in the platform area in the northwestern region, the Dupi Tila Formation lies mostly concealed under the Pleistocene Madhupur Clay or more recent Dihing pebbles or the alluvium (Khan, 1991; Reimann, 1993). The type area of the Dupi Tila Formation is located in the northeast Sylhet area, Bangladesh; the unit was named for sandstone cropping out near a village called “Dupigaon” (Fig. 2.4), where the unit is approximately 300-500 m thick.

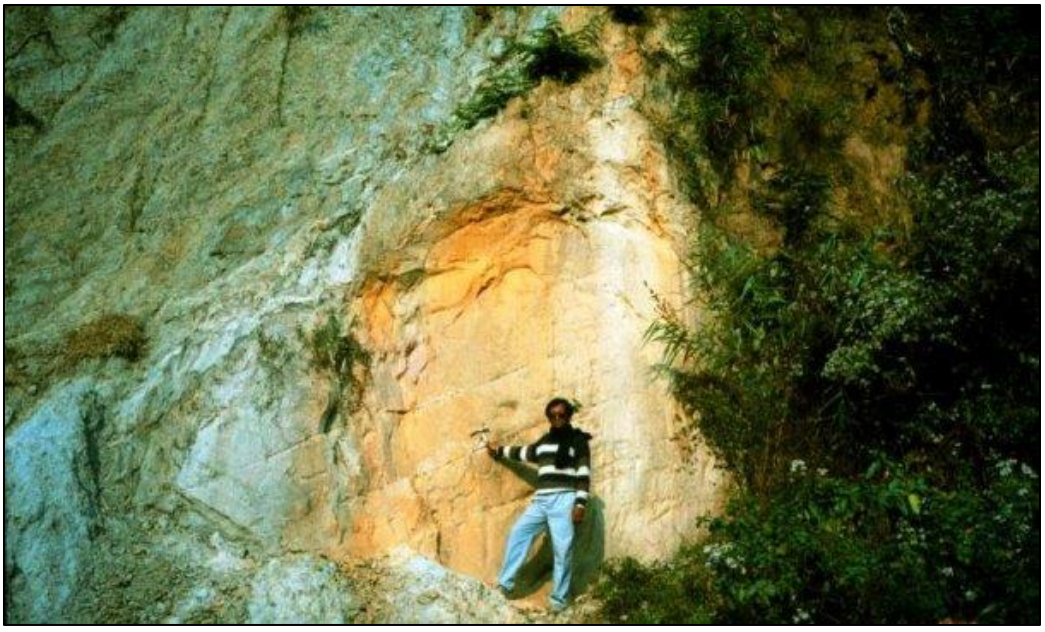

Fig. 2.4 Type area of Dupi Tila Formation, Dupigoan, Sylhet, Bangladesh.

2.5.2 STRATIGRAPHIC CONTEXT

The Dupi Tila Formation unconformably overlies the Girujan Clay in the hilly regions of Sylhet, Chittagong, and Hill Tract districts, and in the eastern part of the Madhupur Tract. In the northwestern platform area, the Dupi Tila Formation unconformably overlies the Surma Group, and in the northeastern Sylhet Trough, it conformably overlies the Tipam Group (Fig. 2.5).

Hiller and Elahi (1988) subdivided the Dupi Tila Formation into the late Pliocene lower Dupi Tila Formation and Pleistocene upper Dupi Tila Formation based on seismic markers referring to the continuous and reasonably traceable seismic reflectors in the Sylhet trough. Khan (1991) subdivided the formation into the late Miocene Dupi Tila Sandstone Formation and Mio-Pliocene Dupi Tila Claystone Formation. The study area includes the northeastern, northwestern, north-central, south-central, and southeastern parts of the Bengal basin.

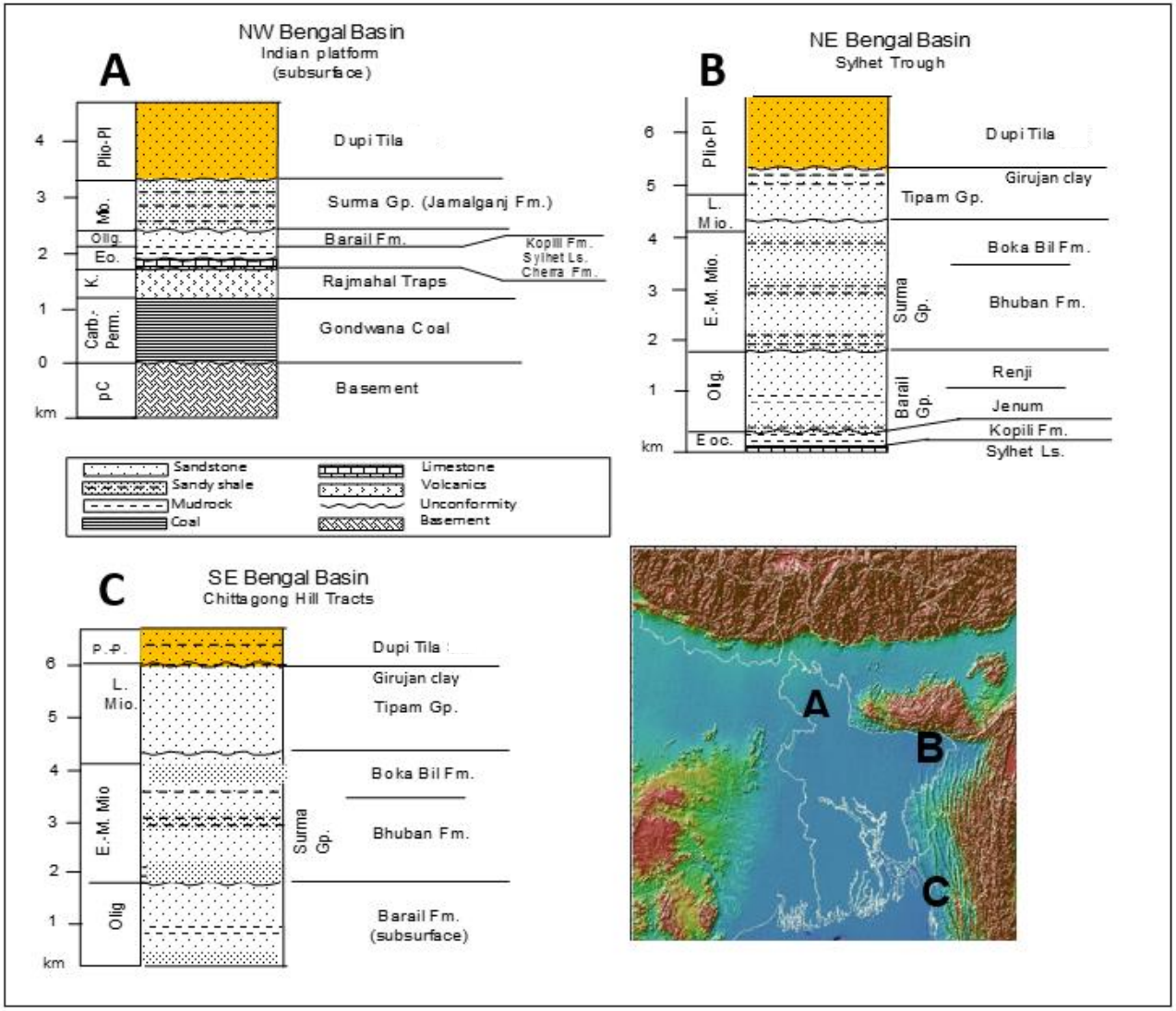

Fig. 2.5 Stratigraphic framework of the Bengal basin, Bangladesh (modified after Uddin and Lundberg, 1998a; Jahan et al., 2017). Orange boxes show the Dupi Tila Formation (also known as Dupi Tila Sandstone) in different parts of the basin.

2.5.3 SEDIMENTOLOGIC CHARACTER

The Dupi Tila Formation is composed of yellow (Fig. 2.6 A), light brown, and pink, medium- to very fine-grained, moderately to poorly indurated sandstone, with interbedded siltstone, silty clay, mudstone, and shale (Fig. 2.6D) and rare pebble beds (Fig. 2.6B) and accumulations of petrified wood (Fig. 2.6C). It includes planar bedded (Fig. 2.6E), planar cross-bedded, trough cross-bedded, convolute bedded (Fig. 2.6F), and massive sandstone, ripple cross-laminated sandstone-siltstone, flaser-laminated sandstone-shale, lenticular laminated sandstone-siltstone-shale, parallel-laminated sandstone-siltstone, wavy laminated shale, parallel-laminated blue shale, and mudstone (Khan, 1991; Reimann, 1993; Gani and Alam, 2002; Alam et al., 2003; Roy, 2012). Locally sediments of the Dupi Tila are bioturbated (Fig. 2.6H) and contain rip-up clasts (Fig. 2.6G).

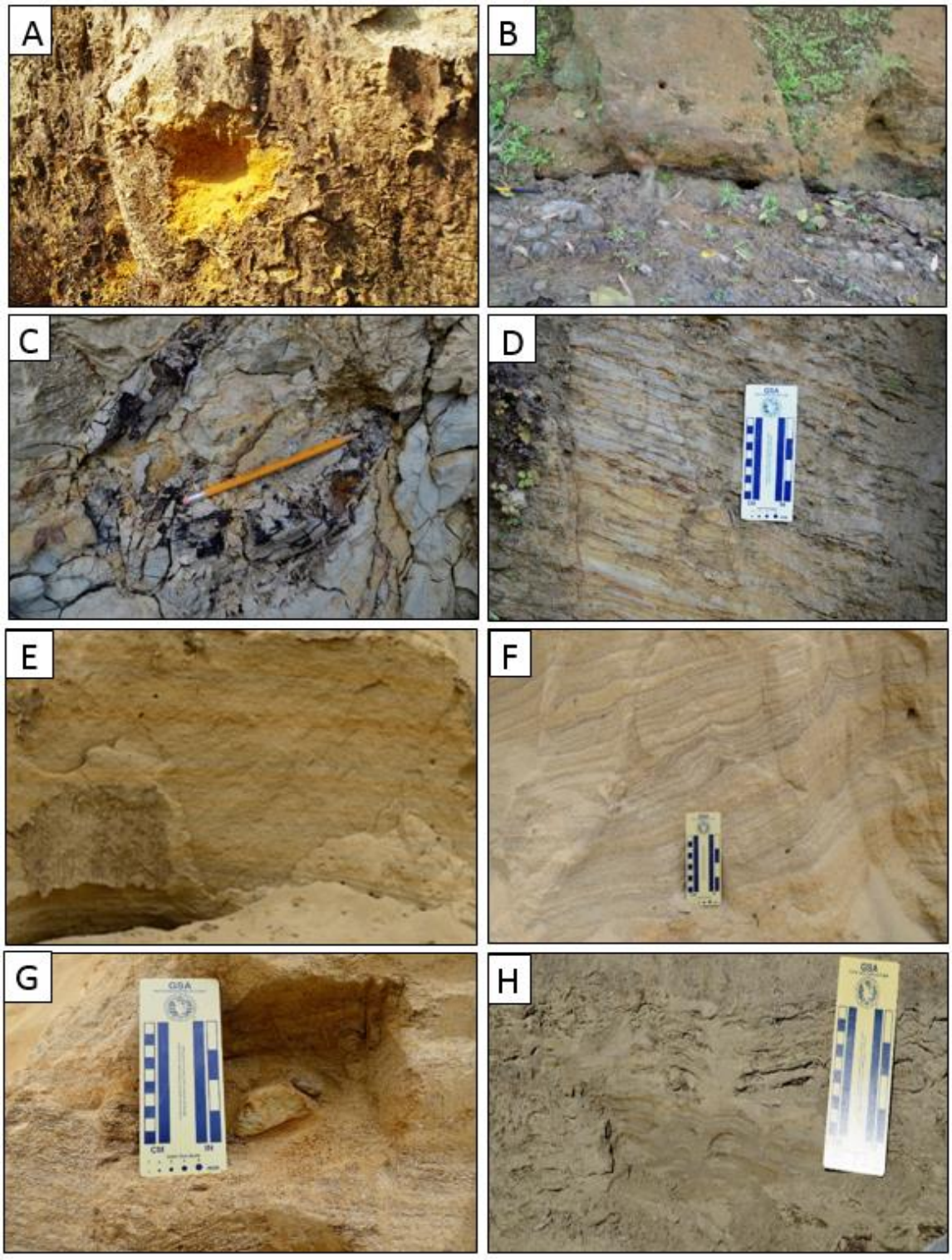

Fig. 2.6 Outcrops showing different characteristics of Dupi Tila Formation; A- typical yellowish brown sandstone; B- pebble beds; C- petrified wood in sandstone; D- sand with clay lenses; E- planar bedding; F- convolute bedding; G- rip-up clasts; and H- bioturbation.

Chapter 3: MATERIALS AND METHODS

3.1 FIELDWORK

Geological field work was carried out in Bangladesh from December 12, 2015, to January 8, 2016. Sixty-one samples were collected from northeastern, northwestern, north-central, south-central and southeastern regions of the Bengal basin, Bangladesh (Fig. 3.1). Among these, fifty-six samples were outcrop samples, and six were drill-core cuttings collected from the northwestern Bengal basin.

Sample-collection sites include: (i) Garo hills, Bijoypur, Netrokona, north-central, Bengal basin; (ii) Sylhet Trough, Shari-Goyain river section, northeastern, Bengal basin; (iii) Lalmai hills, Comilla, south-central, Bengal basin; (iv) Chittagong Hill Tracts, Sitapahar anticline, Kaptai, southeastern, Bengal basin; and (v) the Stable Platform (Dinajpur, and Rangpur), northwestern, Bengal basin (Fig. 3.1).

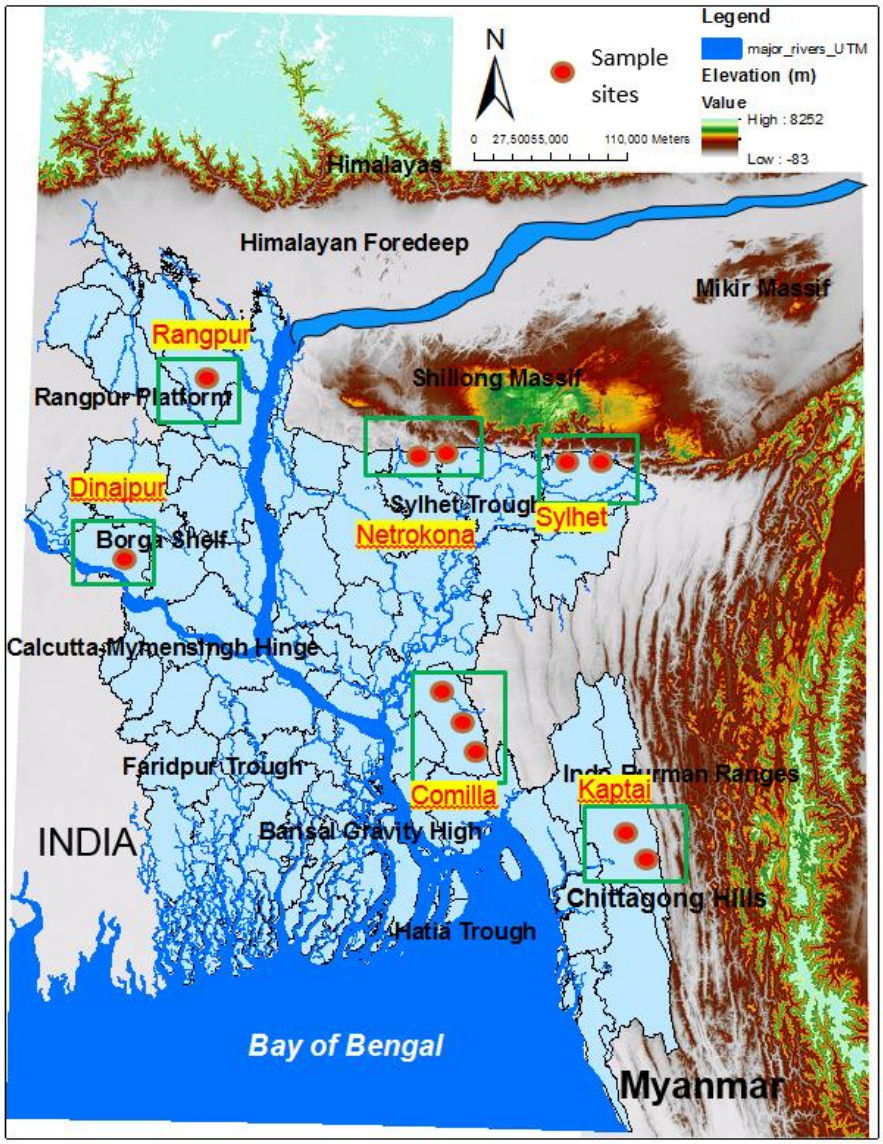

Fig. 3.1 Map showing study locations in the Bengal basin, Bangladesh.

3.1.1 SEDIMENT SAMPLING

Sandstone samples and associated pebbles were collected from both outcrops and drill cores from the Bengal basin. Sediment samples were collected from various locations at an interval of ~5 meters. Outcrop samples were collected using a hand-held auger (Fig. 3.2A, B).

About 200 grams of sample were collected from each sample site. Samples were saved in a sample bag, dated, and numbered. Photographs were taken during the

fieldwork (e.g. outcrop, special features, etc.) using a reference scale (Fig. 3.2A-F). A GPS (Global Positioning System) unit was used during the field operations, and latitude and longitude of each station were recorded. Finally, all the samples were shipped from Bangladesh to Auburn University. Thin sections were prepared from the samples and were analyzed under a petrographic microscope.

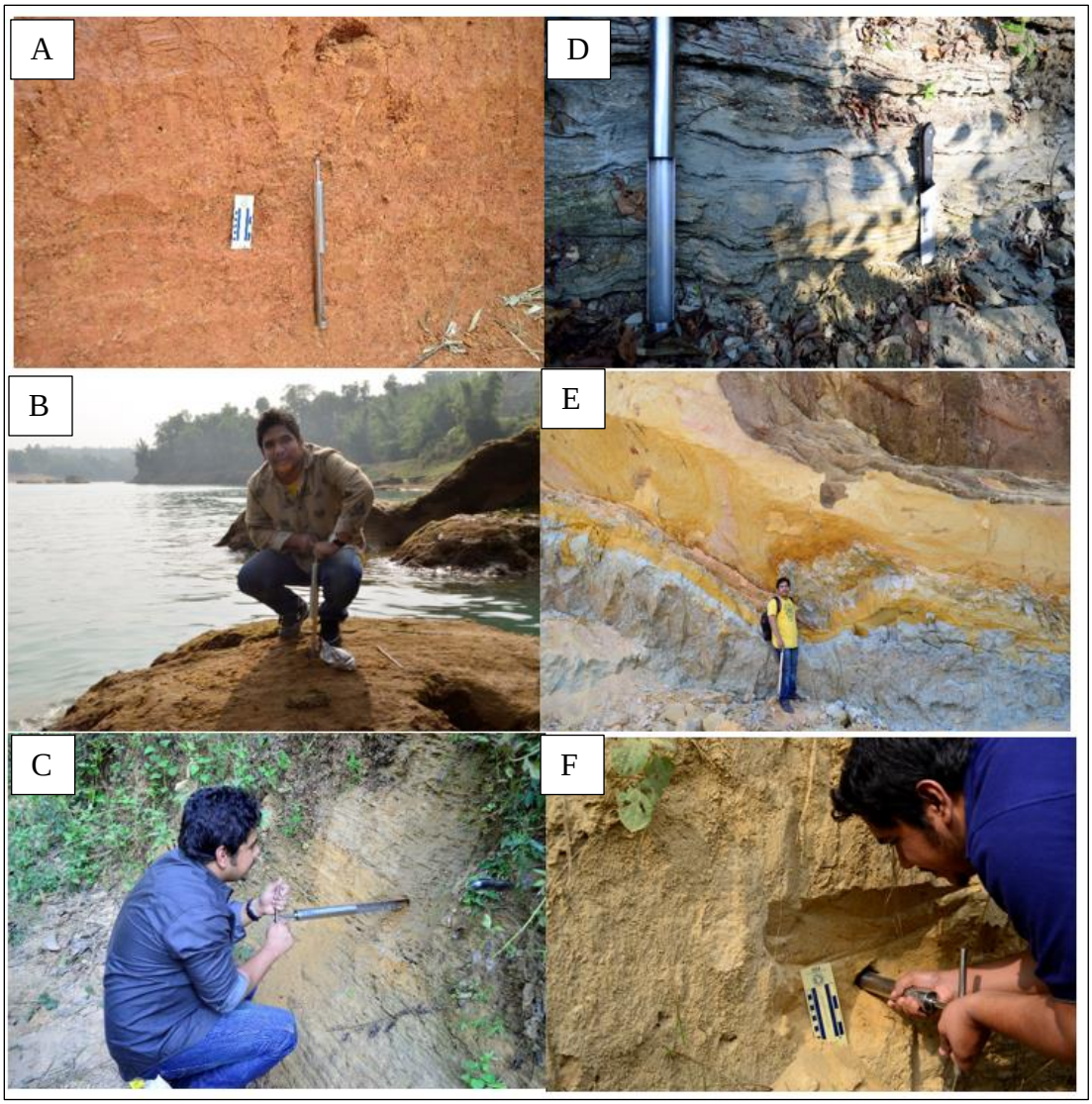

Fig. 3.2. Sampling from different outcrops using hand auger (A, B). Locations shown are the Shari-Goyain river section, Sylhet Trough (C), Garo hills, Bijoypur, Netrokona (D), Lalmai hills, Comilla (E), and Sitapahar anticline, Kaptai, Chittagong hill tracts (D, F).

3.1.2 CORE SAMPLING

Sediment cores were housed at the repositories of the Geological Survey of Bangladesh (GSB). Only six samples were available from the core lab in Bogra, northwestern Bangladesh (Fig. 3.3). Three samples each were collected from core GDH-56, Dangapara, Dinajpur, and core GDH-69, Madarpur, Mithapukur, Rangpur.

Fig. 3.3 Core samples arranged according to drilling depth, Bogra, Bangladesh.

3.2 LABORATORY ANALYSIS

The following provenance indicative methods were performed on the collected samples:

- Petrographic analysis of sandstone samples
- Heavy mineral analysis of intercalated sandstones
- Microprobe analysis on selected heavy minerals
- Whole-rock chemistry on selected mud and sand samples

Among sixty-one (61) samples, thirty (30) samples were prepared for petrographic study, twenty-five (25) for heavy mineral analysis, ten (10) for electron microprobe study, and ten (10) for whole-rock chemistry study. These samples are shown in Table 3.

Table 3. Location and types of analyses completed on the Dupi Tila Formation samples.

Section	Sample no.	Heavy Mineral Analysis	Microprobe analysis	Thin section petrography	Whole-rock Chemistry
Bijoypur, Netrokona outcrop (Garo hills)	BS-1	*	*	*	
	BS-2				
	BS-3				
	BS-4	*		*	
	BS-5				
	BS-6	*	*	*	
	BS-7	*		*	
	BS-8				
	BS-9				*
	BS-10				
Sylhet outcrop (Shari-Goyain river)	SS-1				
	SS-2	*	*	*	
	SS-3	*			
	SS-4	*		*	
	SS-5		*		
	SS-6	*		*	
	SS-7			*	
	SS-8			*	
	SS-9	*		*	
	SS-10				*
Comilla outcrop (Lalmai hills)	CCS-1			*	
	CCS-2	*			
	CCS-3g	*	*	*	
	CCS-4	*		*	
	CWSal-0	*		*	
	CWSal-1	*	*		
	CWSal-2			*	
	CWSal-3				
	CWSal-4	*		*	
	CSSal-1			*	
	CSSal-2				
	Cglau-0	*	*	*	
	CCHS-1	*			
	CCHS-2			*	
	CCol-1				
	CLSal-1	*	*	*	
	CCHz-1				
	CCHz-2				
	CRup-1				
	CRup-2				

Table 3. (Cont.) Location and types of analyses completed on the Dupi Tila Formation samples.

Kaptai outcrop (Sitapahar anticline)	KS-1	*		*	
	KS-2	*	*	*	
	KS-3	*		*	
	KS-4	*	*	*	
	KS-5			*	
	KS-6	*		*	
	KS-7				
	KS-8				*
	KS-9				*
	KS-10				*
	KS-11				*
	KS-12				*
	KS-13a				*
	KS-13b				
Core cuttings (GDH-56)	NWD-1	*			
	NWD-2			*	*
	NWD-3	*		*	
Core cuttings (GDH-69)	NWR-1			*	
	NWR-2	*		*	*
	NWR-3	*			

3.3 SAMPLE PREPARATION

Samples were prepared separately for each analysis. All samples were prepared in the Himalayan Research Laboratory (HRL) in the Department of Geosciences at Auburn University.

3.3.1 PETROGRAPHIC THIN SECTIONS

Approximately 30-40-gm sediment samples were shipped to Wagner Petrographic Ltd for preparation of petrographic thin sections. Mineral assemblages were analyzed with a petrographic microscope (Fig. 3.3). Modal analyses were performed by point-counting using the Gazzi-Dickinson method (Dickinson and Suczek, 1979) in order to minimize control by grain size on sand-grain composition. A total of 300 representative points were counted in each thin section. Framework grains were normalized to 100% using all the end members for quartz, feldspar, and lithic fragments. Careful attention was paid to the classification of lithic fragments and feldspar types (Pettijohn, 1941; Uddin

and Lundberg, 1998a). Thin sections were stained with potassium rhodizonate and sodium 30 cobaltinitrite to distinguish feldspars types.

Fig. 3.3. Using petrographic microscope to do point counting.

3.3.2 HEAVY MINERAL SEPARATION

Twenty-five sandstone samples (five samples from each site) were selected for heavy mineral analysis. Samples were disaggregated and oven-dried. Medium- to fine-grained sand samples were sieved using 4-Ø and 0-Ø screens, and representative 25-g subsamples from the 4-Ø to 0-Ø fraction were used for heavy-mineral separation. Heavy minerals were separated using tetrabromoethane ($C_2B_2Br_4$, density 2.89-2.96 gm/cc), a liquid with a density of 2.9. The mixture was stirred several times to ensure that the grains were thoroughly wetted and not coagulated. As time passed, the heavy minerals settled down to the bottom of the funnel and the lighter fractions floated in the heavy liquid at the top of the separating funnel (Fig. 3.4). After 24 hours, the stopcock was opened slowly and the liquid bearing the heavy mineral fraction in the bottom part of the separating funnel was allowed to flow slowly through a filter paper. Separated heavy minerals were washed with acetone and oven-dried (STABIL-THERM Gravity oven) at 100°C for 12 hours.

Lighter fractions also were cleaned with acetone, dried, and stored. Dry heavy minerals were reweighed to calculate the weight percentage (Fig. 3.5) of heavy minerals.

Fig. 3.4 Heavy minerals separation in the HRL (Himalayan Research Laboratory).

A Frantz magnetic separator (Model- L-1) was used to separate heavy minerals into four subfractions according to their magnetic susceptibility (Hess, 1966) in the Department of Geosciences at Auburn University. Separation was done by applying different slide slope angles and current values (Table 4). These groups include Group-1: Strongly Magnetic (SM); Group-2 and 3: Moderately Magnetic (MM) but different current values; Group-4: Weakly Magnetic (WM); and Group-5: Poorly Magnetic (PM).

Table 4. Five heavy mineral fractions seperated based on different magnetic susceptibility (Hess, 1966).

Side slope 15˚				Side slope 5˚	
Strongly magnetic	Moderately magnetic		Weakly magnetic	Poorly magnetic	
Hand magnet	0.4 Amps	0.8 Amps	1.2 Amps	1.2 Amps	
Magnetite Pyrrhotite Fe-oxides	Illmenite Garnet Olivine Chromite Chloritoid	Hornblende Hypersthene Augite Actinolite Staurolite Epidote Biotite Chlorite Tourmaline (dark)	Diopside Tremolite Enstatite Spinel Staurolite (light) Muscovite Zoisite Clinozoisite Tourmaline (light)	Sphene Leucoxene Apatite Andalusite Monazite Xenotine	Zircon Rutile Anatase Brookite Pyrite Corundum Topaz Fluorite Kyanite Silimanite Anhydrite Beryl
Group 1	Group 2	Group 3	Group 4	Group 5	

Group-1 consists of strongly magnetic minerals, including magnetite, pyrrhotite, and Fe-oxides. This group was separated using a hand magnet. Group-2 minerals include ilmenite, garnet, olivine, chromite and chloritoid. This group was separated using a 15º side slope and a 0.4-Amp current. Group 3 minerals include hornblende, hypersthene, augite, actinolite, staurolite, epidote, biotite, chlorite, and tourmaline. These were separated from weakly to poorly magnetic minerals using a 0.8-amp current and a 15º side slope. Group 4 minerals, including diopside, tremolite, enstatite, spinel, staurolite (light), muscovite, zoisite, clinozoisite, and tourmaline (light), were separated from Group-5 using a 1.2-amp current and a 15º side slope. The remaining heavy minerals were classified as Group 5 (poorly magnetic), which were not separated further due to their presence in small amounts. This group includes slightly magnetic minerals, such as sphene, leucoxene, apatite, andalusite, monazite, and xenotine, and other non-magnetic minerals like zircon, rutile, pyrite, corundum, fluorite, kyanite, sillimanite, and beryl. Separation of heavy minerals belonging to all five groups was not achieved for all samples due to the absence or rarity of minerals from certain groups.

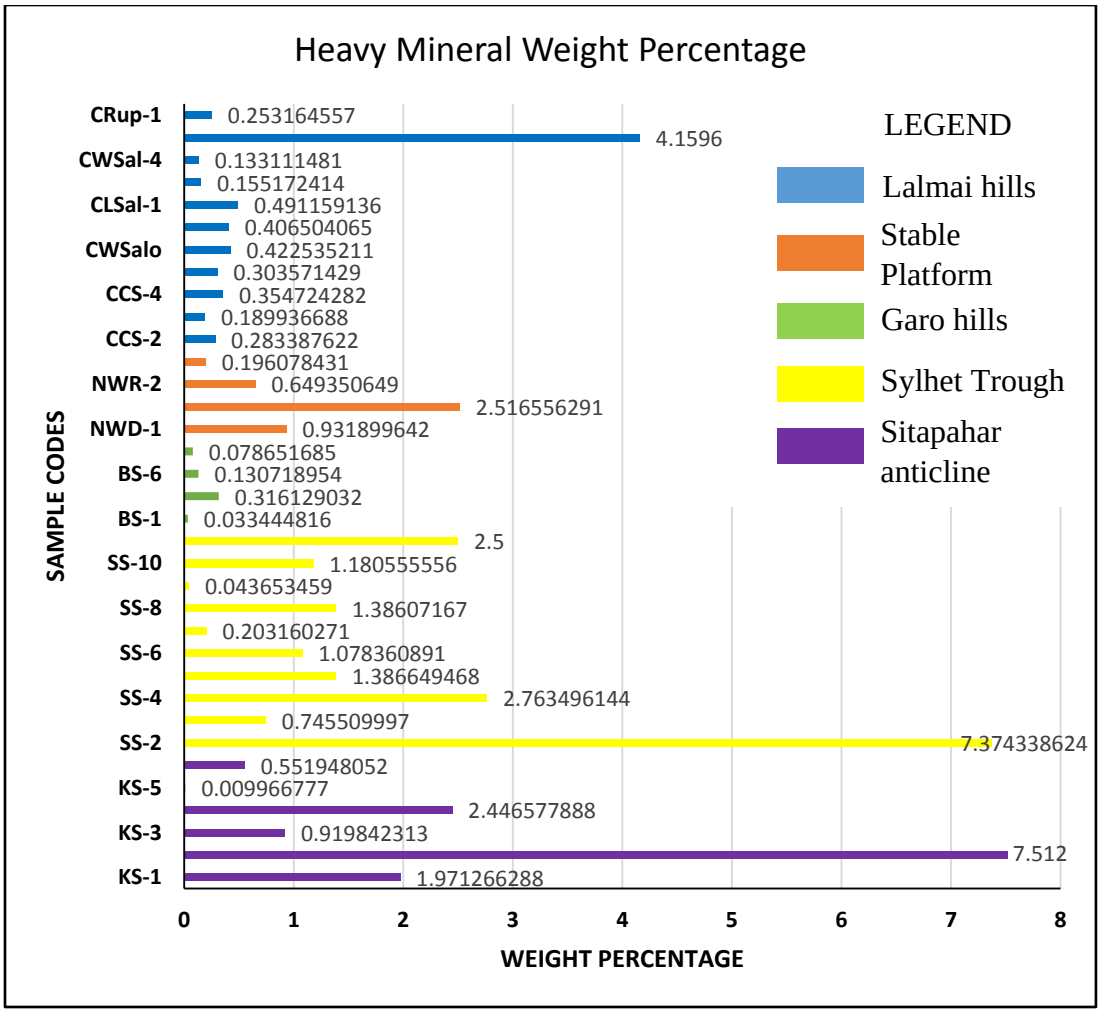

Fig. 3.5 Heavy mineral weight percentage data from selected samples color-coded to indicate study locations (see Appendix-A).

Identification of minerals was carried out using a petrographic microscope and the modified Fleet method. Numbers of grains from each layer were counted and then added together to calculate the percentage of different species of heavy minerals.

3.3.3 PREPARATION FOR MICROPROBE STUDY

Separated heavy minerals were sent to National Petrographics Inc., Texas to prepare multiple-depth polished thin sections for microprobe study. Due to budget constraints, polished thin sections were prepared from only ten (10) samples out of twenty-five (25) samples. Each of the magnetically separated heavy mineral fractions was segregated in different areas of each thin section. Microprobe analysis of ten samples was carried out in

the Central Analytical Facility (CAF) of the University of Alabama in Tuscaloosa, AL under the supervision of Robert Holler.

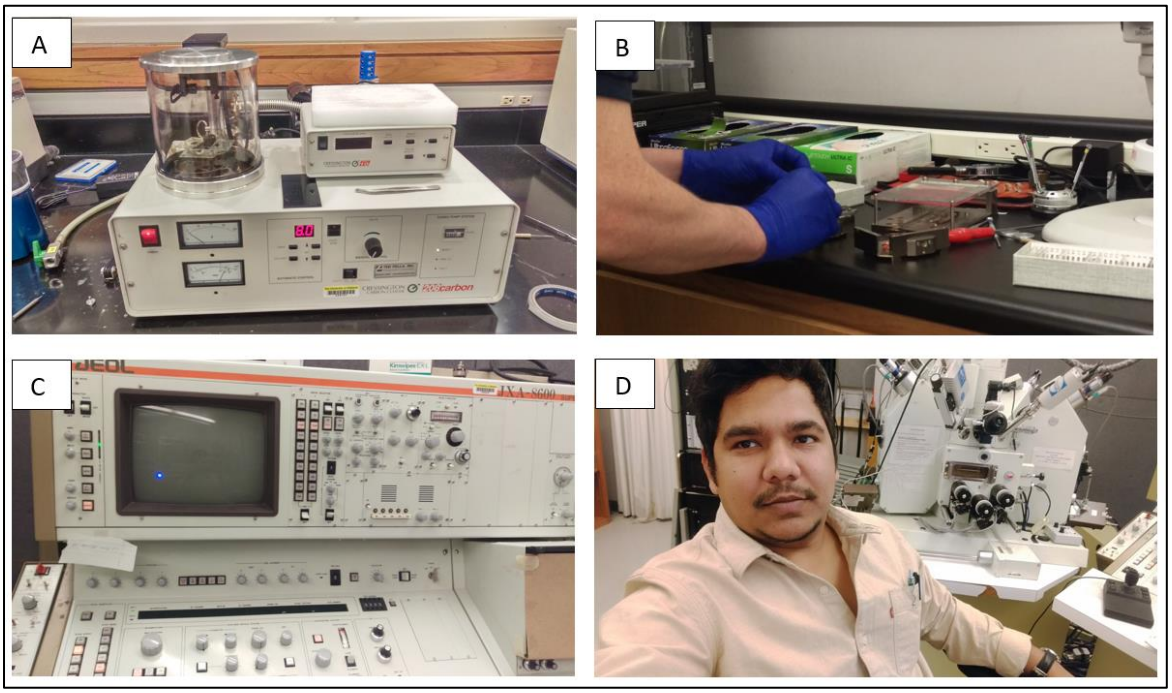

Fig. 3.6 Working on the EPMA machine in the CAF lab at the University of Alabama, A- carbon coating of the multiple-depth polished thin sections, B- using copper tape to tie up thin sections with the probe extension, C- electron scattering during EDS, D- Part of the microprobe machine.

Polished thin sections were carbon coated for 10 minutes (Fig 3.6A) using a Crossington Carbon Coater machine. During the operation, 10-4 mbar pressure was ensured. After carbon coating, samples were attached to the platform of the probe extension interface with copper tape (Fig. 3.6B). Carbon coating and copper tape were used to enhance the conductivity of the thin sections. After the calibration, the probe was employed in EDS (Energy Dispersive Spectroscopy) and WDS (Wavelength Dispersive Spectroscopy) (Fig. 3.6C, D) modes.

3.3.4 SAMPLE PULVERIZATION FOR WHOLE-ROCK CHEMISTRY

Ten mudrock samples were selected from the Dupi Tila Formation in the study area. Samples were dried in an oven at 50°C for nearly 24 hours. Approximately 20 gm of dried sediment for each sample was crushed with a mortar and pestle to a grain size of

<0.63 mm and homogenized. Samples were sent to the ACME Laboratories Ltd., Vancouver, BC, Canada, for analysis. In the lab, splits of 0.2 g of each sample were analyzed by ICP emission spectra following lithium metaborate/tetrabortate fusion and dilute nitric digestion. Loss on Ignition was calculated by weighing the difference after ignition at 1000^{o}C. The geochemical analysis included the measurements of 11 oxides (SiO_2, Al_2O_3, Fe_2O_3, MgO, CaO, Na_2O, K_2O, TiO_2, P_2O_5, MnO, and Cr_2O_3) and 7 trace elements (Ba, Ni, Sr, Zr, Y, Nb, and Sc).

Chapter 4: SANDSTONE PETROGRAPHY

4.1 INTRODUCTION

Sandstone petrography is a widely used technique to infer petrofacies evolution. Sedimentary rocks are principal sources of information in deciphering the paleotectonic history of the Earth's crust. Conventional petrography by point-counting using the Gazzi-Dickinson method is followed in order to minimize control by grain size on sand-grain composition (Dickinson and Suczek, 1979; Ingersoll et al., 1984). Careful attention was paid to the classification of the lithic fragment and feldspar types (Uddin and Lundberg, 1998a). Data were plotted on ternary diagrams to infer tectonic provenance (Dickinson 1985; Ingersoll et al., 1984). Mack (1984) suggested that factors other than the source-rock composition also are important in determining the ultimate composition of sandstones. Sandstone composition is sensitive to several factors, such as climate, relief, transport, and diagenesis, which provide valuable information for paleogeographic reconstructions (Suttner, 1974; Ingersoll et al., 1984; Johnson, 1993). Basin evolution and unroofing history of mountain belts can be best inferred through provenance studies that focus on key attributes of detrital mineralogy (Dorsey, 1988; Cerveny, 1986; Uddin and Lundberg, 1998a, b). Petrofacies evolution through detailed mineralogical analyses is based on the assumption that modes of transportation, depositional environments, climates, and diagenesis have not significantly altered detrital grain composition (Basu et al., 1975; Kumar, 2004; Sitaula, 2009; Alam, 2011; Chowdhury, 2014). Hence, all these factors need to be considered when interpreting sediment provenance (Suttner, 1974; Johnsson, 1993). This chapter deals with sandstone petrography and modal analysis of Pliocene-Pleistocene clastic sequences deposited throughout the Bengal basin.

For petrographic analysis, each of the sandstone thin sections was analyzed under a petrographic microscope to assess size, shape, and composition of the sand grains. The following compositional parameters were distinguished for the sand as appropriate: monocrystalline quartz (Qm); polycrystalline quartz (Qp); sedimentary lithics (Ls) and their types (shale, mudstone, etc.); metamorphic lithics (Lm) and their types; volcanic and plutonic lithics (Lv and Lp) and their types; plagioclase; k-feldspar; chert; and calcite. Metamorphic lithic fragments were identified as very low- to low-grade metamorphic lithic fragments (Lm_1), and medium- to high-grade metamorphic lithic fragments (Lm_2) (Table 5).

Table 5. Recalculated modal parameters of sand and sandstone (after Graham et al., 1976; Dickinson and Suczek, 1979; Dorsey, 1988; Uddin and Lundberg, 1998b).

Qt = Qm + Qp, Where, Qt = total quartzose grains Qm = monocrystalline quartz (> 0.625 mm) Qp = polycrystalline quartz (including chert)
Feldspar Grains (F=P+K), where, F = total feldspar grains P = plagioclase feldspar grains K = potassium feldspar grains
Unstable Lithic Fragments (Lt = Ls + Lv + Lm), where, Lt = total unstable lithic fragments and chert grains Lv = volcanic/metavolcanic lithic fragments Ls = sedimentary/metasedimentary lithic fragments Lm_1 = very low- to low-grade metamorphic lithic fragments Lm_2 = low- to intermediate-grade metamorphic lithic fragments

4.2 PETROGRAPHY OF THE DUPI TILA FORMATION

Dupi Tila sandstones from various part of the Bengal basin include an array of sublithic to subfeldspathic quartz arenites. Thirty thin-sections were analyzed from both outcrops and drill core samples. The Gazzi-Dickinson point-counting method (Ingersoll et al., 1984) was applied and 350-475 framework grains were counted. Types of quartz, feldspar, and lithic fragments were vigilantly observed. The point-count data from thirty thin sections are presented in Table 6. Petrographic results for sandstones are described below.

Table 6. Normalized modal compositions of Dupi Tila Sandstones from different regions of the Bengal basin, Bangladesh (STDEV- Standard Deviation).

Sample number	**QtFL (%)**			**QmFLt (%)**			**QmPK (%)**			**QpLsmLvm (%)**			**LsLvLm (%)**			**$LsLm_1Lm_2$ (%)**			**P/F**
	Qt	**F**	**L**	**Qm**	**F**	**Lt**	**Qm**	**P**	**K**	**Qp**	**Lsm**	**Lvm**	**Ls**	**Lv**	**Lm**	**Ls**	**Lm_1**	**Lm_2**	
Sitapahar anticline, Kaptai																			
KS-1	67	5	28	53	5	42	90	4	6	44	56	0	67	0	33	67	9	24	0.40
KS-2	67	13	20	53	12	35	91	5	4	44	56	0	67	0	33	67	9	24	0.59
KS-3	65	14	21	51	14	35	79	17	4	27	73	0	67	0	33	51	26	24	0.80
KS-4	60	14	26	45	14	41	77	16	7	27	73	0	21	0	79	21	26	53	0.71
KS-5	60	7	33	46	7	47	77	15	8	27	73	0	21	0	79	21	25	54	0.65
KS-6	62	5	33	47	5	48	88	4	8	44	56	0	21	0	79	38	9	54	0.32
MEAN	64	10	27	49	10	41	84	10	6	36	64	0	44	0	56	44	17	39	0.62
STDEV	7	9	13	4	4	6	7	6	2	9	9	0	23	0	23	23	8	15	0.77
Garo Hils, Netrokona																			
BS-1	96	2	2	86	2	12	98	2	0	100	0	0	0	0	0	0	0	0	1.00
BS-4	61	5	34	52	5	43	90	1	9	20	80	0	30	0	70	30	25	45	0.05
BS-6	98	1	1	82	1	17	98	2	0	93	7	0	0	0	0	0	0	0	1.00
BS-7	97	1	2	91	1	8	99	1	0	96	4	0	0	0	0	0	0	0	1.00
MEAN	88	2	10	76	3	21	96	2	2	72	28	0	30	0	70	30	25	45	0.76
STDEV	16	2	15	15	3	13	3	1	4	36	36	0	0	0	0	0	0	0	0.95
Northwest Stable Platform																			
NWD-2	88	6	6	45	3	52	80	18	2	66	34	0	39	0	61	45	25	30	0.89
NWD-3	85	6	9	40	4	56	86	13	1	70	30	0	48	0	52	48	19	33	0.95
NWR-1	85	9	6	47	5	48	85	11	4	69	31	0	53	0	47	53	13	34	0.73
NWR-2	93	3	4	46	3	51	77	5	18	74	26	0	43	0	57	43	26	31	0.23
MEAN	87	6	7	44	4	52	81	12	7	70	30	0	47	0	53	48	19	33	0.70
STDEV	3	2	2	3	1	4	4	6	8	3	3	0	5	0	5	4	6	2	0.52

Sylhet Trough																			
SS-2	69	7	24	49	7	44	87	5	8	50	50	0	57	0	43	57	12	31	0.73
SS-4	69	9	22	49	10	41	86	8	6	50	50	0	57	0	43	57	14	29	0.83
SS-6	67	11	22	47	11	42	83	11	6	38	62	0	57	0	43	44	27	29	1.00
SS-7	63	11	26	44	11	45	80	11	9	38	62	0	26	0	74	26	27	47	1.00
SS-8	63	9	28	44	8	48	80	9	11	38	62	0	26	0	74	26	25	49	0.98
SS-9	65	7	28	45	7	48	84	5	11	50	50	0	26	0	74	39	12	49	0.73
MEAN	66	9	25	46	9	45	83	9	8	44	56	0	42	0	58	42	20	39	0.97
STDEV	3	5	3	2	2	3	3	3	3	6	6	0	15	0	15	15	7	10	0.63
Lalmai hills, Comilla																			
CCS-1	58	5	37	37	5	58	88	6	6	35	65	0	33	0	67	33	32	35	0.47
CCS-3g	63	7	30	32	6	62	85	6	9	45	55	0	41	0	59	41	25	34	0.38
CCS-4	61	8	31	44	8	48	85	9	6	34	66	0	46	0	54	46	26	28	0.61
Cglau-S	66	4	30	54	4	42	93	3	4	30	70	0	23	0	77	23	25	52	0.47
CCHS-2	66	6	28	48	6	46	88	9	3	39	61	0	52	0	48	52	18	30	0.73
CSSal-1	66	7	27	43	7	50	86	10	4	47	53	0	45	0	55	45	17	38	0.73
CLSal-1	67	8	25	49	8	43	87	7	6	41	59	0	23	0	77	23	19	58	0.56
CWSal-0	59	6	35	46	6	48	88	7	5	27	73	0	22	0	78	22	32	46	0.60
CWSal-2	62	8	30	38	8	54	83	11	6	44	56	0	44	0	56	43	19	38	0.65
CWSal-4	68	9	23	47	9	44	84	7	9	47	53	0	49	0	51	49	23	28	0.41
MEAN	64	6	30	43	7	50	87	8	5	39	61	0	38	0	62	39	22	39	0.56
STDEV	4	1	4	6	1	7	3	2	2	7	7	0	12	0	12	12	6	10	0.32

4.2.1 PETROGRAPHY OF DUPI TILA SANDSTONES FROM THE SYLHET TROUGH

Six medium- to fine-grained sandstones were studied from the Sylhet Trough. Sylhet Trough sandstones consist predominantly of mono- and polycrystalline quartz, sedimentary lithic fragments, metamorphic lithic fragments, plagioclase feldspar and rarely orthoclase feldspar (Fig 4.1). These sandstones are quartzolithic to quartzofeldspathic ($Qt_{64}F_{10}L_{27}$). Monocrystalline quartz grains exhibit slightly undulatory extinction and are commonly sutured. No cherts were found. Sedimentary lithic fragments are dominant over metamorphic lithic fragments. Lithic fragments include argillite, slate, phyllite, quartzite, and schist. Metamorphic lithic fragments are mostly low- to intermediate-grade lithic fragments. No volcanic lithic fragments were found.

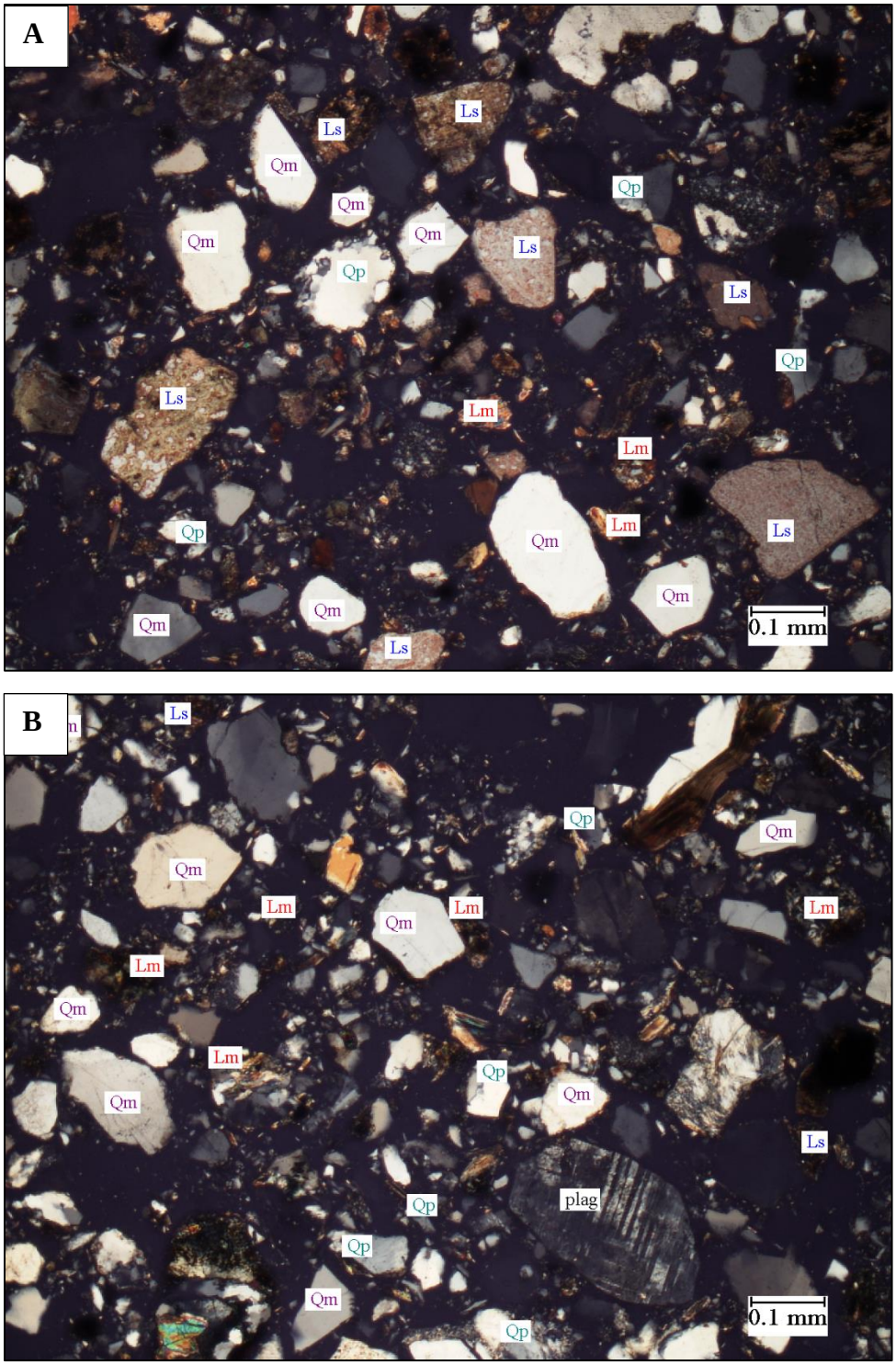

Fig. 4.1 Representative photomicrographs of sandstone of Dupi Tila Formation from the Sylhet Trough, Bengal basin showing (A) mono- (Qm) and polycrystalline quartz (Qp), sedimentary (Ls) and metamorphic lithic (Lm) grains (sample SS-2, 4X, crossed polar), (B) mono- (Qm) and polycrystalline quartz (Qp), feldspars (plag), sedimentary (Ls), and metamorphic lithic (Lm) fragments (sample SS-9, 4X, crossed polar).

4.2.2 PETROGRAPHY OF DUPI TILA SANDSTONES FROM THE GARO HILLS

Four medium- to fine-grained sandstones were studied from the Garo hills. These consist predominantly of monocrystalline quartz, sedimentary lithic fragments, metamorphic lithic fragments, and rare feldspars (Fig 4.2). Sandstones are quartz arenites ($Qt_{88}F_2L_{10}$). Lithic fragments are relatively fine-grained and are generally sparse. Only one sample (BS-4) contained high amounts of sedimentary and metamorphic lithic fragments. Metamorphic lithic fragments are common and include slate, phyllite, quartzite, and schist. No volcanic lithic fragments were found. The Garo hills sediments are more mature than those from other areas based on the Q/(Lt+F) maturity index.

4.2.3 PETROGRAPHY OF DUPI TILA SANDSTONES FROM THE LALMAI HILLS

Ten medium- to fine-grained sandstones from the Lalmai hills consist predominantly of mono-, poly-, and microcrystalline quartz, sedimentary lithic fragments, metamorphic lithic fragments, plagioclase feldspar and rare orthoclase feldspar (Fig 4.3). These sandstones are mostly quartzolithic ($Qt_{64}F_6L_{30}$). Few chert grains were observed. Lithic fragments are relatively abundant, metamorphic lithic fragments are more common than sedimentary lithic fragments. Lithic fragments include argillite, slate, phyllite, quartzite, and schist. No volcanic lithic fragments were found.

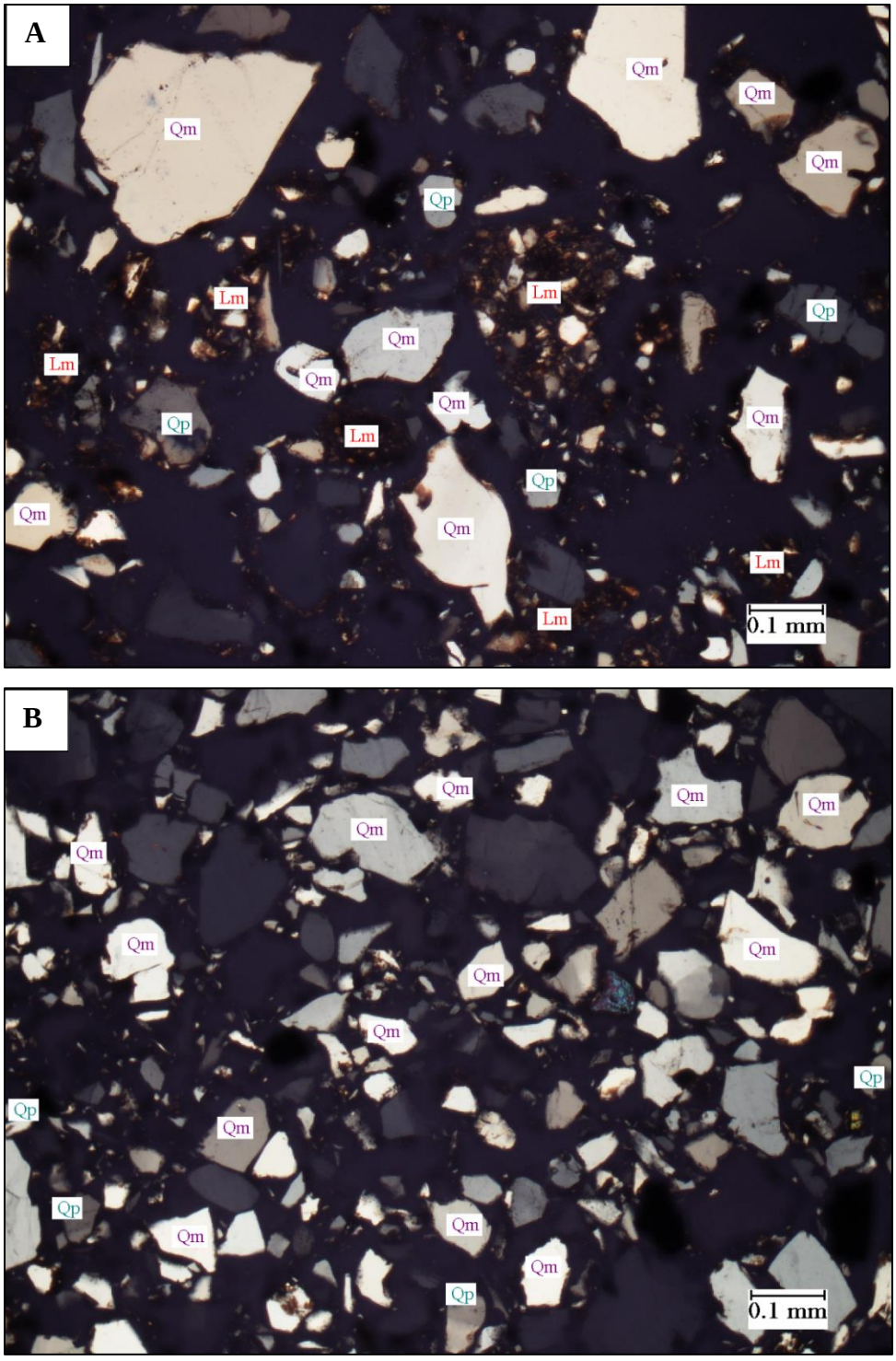

Fig. 4.2 Representative photomicrographs of sandstone of Dupi Tila Formation from the Garo hills, Bengal basin showing (A) mono- (Qm) and polycrystalline quartz (Qp), and metamorphic lithic (Lm) grains (sample BS-4, 4X, crossed polar), (B) monocrystalline (Qm) quartz, and polycrystalline quartz (Qp) (sample BS-7, 4X, crossed polar).

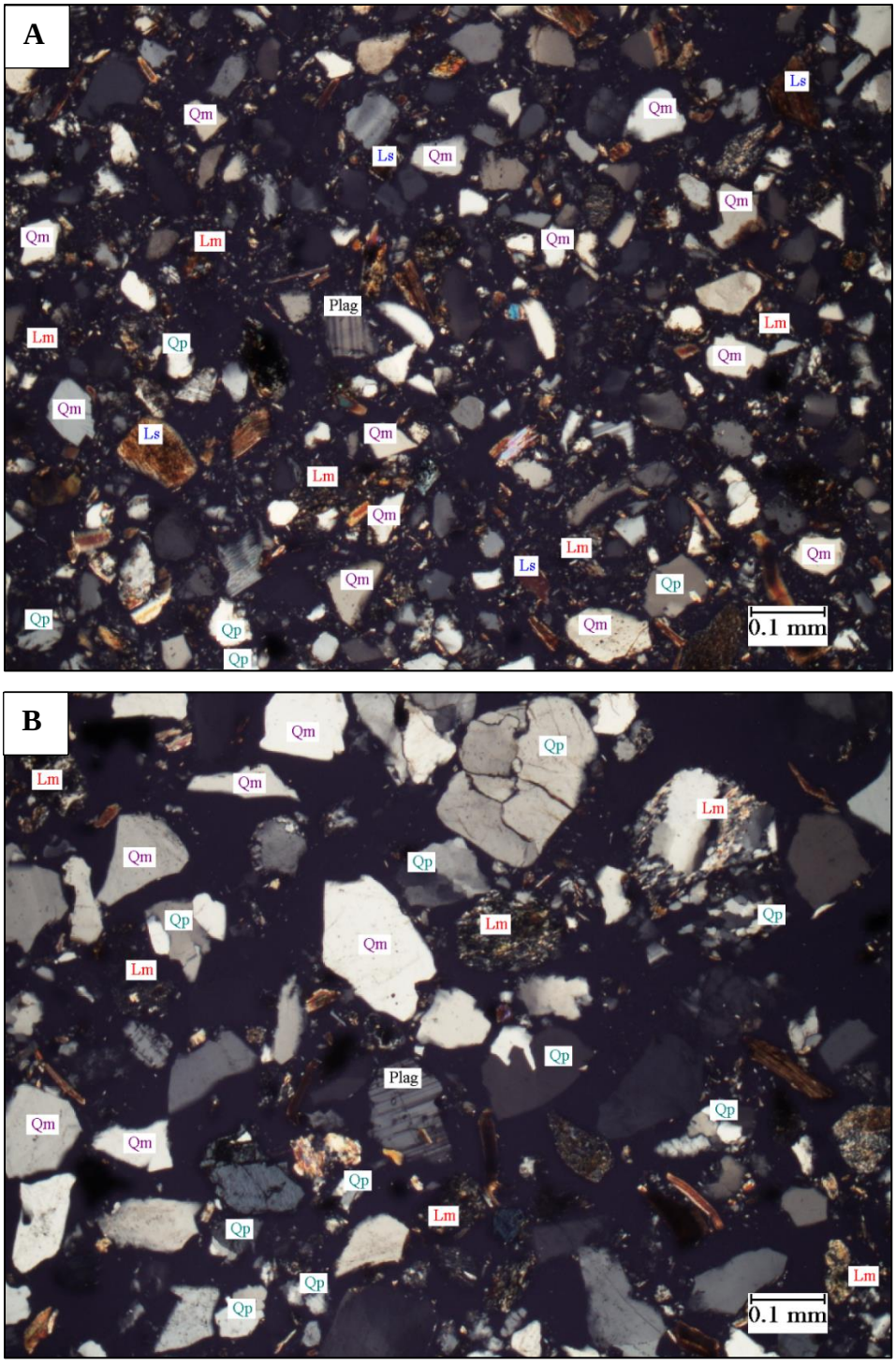

Fig. 4.3 Representative photomicrographs of sandstone of Dupi Tila Formation from the Lalmai hills, Bengal basin showing (A) mono- (Qm)and polycrystalline quartz (Qp), plagioclase feldspars (plag.), sedimentary (Ls) and metamorphic lithic (Lm) grains (sample CCHS-2, 4X, crossed polar), (B) mono- (Qm) and polycrystalline quartz (Qp), plagioclase feldspar (plag.), sedimentary (Ls), and metamorphic lithic fragments (Lm) (sample CWSal-4, 4X, crossed polar).

4.2.4 PETROGRAPHY OF DUPI TILA SANDSTONES FROM THE NORTHWEST STABLE PLATFORM

Four coarse- to medium-grained sandstones, two from core GDH-56 and two from core GDH-69, were studied from the Stable Platform part of the Bengal basin. These sandstones consist predominantly of mono- and polycrystalline quartz, sedimentary lithic fragments, metamorphic lithic fragments, plagioclase feldspar and rare orthoclase feldspar (Fig 4.4). Sandstones are quartz arenites ($Qt_{87}F_6L_7$). Metamorphic lithic fragments are dominant over sedimentary lithic fragments. Lithic fragments include argillite, slate, phyllite, mudstone, siltstone, quartzite, and schist. No volcanic lithic fragments were found.

4.2.5 PETROGRAPHY OF DUPI TILA SANDSTONES FROM THE SITAPAHAR ANTICLINE

Six mostly medium- to fine-grained sandstones were studied from the Sitapahar anticline. These consist predominantly of mono- and polycrystalline quartz, sedimentary lithic fragments, metamorphic lithic fragments, plagioclase feldspar, microcline, and orthoclase (Fig 4.5). These sandstones are quartzolithic to quartzofeldspathic ($Qt_{64}F_{10}L_{27}$). Mono- and polycrystalline quartz grains exhibit both straight and undulatory extinction and are commonly sutured. Lithic fragments include metamorphic lithic fragments and subordinate sedimentary lithic fragments. Lithic fragments include argillite, mudstone, siltstone, slate, phyllite, quartzite, and schist. Like samples from other regions, no volcanic lithic fragments were found.

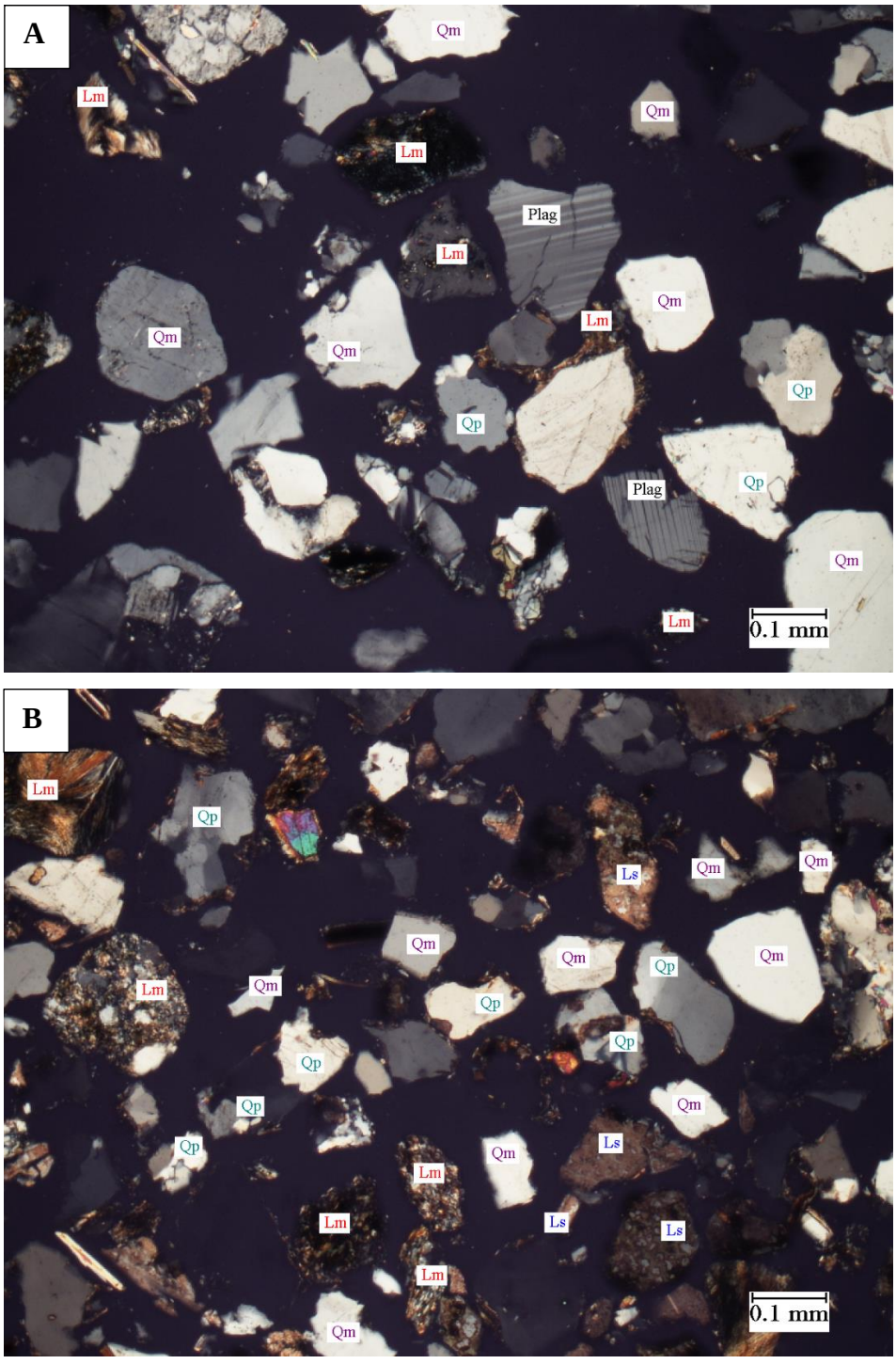

Fig. 4.4 Representative photomicrographs of sandstone of Dupi Tila Formation from the northwest Stable Platform, Bengal basin showing (A) mono- (Qm) and polycrystalline quartz (Qp), plagioclase feldspars (plag.), and metamorphic lithic (Lm) fragments (sample NWD-2, GDH- 56, 4X, crossed polar), (B) mono- (Qm) and polycrystalline quartz (Qp), sedimentary (Ls), and metamorphic lithic fragments (Lm) (sample NWR-1, GDH-69, 4X, crossed polar).

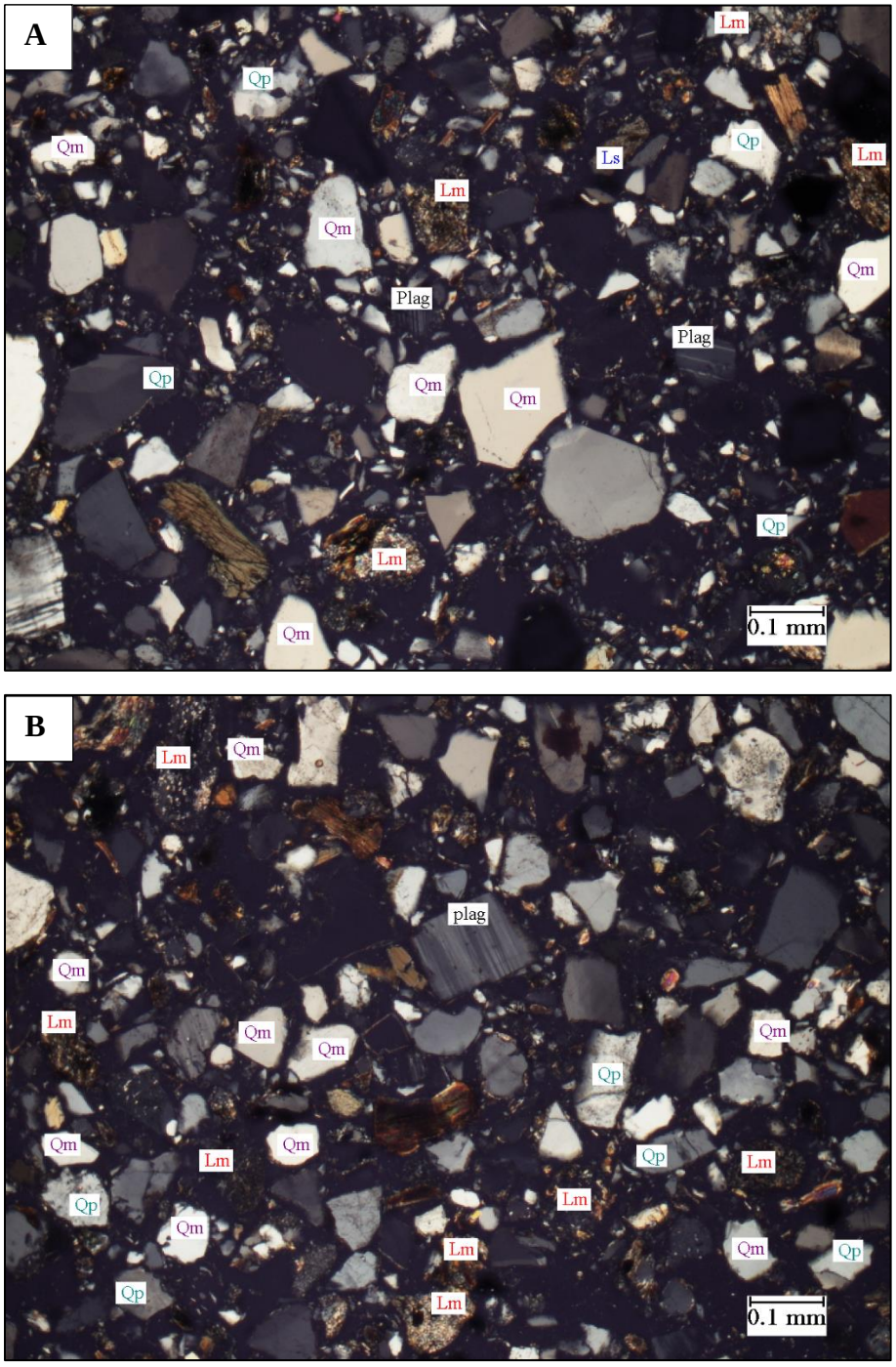

Fig. 4.5 Representative photomicrographs of sandstone of Dupi Tila Formation from the Sitapahar anticline, Bengal basin showing (A) mono- (Qm) and polycrystalline quartz (Qp), plagioclase feldspars (plag.), and metamorphic lithic (Lm) grains (sample KS-2, 4X, crossed polar), (B) mono- and polycrystalline quartz, and metamorphic lithic fragments (Lm) (sample KS-7, 4X, crossed polar).

4.3 SANDSTONE MODES

The relative abundance of major framework grain types in samples from each of the five localities is shown in figure 4.6. The Dupi Tila Formation contain high percentages of monocrystalline quartz in all localities, but particularly in the Garo hills samples. Polycrystalline quartz is most abundant in the Stable Platform area. Lithic fragments are abundant in Lalmai hills, Sylhet Trough, and Sitapahar anticline regions. This plot suggests that modal percentages of lithic fragments decrease from the northeast to northwest whereas modal polycrystalline quartz decreases from the northwest to northeast part of the basin. Modal feldspar contents are consistently low throughout the basin.

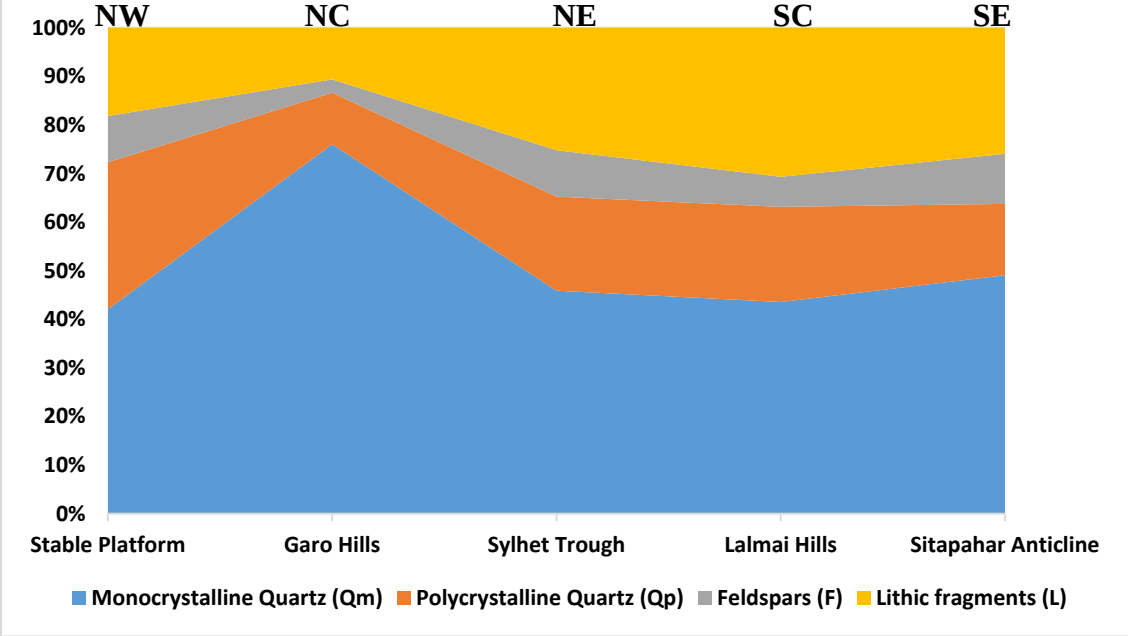

Fig. 4.6 Variation of modal sandstone composition of Dupi Tila Formation from various regions of the Bengal basin, Bangladesh (NW- Northwest, NC- North-central, NE- Northeast, SC- South-central, and SE- Southeast) .

4.4 PETROFACIES EVOLUTION

Ternary diagrams were prepared reflecting the petrofacies evolution using modal analyses of Dupi Tila Formation from various regions of the Bengal basin, Bangladesh. Tectonic discrimination plots from Dickinson (1985), were prepared based on the modal compositional analysis of sandstone framework grains. The QtFL (Fig. 4.7) plot shows

that sands of the Dupi Tila Formation were derived from "recycled orogenic" sources. The higher percentage of lithic fragments and a lower percentage of feldspars reflect various tectonic settings. Moreover, another controlling factor during the Pliocene-Pleistocene was climate. The relief of the source areas (the Himalayas, Indo-Burman ranges) inhibited intensive weathering. In the QmFLt diagrams (Fig. 4.8), sandstones of the Dupi Tila Formation plot in the "transitional recycled" field, except for the Garo hills samples. Plagioclase feldspars are relatively more abundant than potassium feldspars (see QmPK plot in figure 4.9). Feldspars are very rare in the Dupi Tila samples.

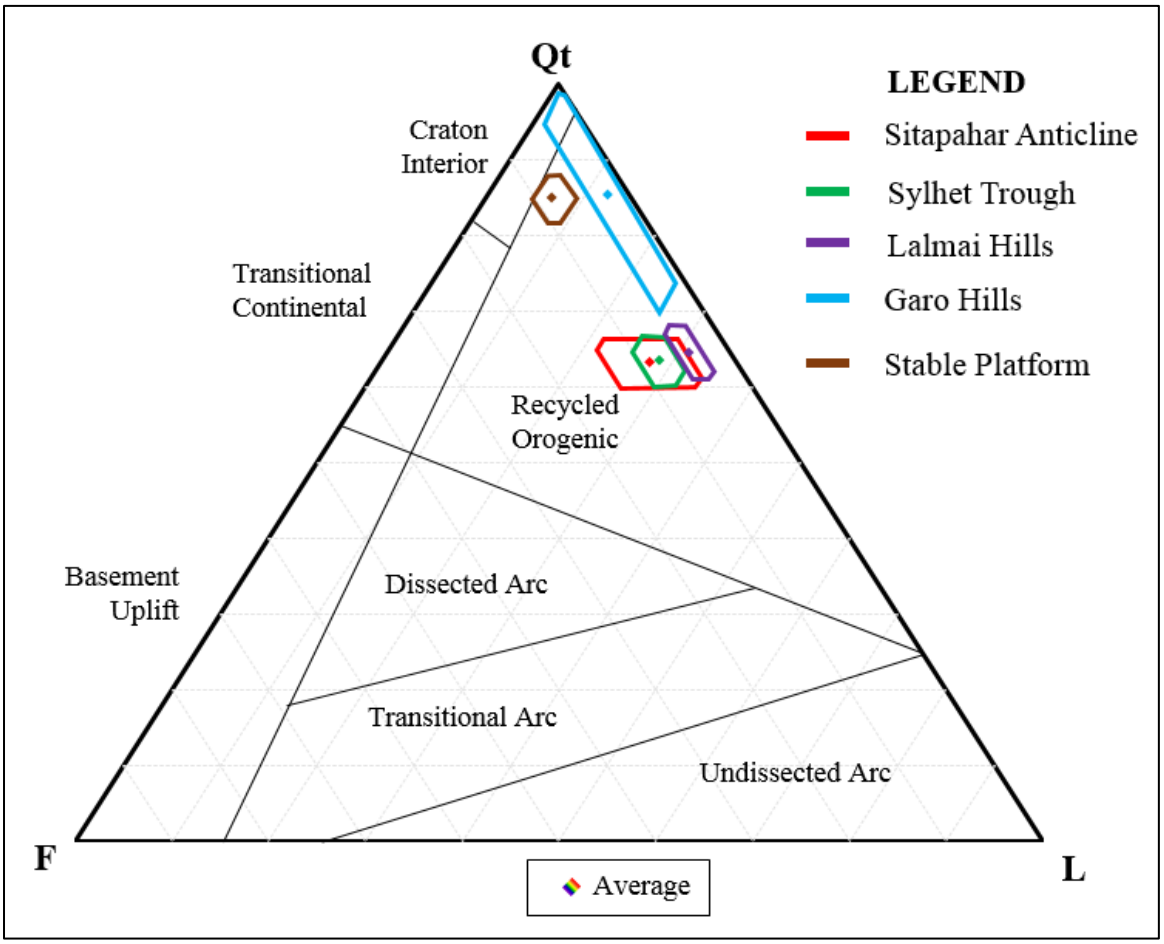

Fig. 4.7 QtFL plot of the Dupi Tila Formation from the Sitapahar anticline, Sylhet Trough, Lalmai hills, Garo hills, and Stable Platform showing mean and standard deviation polygons (provenance fields are taken from Dickinson, 1985).

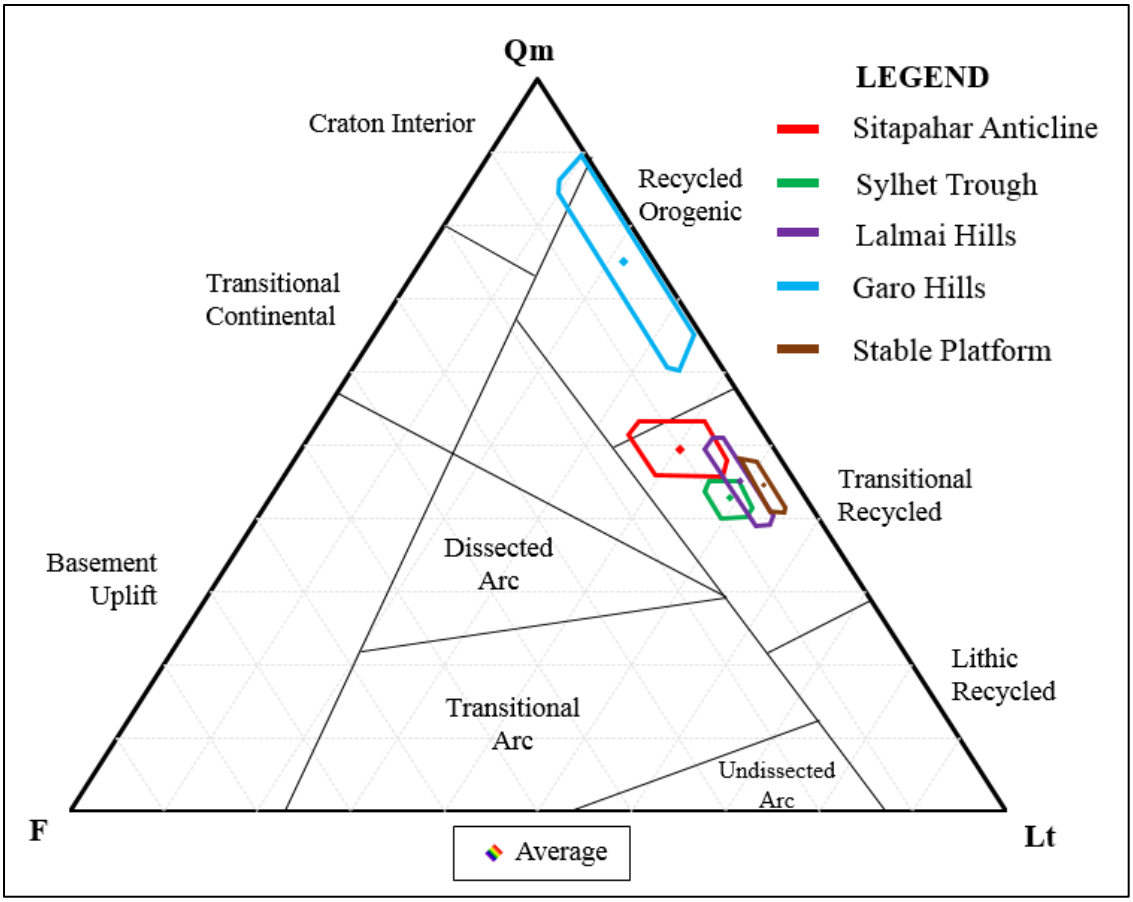

Fig. 4.8 QmFLt plot of the Dupi Tila Formation from the Sitapahar anticline, Sylhet Trough, Lalmai hills, Garo hills, and Stable Platform showing mean and standard deviation polygons (provenance fields are taken from Dickinson, 1985).

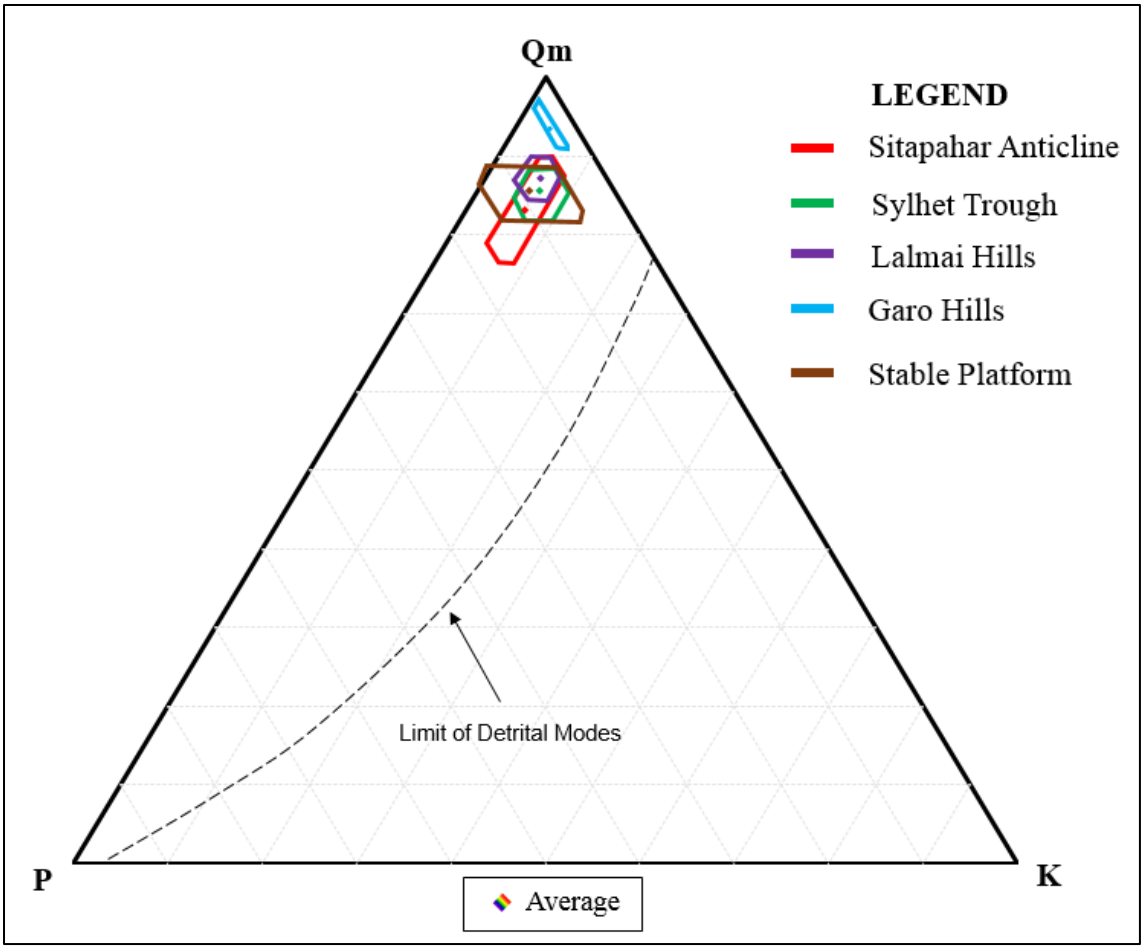

Fig. 4.9 QmPK plot of the Dupi Tila Formation from the Sitapahar anticline, Sylhet Trough, Lalmai hills, Garo hills, and Stable Platform showing mean and standard deviation polygons.

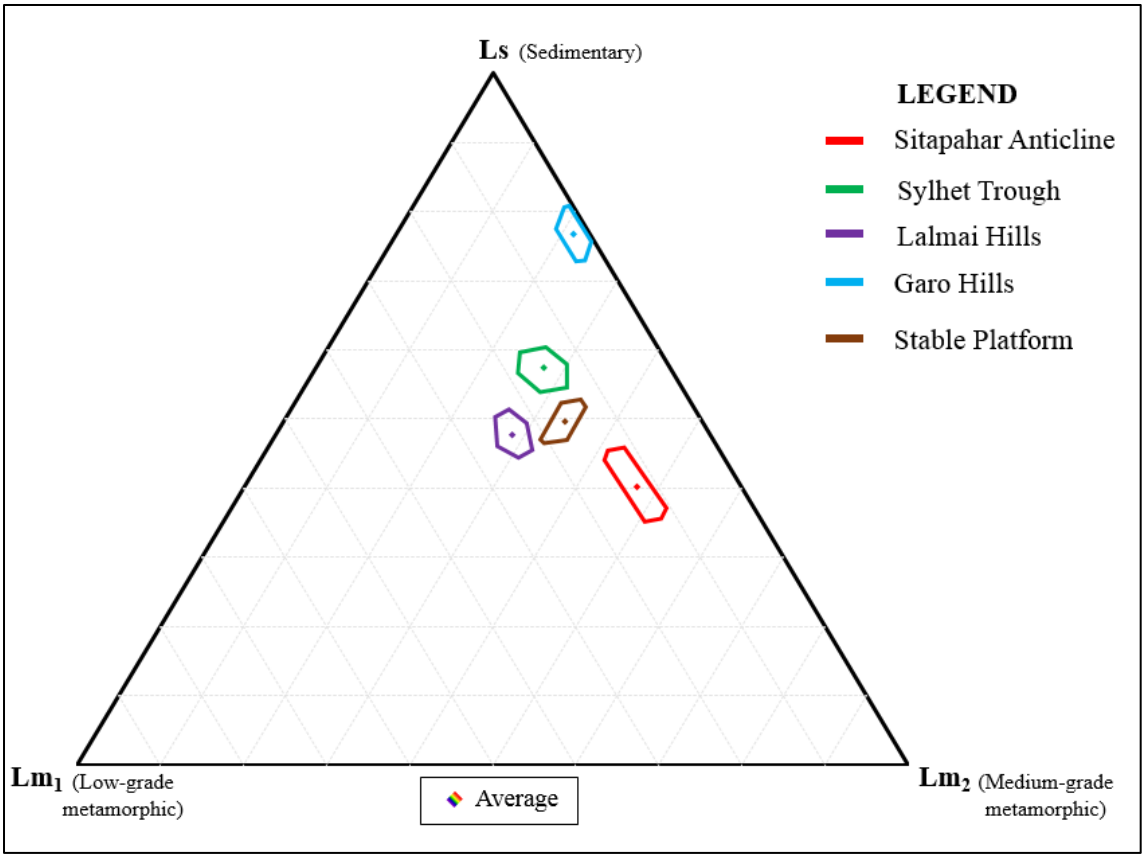

Fig. 4.10 $LsLm_1Lm_2$ plot of Dupi Tila Formation from different parts of the Bengal basin showing variation in the composition of lithic fragments. Ls = sedimentary lithic fragments, Lm_1 = very low- to low-grade metamorphic rock fragments, and Lm_2 = low- to intermediate-grade metamorphic lithic fragments.

The Sitapahar anticline, Sylhet Trough, and Lalmai hills samples are quartzolithic or quartzofeldspathic in modal composition. However, the Garo hills and Stable Platform samples are more quartzose. Modal analyses of the sandstones of the Dupi Tila Formation from Sitapahar anticline ($Qt_{64}F_{10}L_{27}$), Garo hills ($Qt_{88}F_2L_{10}$), northwest Stable Platform ($Qt_{87}F_6L_7$), Sylhet Trough ($Qt_{66}F_9L_{25}$) and Lalmai hills ($Qt_{64}F_6L_{30}$) suggest that the sandstones had an orogenic source. Only samples from the Garo hills contains a high amount of mono- and polycrystalline quartz; QtFL, and QmFLt diagrams differ from the other area samples.

Lithic fragments were dominant in the north-central-south part of the basin and are relatively sparse in the northwest region. Metamorphic lithic fragments are more common than sedimentary lithic fragments (Fig. 4.10), while volcanic lithic fragments are absent in the studied sediments. Due to the absence of volcanic lithic fragments or ash

beds in the Dupi Tila Formation, it can be concluded that the Rajmahap traps did not contribute significantly to the Bengal basin. A high number of low- to intermediate-grade metamorphic lithic fragments, dominated by slate and phyllite, occur throughout the Dupi Tila Formation. The abundance of low- to intermediate-grade lithic fragments (Lm_2) in all samples suggest unroofing of deep crustal levels of orogens.

Very few microcline and untwined orthoclase feldspars were found in the Sylhet Trough and Sitapahar anticline samples. Ratios of plagioclase feldspar to total feldspar are shown in the box plot (Fig 4.11). Sylhet Trough samples have the highest feldspar contents. Plagioclase feldspars are relatively more adundant than potassium feldspars in all regions.

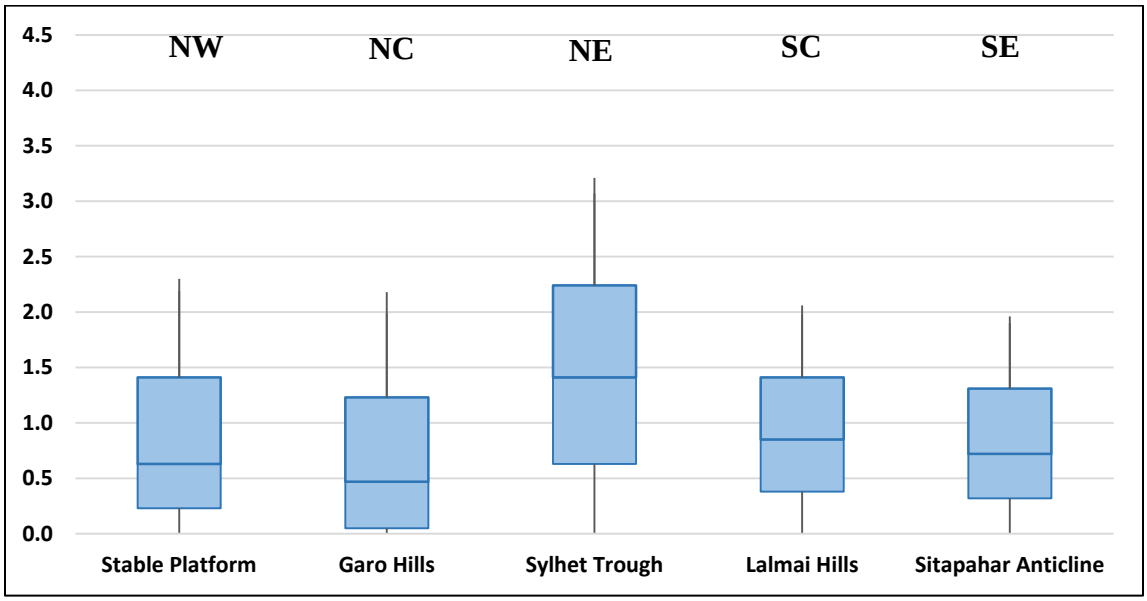

Fig. 4.11 Ratios of plagioclase feldspar to total feldspar (P/F) in the Dupi Tila sandstones from various regions of the Bengal basin, showing distribution of feldspar ratios for each area samples (NW- Northwest, NC- North-central, NE- Northeast, SC- South-central, and SE- Southeast).

Due to the uplift of the Himalayas followed by erosion, voluminous siliciclastic sediments were funneled into the Bengal basin. The Indo-Burman ranges to the east also contributed detritus to the Bengal basin (Uddin and Lundberg, 1988a). Sediment compositions from the Bengal basin from Oligocene to Pliocene-Pleistocene show a temporal increase in higher-grade metamorphic lithic fragments derived from the orogens

(Uddin and Lundberg, 1998b). The Dupi Tila Formation has significant amounts of untwinned potassium feldspars (Uddin et al., 1998b) compared to the plagioclase-rich Miocene sandstones of the Surma Group. This suggests a plutonic source for Dupi Tila Formation, and/or an increase in mechanical weathering relative to chemical weathering in the source areas during the Pliocene-Pleistocene (Mack, 1978). Miocene leucogranites of the High Himalayan Crystalline terrane (France-Lanord et al., 1993) may be a principal source of these feldspars (Harrison et al., 1997; and many others).

Based on the Basu et al., 1975 diamond diagram, the Dupi Tila Formation sourced from low, middle and upper rank metamorphic rocks. Most quartz grains exhibit undulatory extinction. In the Stable Platform region, most samples fall into middle and upper-rank metamorphic rock fields (Fig. 4.12).

Based on the immature subangular to angular grain shapes and compositional analyses, a proximal source is suggested. The Pliocene-Pleistocene Dupi Tila Formation is most likely derived from the Himalayas and the Indo-Burman ranges.

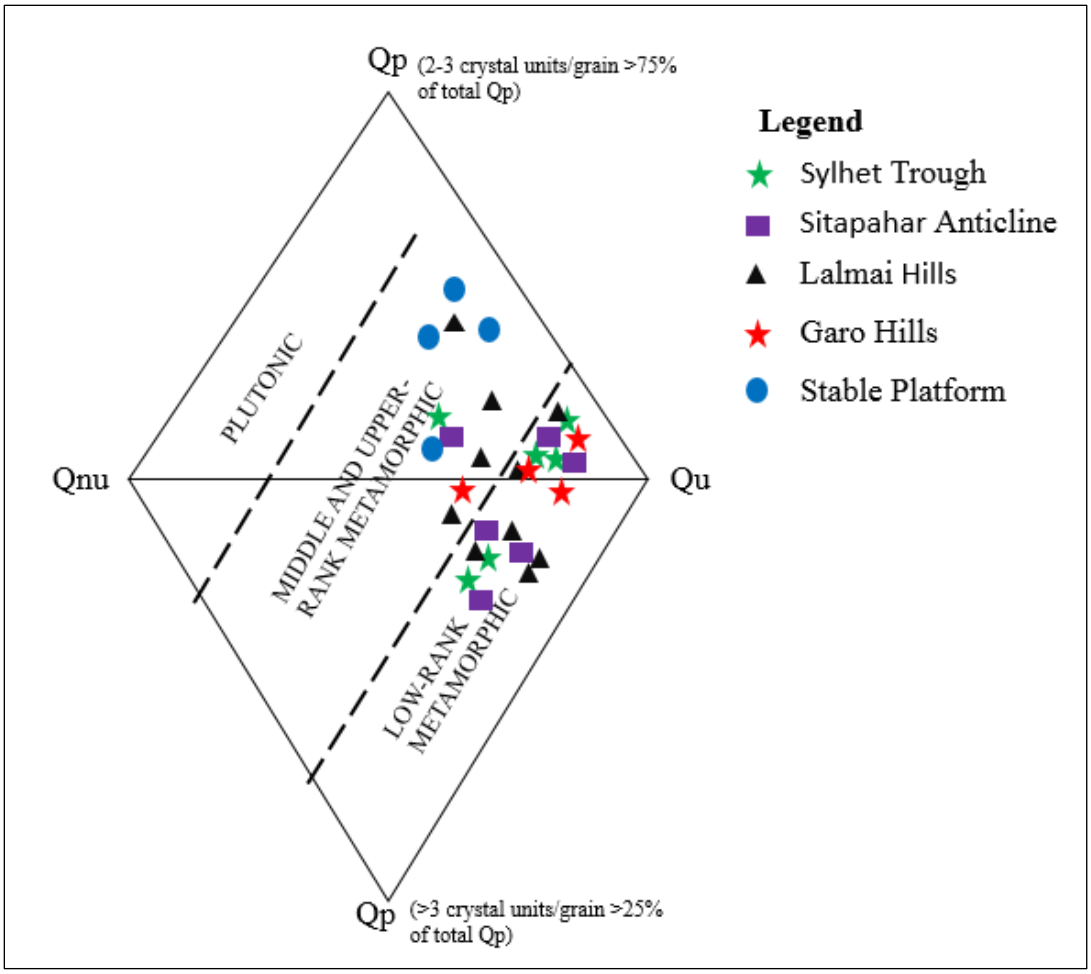

Fig. 4.12 Diamond diagram plots of the Dupi Tila sandstone samples from the different regions of the Bengal basin, Bangladesh (based on Basu et al., 1975).

Chapter 5: HEAVY MINERAL ANALYSIS

5.1 INTRODUCTION

This study reports semi-quantitative analyses of heavy minerals, i.e., those having a specific gravity of 2.9 or higher (Morton, 1985; Tucker, 1988). Although heavy-mineral assemblages are greatly controlled by provenance, they are also influenced by other extrabasinal and intrabasinal factors such as weathering, transport, deposition, and diagenesis (Morton and Hallsworth, 1999). Many heavy minerals are indicative of particular source rocks and, thus, are commonly used in foreland-basin studies (Najman et al., 2008; Garzanti et al., 2007; Uddin et al., 2007). Because they are generally resistant enough to endure transport, heavy minerals are generally sensitive indicators of the nature of provenance. Over thirty common translucent detrital mineral species can be used as provenance indicators (Mange and Maurer, 1992; Morton and Hallsworth, 1999).

Heavy mineral analysis has been used widely in provenance studies of siliciclastic rocks. Studies of sediment composition can help constrain source-rock lithology. Common minerals (like quartz and feldspars) that constitute the bulk sediment composition are contributed by a variety of rocks. However, many heavy minerals are restricted to specific source rocks. Thus, heavy mineral suites can provide clues to decipher provenance lithology (Mandal, 2009; Chowdhury, 2014). Different sources within the same tectonic setting even can be distinguished by heavy mineral analyses (Morton, 1985; Najman and Garzanti, 2000; Garzanti et al., 2007).

Among the large variety of heavy mineral species found in sandstones, approximately thirty are used in source-rock identification (Morton, 1985; Mange and Maurer, 1992). Heavy mineral assemblages are generally resistant enough to endure transport (Morton and Hallsworth, 1999; Uddin et al., 2007). Several sedimentary processes such as weathering of source rock, mechanical breakdown, and hydraulics during transportation,

alluvial storage, and burial diagenesis may change the original relative abundances of heavy mineral assemblages (Morton, 1985; Morton and Hallsworth, 1999). However, some minerals are more stable (Table 7), including apatite, TiO_2 polymorphs (rutile, anatase, and brookite), tourmaline, and zircon (Morton, 1986, Mange and Maurer, 1992; Morton and Hallsworth, 1999).

Table 7. Relative stability of minerals with similar hydraulic and diagenetic behaviors (stability increases towards the top part of the table).

Stability in weathering profiles (Grimm, 1973; Bateman and Catt, 1985; Dryden and Dryden, 1946)	Mechanical stability during transport (Freise, 1931)	Burial persistence North Sea (Morton, 1984, 1986)	Chemical weathering (Pettijohn, 1941)
Zircon, Rutile Tourmaline, Andalusite, Kyanite, Staurolite Garnet Epidote Calcic Amphibole Clinopyroxene Orthopyroxene Apatite	Tourmaline Corundum Chrome-spinel Spinel Rutile Staurolite Augite Topaz Garnet Epidote Apatite Zircon Kyanite Olivine Andalusite Diopside Monazite	Apatite, Monazite, Spinel, TiO2 minerals, Tourmaline, Zircon Chloritoid, Garnet Staurolite Kyanite Titanite Epidote Calcic Amphibole Andalusite Sillimanite Pyroxene Olivine	TiO_2 minerals Zircon Tourmaline Sillimanite Andalusite Kyanite Staurolite Topaz Titanite Monazite Garnet Epidote Calcic amphibole Orthopyroxene Clinopyroxene Olivine Apatite

Morton and Hallsworth (1999) proposed the method of varietal studies of heavy minerals that focus on the relative abundances of more stable species (i.e., those that are less impacted by diagenesis and hydraulic behavior). Determination of relative proportions of specific minerals that behave in a similar way during diagenesis and

transportation can be very useful (Morton and Hallsworth, 1999). Several mineral ratios and indices have been proposed by Morton and Hallsworth (1999). These include ATi (apatite and tourmaline index), GZi (garnet and zircon index), CZi (chrome spinel and zircon index), MZi (monazite, zircon index), and RZi (TiO_2 group and zircon ratio). However, these methods are not applicable if the rock unit does not contain abundant heavy minerals. In the absence of full suites of heavy minerals, analyses can be accomplished by determining the relative abundance of all important heavy mineral species preserved in each stratigraphic unit, recognizing dominant members of mineral groups, and establishing index minerals from different stratigraphic levels (Peavy, 2008; Rahman, 2008; Alam, 2011; and Chowdhury, 2014)).

Semi-quantitative analyses of heavy mineral assemblages in the representative Dupi Tila sandstones from various regions from the Bengal basin were performed in order to assess source-rock types and to help reconstruct paleogeography of the northeastern Himalayas.

5.2 RESULTS

Semi-quantitative point-counting results for heavy minerals in the Dupi Tila sandstones from the different part of the Bengal basin are presented in Table 8. Total heavy mineral contents vary from 0.02 to 1.4% (average = 0.08%). Samples from the Sitapahar anticline (KS samples) and Sylhet Trough (SS samples) have higher heavy mineral contents than samples from other parts of the Bengal basin. Percentage and average frequency of distribution of heavy minerals are plotted on bar diagrams in figures 5.1-5.2. The opacity of the samples decreases with decreasing magnetic susceptibility for all samples (Table 4). Opaque minerals recognized in the present study are mostly oxides and hydroxides of iron (e.g., magnetite, pyrrhotite, hematite, limonite and ilmenite). Similar varieties of opaque minerals were also observed in the Dupi Tila sediments, but they are relatively sparse. Percentages of opaque mineral assemblages in the Garo hills section are notably higher than those for other samples from the basin. Highly stable minerals (e.g., zircon, tourmaline, and rutile) are significantly more abundant in the Lalmai hills. The order of dominance of heavy minerals in the Dupi Tila

Formation, from high to low is- opaque minerals, garnets, sillimanite, tourmaline, kyanite, andalusite, epidote group, chlorite & chloritoid, and staurolite.

Table 8. Normalized abundances of heavy minerals in the Dupi Tila Formation from various locations of the Bengal basin, Bangladesh.

Sample No	SS-2		SS-4		SS-11		BS		NWD	
Location	Sylhet Trough						Garo hills		Stable Platform	
Heavy Minerals	No. of grains	Percentage	No. of grains	Percentage	No. of grains	Percentage	No. of grains	Percentage	No. of grains	Percentage
Zircon	4	2.41	2	1.13	2	1.18	2	1.37	2	1.04
Rutile	1	0.60	2	1.13	3	1.76	3	2.05		
Tourmaline	16	9.63	13	7.34	21	12.35	5	3.42	16	8.29
Garnet	25	15.06	31	17.51	15	8.82	13	8.90	17	8.80
Apatite	5	3.01			2	1.18			5	2.59
Epidote	5	3.01	4	2.26	3	1.76	1	0.68	7	3.63
Hornblende	3	1.81	6	3.39	5	2.94	2	1.37	5	2.59
Tremolite					3	1.76			4	2.08
Actinolite	3	1.81	1	0.56	5	2.94			6	3.12
Chloritoid + Chlorite	1	0.60	3	1.69	2	1.18	6	4.11	11	5.70
Biotite			1	0.56			3	2.05	2	1.04
Staurolite	5	3.01	4	2.26	1	0.59	4	2.74	6	3.12
Sillimanite	13	7.83	16	9.04	11	6.47	14	9.59	32	16.58
Kyanite	2	0.60	6	3.39	6	1.76	2	1.37	4	2.08
Andalusite	1	1.20	3	1.69	3	3.53			11	5.70
Muscovite	3	1.81								
Pyroxenes	3	1.81	7	3.95	6	3.53			9	4.66
Opaque	76	45.78	78	40.07	82	48.24	91	62.2	56	29.12
Total	166	100	177	100	170	100	146	100	193	100
Other heavy minerals	clinozoisites, xenotine, monazite						anhydrite, beryl		phengite	

Table 8. (Cont.) Normalized abundances of heavy minerals in the Dupi Tila Formation from various locations of the Bengal basin, Bangladesh.

Sample No	KS-2		KS-4		CCS		CWSalLDT		NWR	
Location	Sitapahar anticline				Lalmai hills				Stable platform	
Heavy Minerals	No. of grains	Percentage	No. of grains	Percentage	No. of grains	Percentage	No. of grains	Percentage	No. of grains	Percentage
Zircon	4	1.44	4	1.82	6	2.74	4	1.89	2	1.06
Rutile	6	2.17	2	0.91	8	3.65	11	5.19	6	3.17
Tourmaline	10	3.61	12	5.45	14	6.39	14	6.60	6	3.17
Garnet	32	11.55	18	8.18	21	9.59	17	8.02	26	13.76
Apatite	4	1.44			2	0.91	3	1.42	4	2.12
Epidote	12	4.33	14	6.36	6	2.74	4	1.89	6	3.17
Hornblende	12	4.33	7	3.18	4	1.83	7	3.30	1	0.53
Tremolite	6	2.17	6	2.73	2	0.91	4	1.89		
Actinolite	8	2.89	2	0.91	3	1.37	6	2.83	3	1.59
Chloritoid + Chlorite	15	5.42	16	7.27	6	2.74	2	0.94	9	4.76
Biotite			2	0.91	4	1.83	1	0.47		
Staurolite	18	6.50	7	3.18	6	2.74	2	0.94	6	3.17
Sillimanite	8	2.89	14	6.36	26	11.87	35	16.51	27	14.29
Kyanite	14	2.17	16	1.82	7	3.20	14	6.60	12	6.35
Andalusite	6	5.05	4	7.27	11	5.02	4	1.89	8	4.23
Muscovite									3	1.59
Pyroxenes	25	9.03	18	8.18	13	5.92	17	8.02	8	4.23
Opaque	97	35.02	78	35.45	80	36.53	67	31.60	62	32.80
Total	277	100	220	100	219	100	212	100	189	100
Other heavy minerals	fluorite, beryl, clinozoisites				beryl, xenotine, margarite, leucoxene				phengite	

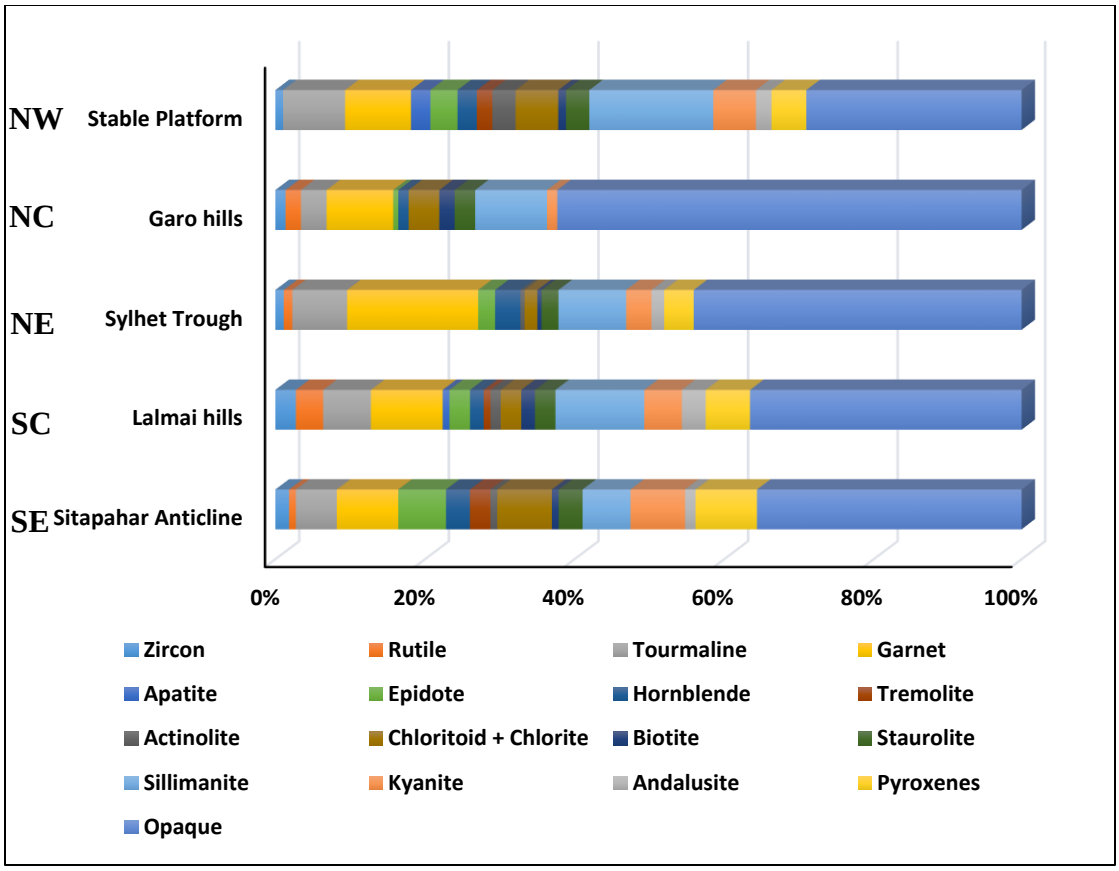

Fig. 5.1 Heavy mineral frequencies in the Dupi Tila Formation samples from various parts of the Bengal basin (NW- Northwest, NC- North-central, NE- Northeast, SC- South-central, and SE- Southeast; mineral color codes are distributed horizontally from left to right in the legend).

Heavy mineral assemblages (SS-2, SS-4, SS-11 thin section; SS-3, SS-5. SS-6, SS-7, SS-8, SS-9, and SS-10 smear slides) from the Sylhet Trough contain 45% opaque minerals, high amounts of aluminosilicates (sillimanite, kyanite, andalusite), and a few stable minerals, especially tourmaline, zircon, rutile (Fig. 5.3B). Other minerals present include garnets, epidote-group minerals, apatite, staurolite, hornblende, actinolite, orthopyroxenes (e.g., hypersthene), clinopyroxenes, and clinozoisite. Among all the sites, Sylhet Trough samples have more garnets (Fig. 5.3A) and tourmalines. Tourmaline grains are angular and has sharp edges in these samples.

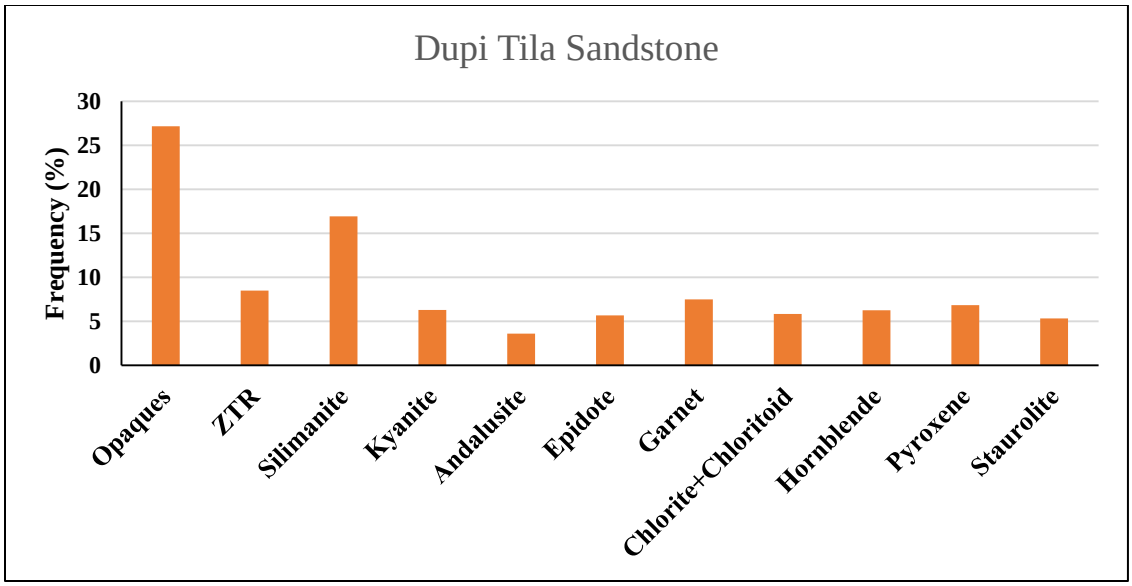

Fig. 5.2 Average heavy mineral frequency in samples of the Dupi Tila Formation combined (ZTR- zircon-tourmaline-rutile).

Heavy mineral assemblages (BS thin section; BS-1, BS-5. BS-6, and BS-8 smear slides) in the Garo hills samples include 60% opaque minerals, and high amounts of garnet and sillimanite. They also contain common tourmaline, chlorite & chloritoid, staurolite, and epidote-group minerals (Fig. 5.4A, B). Anhydrite and beryl also are found in some samples. Tourmaline grains have subangular to subrounded shape in these samples.

Heavy mineral assemblages (CCS, CWSalLDT thin section; CRup-1, CWSal-1, CWSal-4, CLSal-1, Cglau, CWSalo, CCHS-1, CCS-2, CCS-3, and CCS-4 smear slides) in the Lalmai hills samples contain 35% opaque minerals, 10% ZTR stable minerals, garnet, and sillimanite. Other minerals observed include kyanite, andalusite, orthopyroxenes (e.g., hyperthene), epidote-group minerals, chlorite & chloritoid, and staurolite (Fig. 5.5A). The index heavy mineral in the Lalmai hills samples is sillimanite (Fig. 5.5B).

Heavy mineral assemblages (NWD, NWR thin section; NWD-1, NWD-3, NWR-2 and NWR-3 smear slides) from the Stable Platform samples contain 32% opaque minerals, 8% ZTR stable minerals, 12% garnet, 15% sillimanite, and 6% andalusite. Other accessory minerals include epidote-group minerals, apatite, hornblende, chlorite

& chloritoid, kyanite, tremolite, and pyroxenes (Fig. 5.6A). Fibrolite, a sillimanite that crystallizes as fine, parallel or subparallel fibrous needles and interlaced mats of fibers, is considered as the index mineral in the Dupi Tila Formation of Stable Platform samples (Fig. 5.6B).

Heavy mineral assemblages in samples (KS-2, KS-4 thin section; KS-1, KS-3, KS-5, and KS-6 smear slides) from the Sitapahar anticline contain 35% opaque minerals, 12% aluminosilicates, 10% garnets, 8% ZTR stable minerals, 8% pyroxenes, 5% staurolites, and epidote-group minerals. Other minerals observed include chloritoid & chlorite, hornblende, tremolite, fluorite, beryl, and clinozoisite (Fig. 5.7A, B). Tourmaline grains are angular and have sharp edges in this area samples.

Drill core samples from the Stable Platform (NWD and NWR) have high percentages of heavy minerals, whereas Garo hills samples have limited amounts of heavy minerals. Samples from the Sitapahar anticline, Lalmai hills, and Sylhet Trough contain considerably high amounts of heavy minerals. Aluminosilicates are the predominant type of heavy minerals. Sillimanite (fibrolite), kyanite and andalusite are found to be abundant in all samples, especially those from the Stable Platform and Lalmai hills.

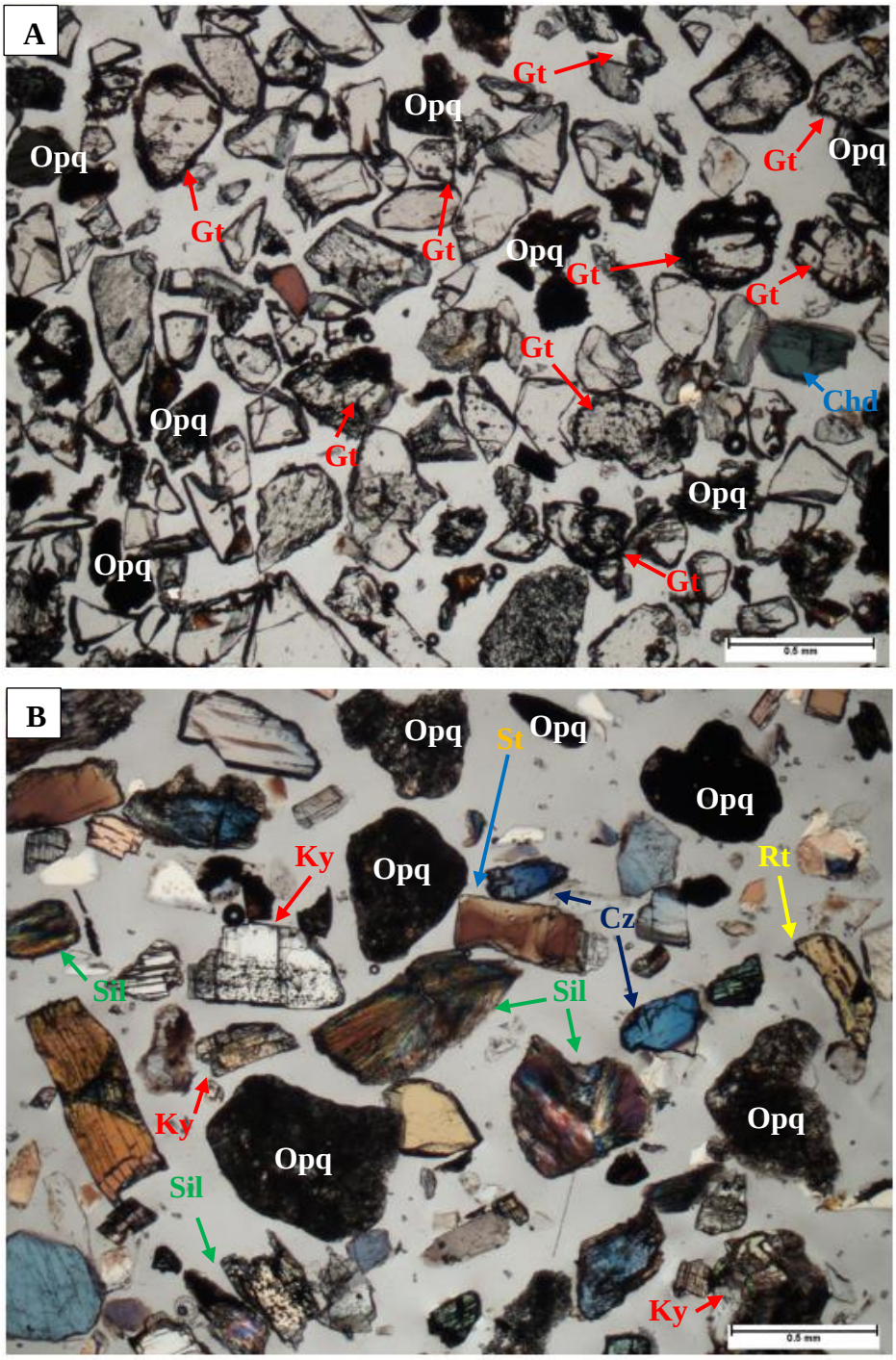

Fig. 5.3 Representative photomicrographs of heavy minerals from the Sylhet Trough, Bengal basin showing (A) garnet and opaque minerals (sample SS-4, fraction B, 10X, plane polar), (B) Aluminosilicates, ZTR and other minerals minerals (sample SS-4, fraction E, 10X, crossed polar) (Ctd= Chloritoid, Gt= Garnet, Ky= Kyanite, Sil= Sillimanite, Rt= Rutile, St= Staurolite, Cz= Clinozoisites, ZTR= Zircon Rutile Tourmaline, Opq= Opaque minerals).

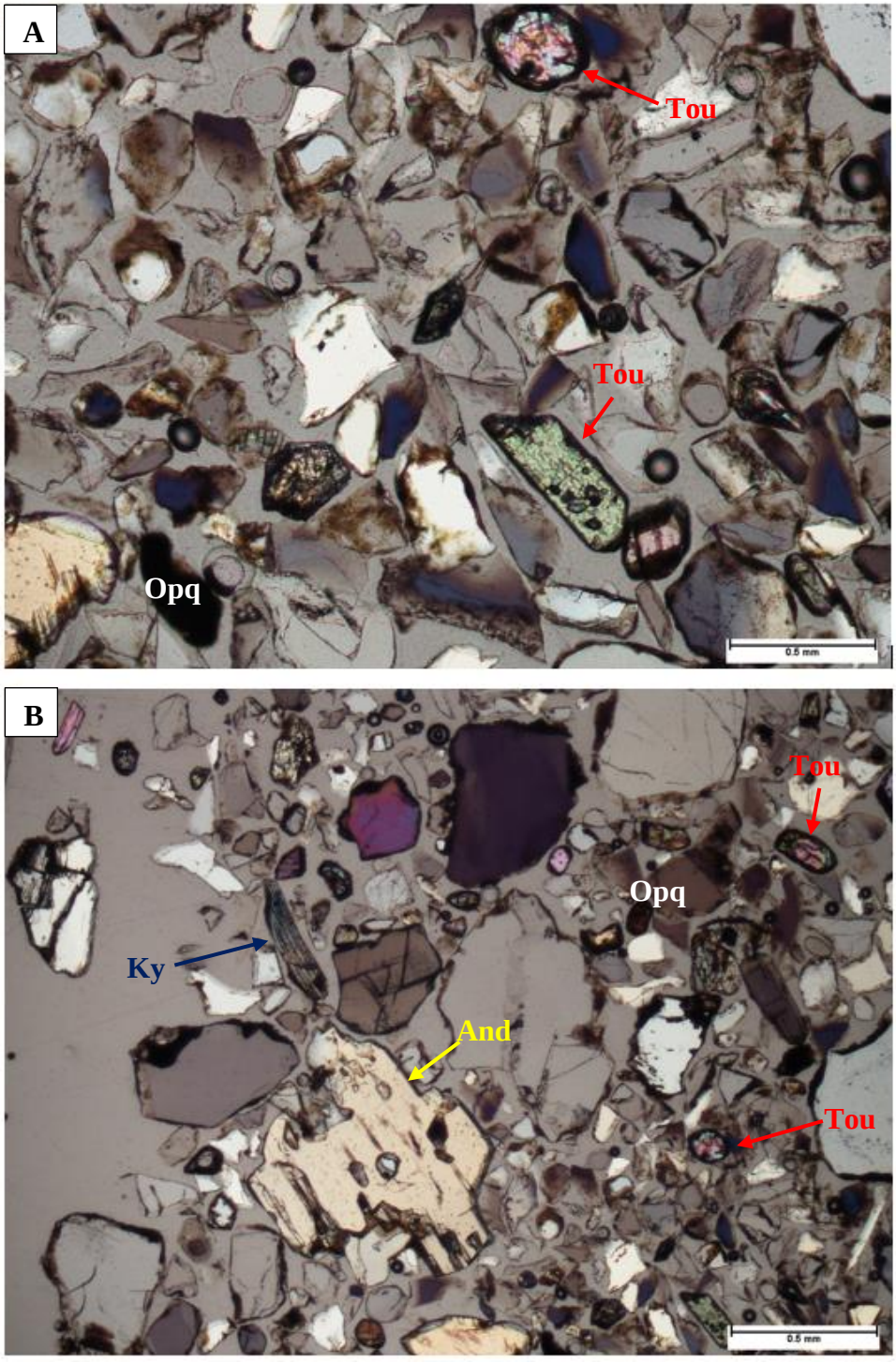

Fig. 5.4 Representative photomicrographs of heavy minerals from the Garo hills, Bijoypur, Netrokona, Bengal basin showing (A) ZTR minerals (sample BS, fraction C, 10X, crossed polar), (B) Aluminosilicates, ZTR and other minerals (sample BS, fraction E, 10X, crossed polar) (ZTR= Zircon Rutile Tourmaline, Tou= Tourmaline, Ky= Kyanite, And= Andalusite, Opq= Opaque minerals).

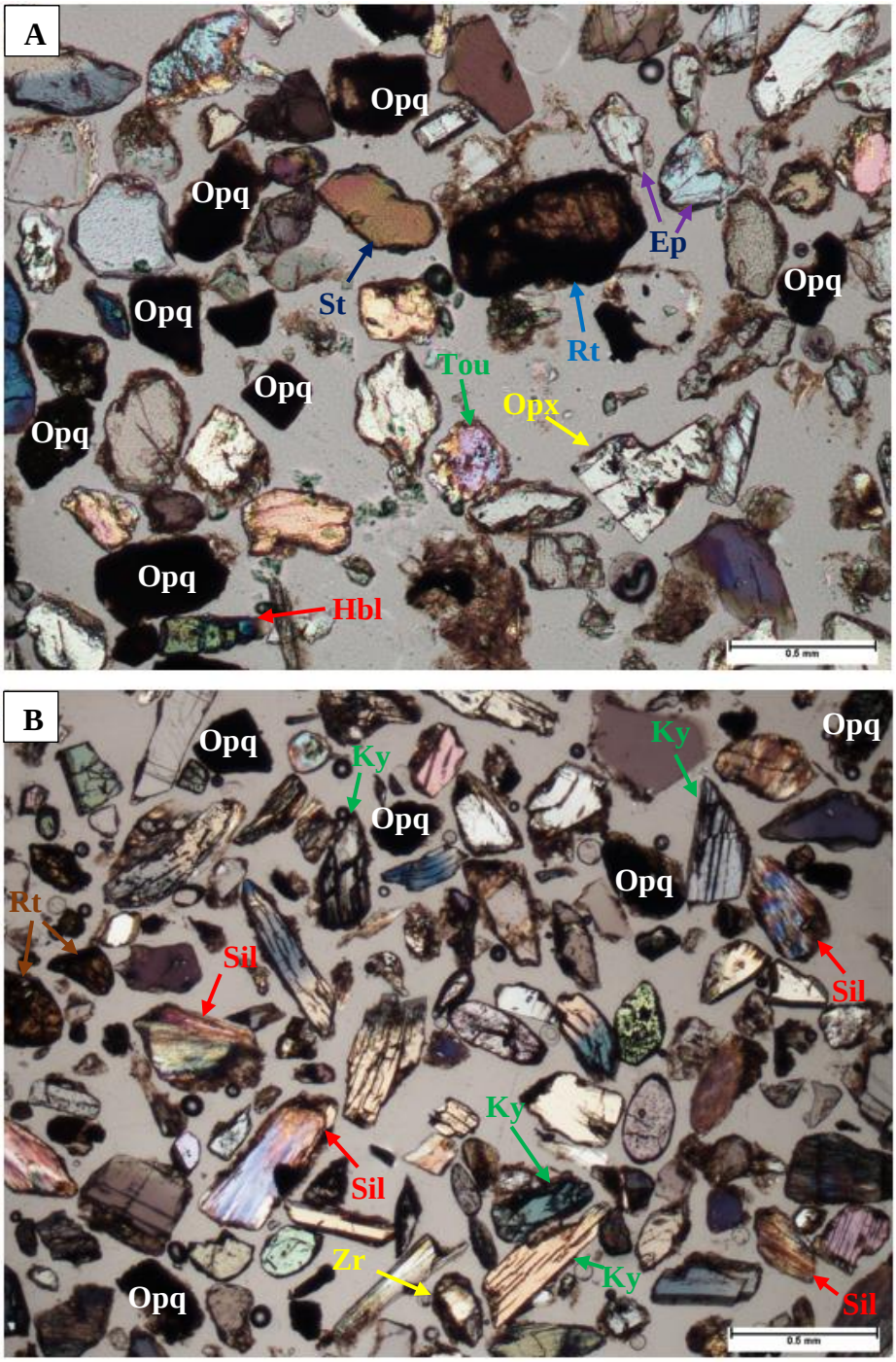

Fig. 5.5 Representative photomicrographs of heavy minerals from the Lalmai hills, Comilla, Bengal basin showing (A) heavy and opaque minerals (sample CCS, fraction C, 10X, crossed polar), (B) Aluminosilicates, ZTR, and other minerals (sample CLDT, fraction E, 10X, crossed polar) (Ky= Kyanite, Sil= Sillimanite, Opq= Opaque minerals, Zr= Zircon, Rt= Rutile, Hbl= Hornblende, St= Staurolite, Ep= Epidote, Opx= Orthopyroxene, Tou= Tourmaline).

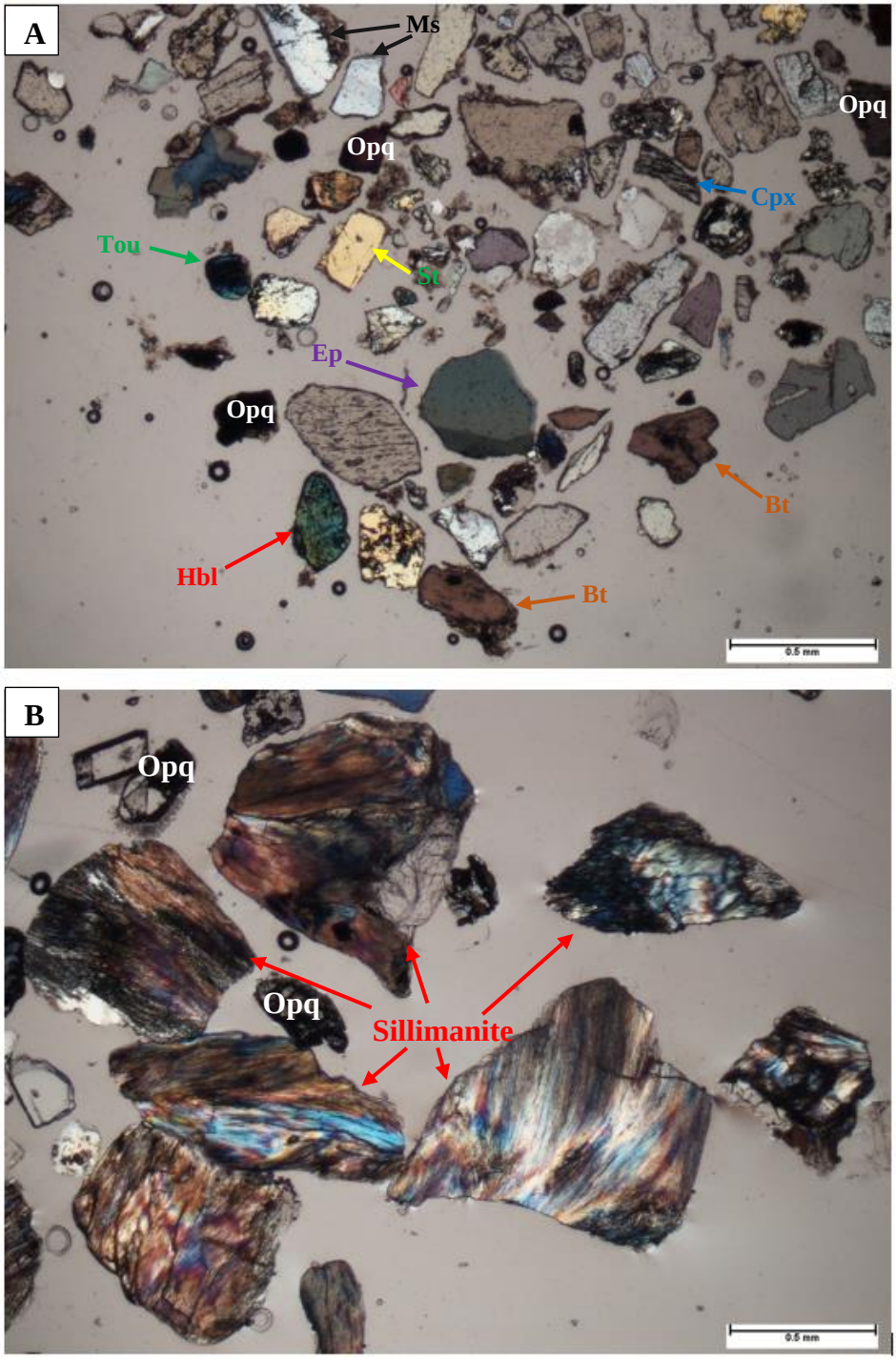

Fig. 5.6 Representative photomicrographs of heavy minerals from the northwest Stable Platform, Bengal basin showing (A) heavy and opaque minerals (sample NWR, GDH-69, fraction C, 10X, crossed polar), (B) Aluminosilicates, Sillimanite/ fibrolitic sillimanite (sample NWD, GDH-56, fraction E, 10X, crossed polar) (Ky= Kyanite, Sil= Sillimanite, St= Staurolite, Bt= Biotite, Tou= Toumaline, Hbl= Hornblende, Cpx= Clinopyroxene, Ms= Muscovite, Opq= Opaque minerals).

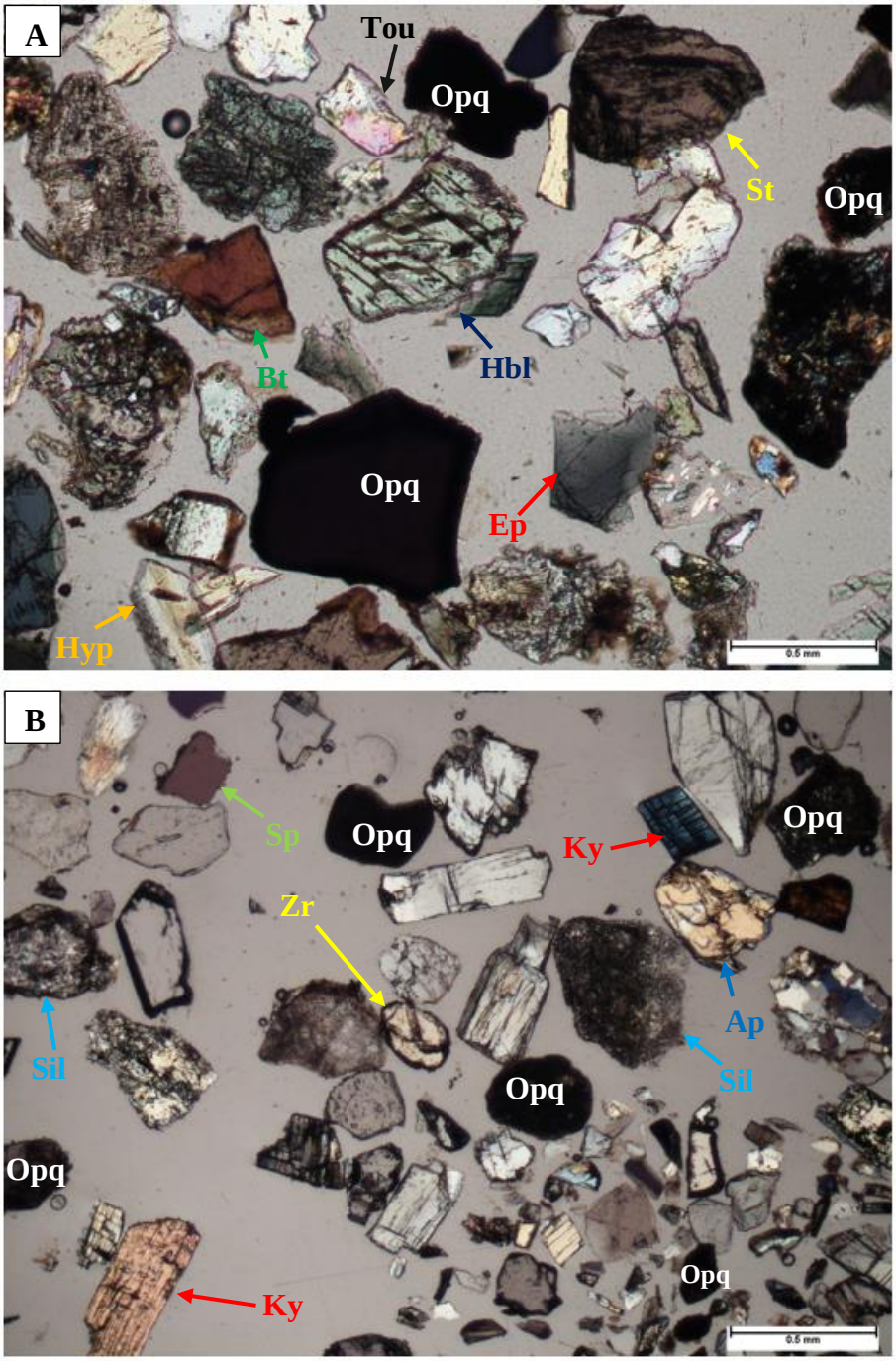

Fig. 5.7 Representative photomicrographs of heavy minerals from the Sitapahar anticline, Kaptai, Chittagong, Bengal basin showing (A) heavy and opaque minerals (sample CCS, fraction C, 10X, crossed polar), (B) Aluminosilicates, ZTR, and other minerals (sample CLDT, fraction E, 10X, crossed polar) (ZTR= Zircon Rutile Tourmaline, Ky= Kyanite, Sil= Sillimanite, Opq= Opaque minerals, Ep= Epidote, Bt= Biotite, Hbl= Hornblende, Zr= Zircon, St= Staurolite, Tou= Tourmaline, Hyp= Hypersthene, Sp= Sphene, Ap= Apatite).

5.3 PROVENANCE

Studies of the provenance of clastic sediments in sedimentary basins are important in paleogeographic and tectonic reconstructions. Heavy mineral assemblages consisting of ultrastable (zircon, tourmaline, rutile), stable (garnet, apatite, epidote), and unstable (e.g., hornblende) grains mostly indicate different source rocks for the present study. This study also suggests possible paleo-drainage patterns and infers climatic conditions prevailing during deposition of the Dupi Tila Formation.

Garnets dominate in all studied samples of the studied Dupi Tila Formation except in the Garo hills region (Fig. 5.8). Variations in garnet abundances in vertical sequences also are observed, and these may reflect temporal changes in source rock. The Dupi Tila Formation contains significant amount of ultrastable heavy minerals (ZTR). Tourmaline is the predominant of ultrastable minerals (Fig. 5.9). The 'ZTR index', which is the combined percentage of zircon, tourmaline, and rutile among the transparent heavy minerals, is a useful tool to quantify mineralogical maturity in heavy mineral suits (Hubert, 1962). Considerable textural immaturity, subangular to subrounded nature of detrital grains, suggest a short transport distance along a pathway of low relief. Also, tourmaline grains are not polycyclic, indicating a crystalline source (Krynine, 1946).

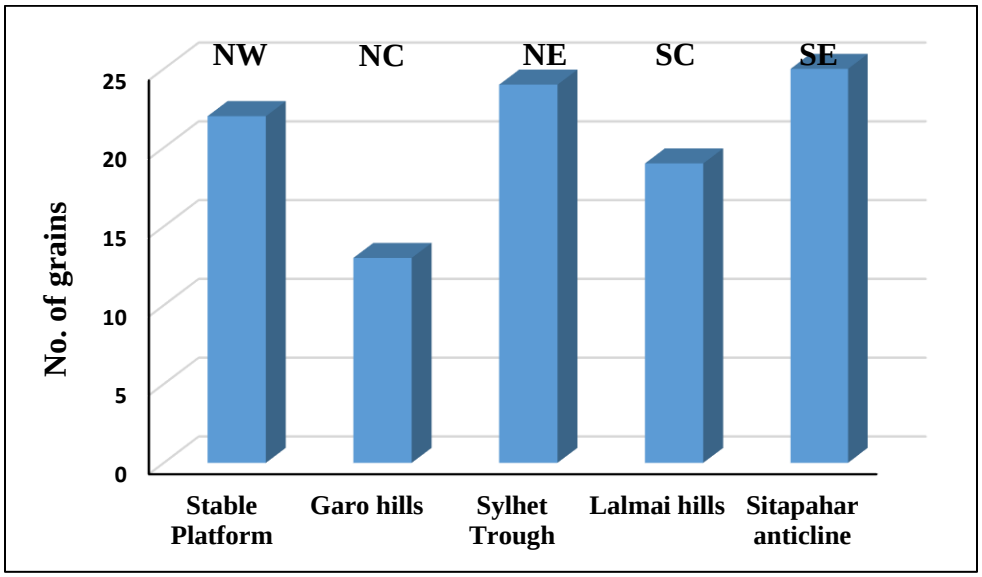

Figure 5.8 Variation in distribution of garnets in the Dupi Tila samples collected from different parts of the Bengal basin, Bangladesh (NW- Northwest, NC- North-central, NE- Northeast, SC- South-central, and SE- Southeast).

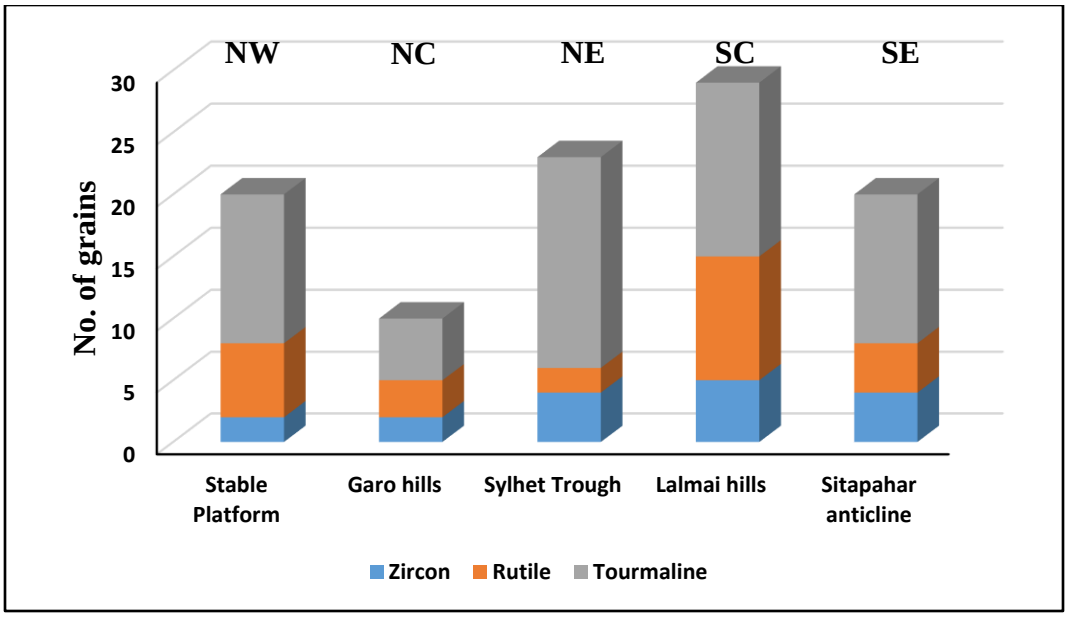

Figure 5.9 Variation in distribution of ZTR minerals in the Dupi Tila samples collected from different parts of the Bengal basin, Bangladesh (ZTR= Zircon Rutile Tourmaline; NW- Northwest, NC- North-central, NE- Northeast, SC- South-central, and SE- Southeast).

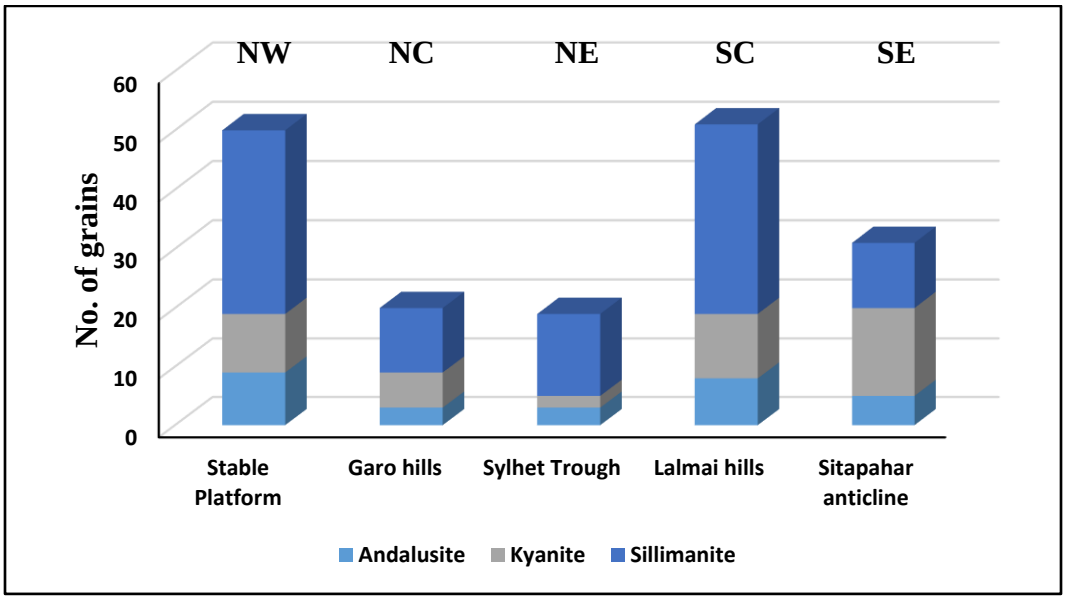

Figure 5.10 Variation in distribution of aluminosilicates in the Dupi Tila samples collected from different parts of the Bengal basin, Bangladesh (NW- Northwest, NC- North-central, NE- Northeast, SC- South-central, and SE- Southeast).

The Dupi Tila Formation from different regions of the Bengal basin has a substantial amount of aluminosilicates. Sillimanite is the predominant mineral throughout the basin,

especially in the Stable Platform and Lalmai hills area (Fig. 5.10). Sillimanite and kyanite intergrowths are observed in the Sitapahar anticline area.

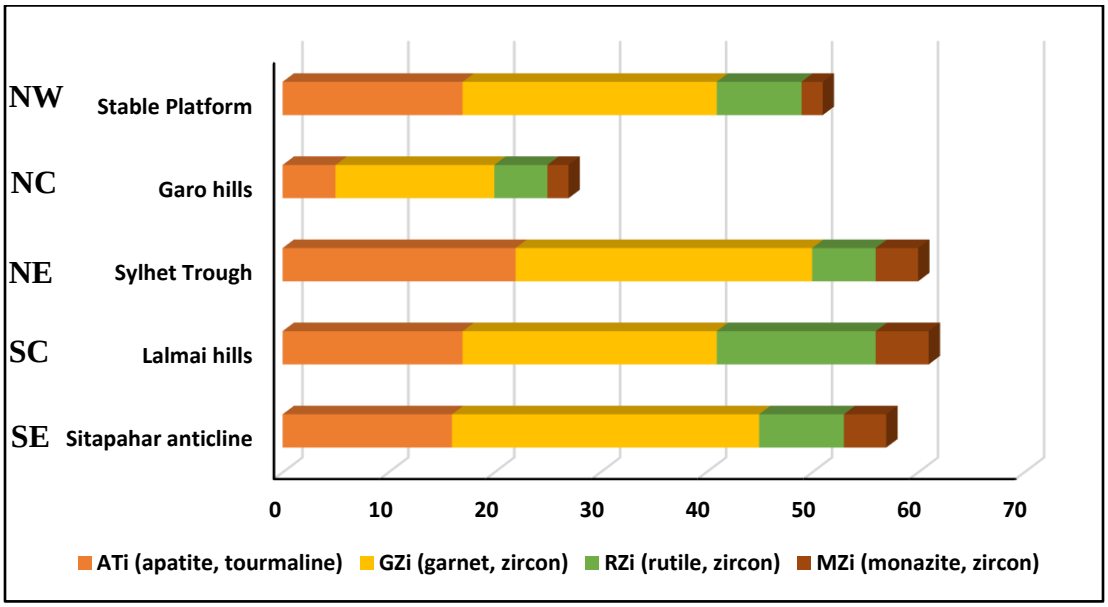

Figure 5.11 Plots of ATi (apatite, tourmaline), GZi (garnet, zircon), ATi (apatite, tourmaline), RZi (rutile, zircon), and ATi (apatite, tourmaline), MZi (monazite, zircon) indices of Dupi Tila samples collected from different parts of the Bengal basin, Bangladesh (NW- Northwest, NC- North-central, NE- Northeast, SC- South-central, and SE- Southeast).

Ratios of highly stable mineral indices also suggest variations in sources among the study areas. The Dupi Tila Sandstone samples plot in five different localities on the GZi to ATi, RZi to ATi, and MZi to ATi stacked bar diagrams (Fig. 5.11) showing the Garo hills are different from the other localities. ATi and GZi indices are higher in the Sylhet Trough samples, whereas RZi and MZi indices are higher in the Lalmai hills samples.

All these observations suggest that sediments of the Dupi Tila Formation were derived from an orogenic source. The relative abundance of aluminosilicates and related heavy minerals in the Dupi Tila Formation throughout the Bengal basin reflect unroofing of deeper crustal levels in the eastern Himalaya. Sillimanite (fibrolites) crystallizes during high-temperature metamorphism and occurs in sillimanite-cordierite gneiss and biotite-sillimanite hornfels, indicating the samples are sourced from high-grade regional metamorphic protoliths. Andalusite occurs chiefly in metamorphic rocks that usually forms in high temperature and low-pressure regimes (< 4Kbar). Due to high heat from

magmatic plutons in relatively low burial depth country rocks turned into metamorphic rocks, indicating the samples are sourced from high-grade contact or regional metamorphic protoliths (Visona et al., 2012).

Mountain building in the eastern Himalaya and Indo-Burman ranges was significant and the orogenic fronts were presumably encroaching on the basin from the north and east by Pliocene-Pleistocene time (Uddin and Lundberg, 1998a; Uddin et al., 2007). Orthopyroxenes, especially abundant hypersthene, further suggest unroofing and erosion of high-pressure mafic rocks, including ophliolites in both the Himalayas and the Indo-Burman ranges.

Chapter 6: MICROPROBE ANALYSIS

6.1 INTRODUCTION

In addition to studying overall heavy mineral suites, provenance analysis of clastic sediments also can be facilitated by chemical analyses of specific heavy mineral species (e.g., garnet, zircon, tourmaline, rutile, ilmenite, chlorite, spinel, etc.), the compositions of which are related to the formative conditions of their parent rocks (Morton and Taylor, 1991). Density and stability (both chemical and mechanical) variations among different heavy minerals may obscure the signature of the source. Reliability of provenance interpretation can be increased greatly by eliminating or reducing these variations. Density and stability of a specific mineral species are relatively homogeneous. Thus, varieties of key minerals present in a sedimentary unit are independent of influences such as hydrodynamic sorting and diagenesis. Hence, they can provide a more reliable guide to provenance than the simple presence/absence or relative abundance of different mineral species.

Interpretation of provenance is considerably enhanced by determining the composition of individual detrital grains. The advancement of the electron microprobe made it possible to determine compositional variations in particular species of a heavy mineral accurately and quickly. Electron microprobe analysis provides a complete micrometer-scale quantitative chemical analysis of inorganic solids. To constrain provenance, the chemical composition of selected detrital heavy-mineral grains (i.e., potentially garnet) were assessed via microprobe analysis. Microprobe analysis of ten samples was carried out in the Central Analytical Facility of the University of Alabama in Tuscaloosa, AL under the supervision of Robert Holler.

6.2 MINERAL CHEMISTRY

Specific heavy minerals, such as garnet, epidote, chloritoid, chrome-spinel, and amphibole, have been used by previous workers to determine provenance of sediments (Morton, 1985; Henry and Dutrow, 1990; Morton and Taylor, 1991; Nanayama, 1997; Kumar, 2004; Zahid, 2005; Rahman, 2008).

In this study, five mineral groups (garnet, tourmaline, epidote, chloritoid and ilmenite) were subjected to microprobe analysis. Compositional variations in their mineral chemistry can be used to discriminate various source rocks (Enami and Banno, 1980; Chopin and Schreyer, 1983; Morton, 1985; Darby and Tsang, 1987; Henry and Guidotti, 1985; Henry and Dutrow, 1990; Morton and Taylor, 1991; Nanayama, 1997).

Garnet is commonly found in a variety of metamorphic rocks, as well as in plutonic igneous rocks, pegmatites, and some volcanic igneous rocks (Mange and Maurer, 1989). The chemical formula of garnet is $[X_3Y_2(SiO_4)_3]$, where X is replaced by bivalent cations like Fe^{2+}, Mg^{2+}, Ca^{2+}, or Mn^{2+}, and Y is replaced by trivalent cations like Al^{3+}, Fe^{3+} or Cr^{3+}. The specific cations in the garnet structure can be related to the type of source rocks. The ratio of $(Fe^{2+} + Mg^{2+}) / (Ca^{2+} + Mn^{2+})$ in the garnet structure increases with the degree of metamorphism in metamorphic source terranes (Sturt, 1962; Nandi, 1967).

Tourmaline can be found in various rock types as a common accessory mineral (Henry and Guidotti, 1985). The general formula of tourmaline is $XY_3Z_6(BO_3)Si_6O_{18}(OH)_4$, where X is occupied by Na^+ and/or Ca^{2+}, Y is occupied by Mn^{2+}, Fe^{2+}, Al^{3+}, Li^{2+}, and/or Mg^{2+}, and Z is occupied by Al^{3+}, Cr^{3+}, Mn^{2+} and/or Mg^{2+} (Deer et al., 1992). Tourmaline occurs in granites, granite pegmatites, and in contact- or regionally metamorphosed metamorphic rocks (Mange and Maurer, 1989). End-member calculations of tourmaline chemistry can help in distinguishing source rock types. Previous workers have used Al-Fe (tot)-Mg and Ca-Fe (tot)-Mg plots for provenance analysis (e.g., Henry and Guidotti, 1985; Henry and Dutrow, 1992; Kumar, 2004; Zahid, 2005; Rahman, 2008; Sitaula, 2009; Alam, 2011).

The ratio of $Fe^{3+}/ (Al+Fe^{3+})$ in epidote group minerals can help to distinguish source rock and its temperature conditions (Enami and Banno, 1980, Nanayama, 1997).

Variations in the chemical composition of chloritoid are generally defined by variations in the abundance of Fe, Mg, and Mn (Morton, 1991), which reflect different source-rock types (Chopin and Schreyer, 1983). Ilmenite chemistry is a viable approach to determine provenance for sands in a depocenter along with heavy mineral suites, quartz types, and Fourier analysis of grain shape (Darby and Tsang, 1987).

6.3 ELECTRON MICROPROBE

The electron probe microanalyzer (EPMA) provides a complete micron-scale quantitative chemical analysis of solids. This method utilizes characteristic x-rays excited by an electron beam incident on a flat surface of the sample. As the electron beam hits the surface of grains it responses in two different ways. Some of the beam electrons will be scattered backward. These backscattered electrons carry information about chemical composition of the grain. Backscattered electrons are a result of multiple elastic scattering and have energies between 0 and E0 (the beam energy). When the electron beam hits the sample, it loses some energy, which is received by the electrons in the outer shell of atoms of the sample. By receiving this energy, electrons in the sample become excited and jump from one shell to another and emit a certain amount of energy. This emitted energy (thrown by the sample electrons) is related to chemical composition. Some secondary electrons are also mobilized by the beam through inelastic scattering. These electrons have energies in the range 0-50 eV with a most probable energy of 3-5 eV. Different detector setups are required to detect different types of signals as there are energy differences between backscattered X-rays and secondary electrons.

EPMA provides a complete quantitative chemical analysis of solid materials, as well as high-resolution scanning electron and scanning x-ray images (concentration maps). There are two types of scanning electron images: backscattered electron (BSE) images and secondary electron (SE) images. BSE images show compositional contrast, while SE images show enhanced surface and topographic features.

A JEOL 8600 microprobe at the Central Analytical Facilities in the University of Alabama was used for this study. The probe is automated by Geller Micro analytical laboratory dQANT automation and uses an accelerating voltage of 15 KV and a beam

current of 15 nano amps. Both natural and synthetic standards were used to calibrate the data.

6.4 STANDARD INTENSITY CALIBRATION

Appropriate standards were chosen to obtain standard X-ray intensities of the substances measured during microprobe analysis. Different standards were used for different substances. Secondary standards were analyzed as unknowns to check if their known compositions are reproduced. Analytical conditions (e.g., accelerating voltage, beam current, etc.) were maintained throughout the session.

The standards used for this analysis are listed in Table 9. Most of them come from the C. M. Taylor Corp. The USNM standards come from the National Museum of Natural History, a branch of the Smithsonian Institution. This study used two synthetic standards obtained from the University of Oregon microprobe lab, and an almandine standard obtained from the Harvard Mineral Museum. Calibration for each analytical session was checked using the Kakanui Hornblende (USNM) and Pryope #39 (C. M. Taylor) standards.

Table 9. Electron microprobe standards used for this study.

Electron Microprobe Standards			
Element	Standard	Source	Comment
Cr	Chromite#5	C M Taylor Corp	
Mn	Spessartine#4b	C M Taylor Corp	
TiO_2	Rutile	C M Taylor Corp	
Ca	Sphene# 1A	C M Taylor Corp	
Fe	Hematite# 2	C M Taylor Corp	Used for oxide (spinel) analysis
Fe	Syn. Fayalite Ol-11	Univ. of Oregon	Used for silicate analysis
Ni	Ni metal	C M Taylor Corp	
Si	Diopside 5A	C M Taylor Corp	Si standard for all phases except garnet
Mg	Olivine #1	C M Taylor Corp	
Al	Syn. Spinel	C M Taylor Corp	
K	Orthoclase MAD-10	C M Taylor Corp	
Na	Ameila Albite	USNM	This is a ubiquitous Na Standard
Si	Almandine	Harvard Mineral Museum oxygen standard # 112140	Si standard for garnet analyses
F	Syn. Fluoro-Phologopite	University of Oregon M-6	
Cl	Scapolite	USNM R 6600-1	

6.5 RESULTS

Nine (9) carbon coated multiple-depth polished thin sections (SS-2, SS-4, SS-11, KS-2, KS-4, CCS, CWSaLDT, NWD, and NWR) were subjected to EDS and WDS. Polished thin sections were devided into four quadrants, each containing a different heavy mineral fraction: Group 2; Group 3; Group 4; and Group 4/5 (see Table 4).

Under the supervision of Robert Holler, 315 heavy mineral grains were analyzed. Observed minerals include garnets, tourmalines, sillimanite, kyanite, staurolite, epidote, chloritoid, ilmenite, hornblende, hypersthene, clinopyroxene, apatite, rutile, zircon, sphene, clinozoisite, vermiculite, biotite, muscovite, chlorite, magnetite, and hematite.

Chemical mapping also helped to evaluate element contents in minerals of interest (Fig. 6.1). The EDS spectrum recorded and WDS element weight percentage was recorded (Fig. 6.2)

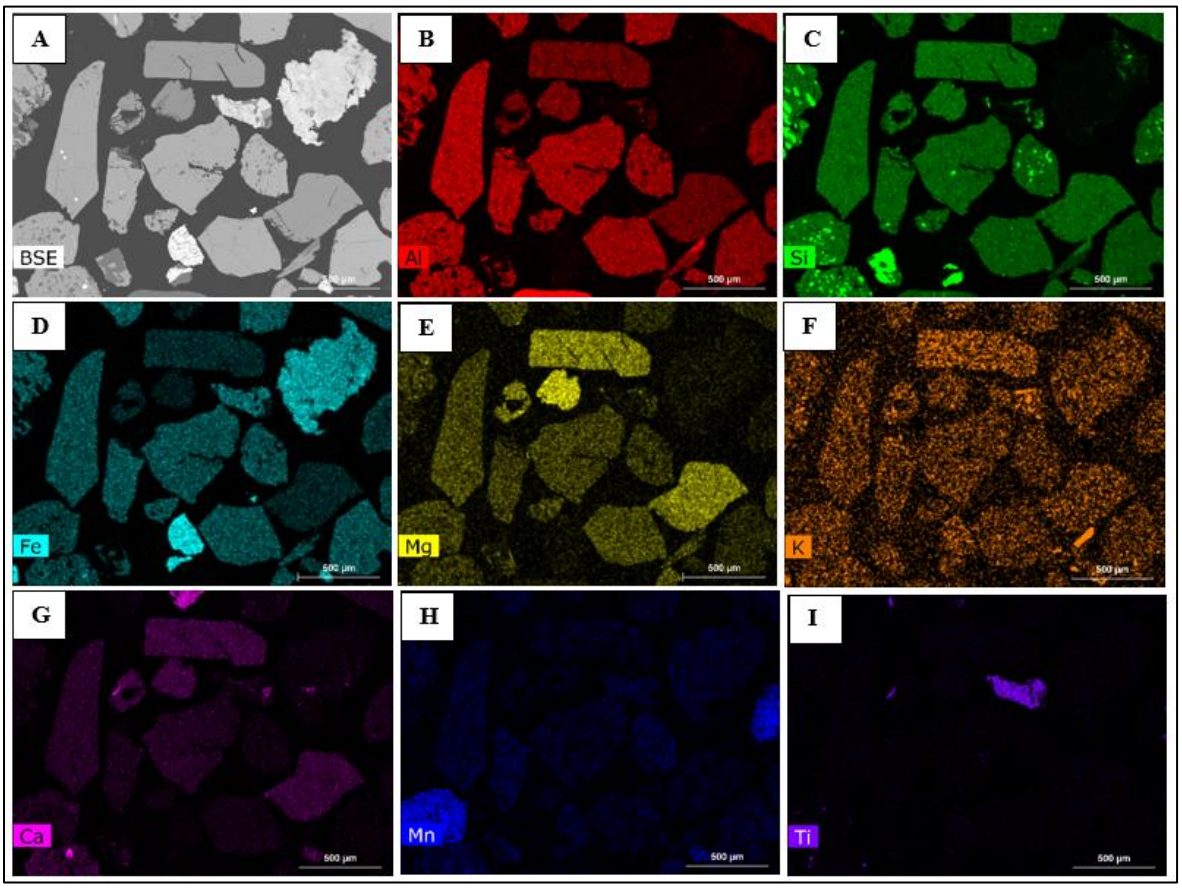

Fig. 6.1 Chemical mapping of mineral grains during spectroscopy showing different element contents on the thin sections, A- BSE image, B-I primary element contents in heavy minerals- B- aluminum, C- silicon, D- iron, E- magnesium, F- potassium, G- calcium, H- manganese, and I- titanium element contents respectively (Sample- NWD, fraction B).

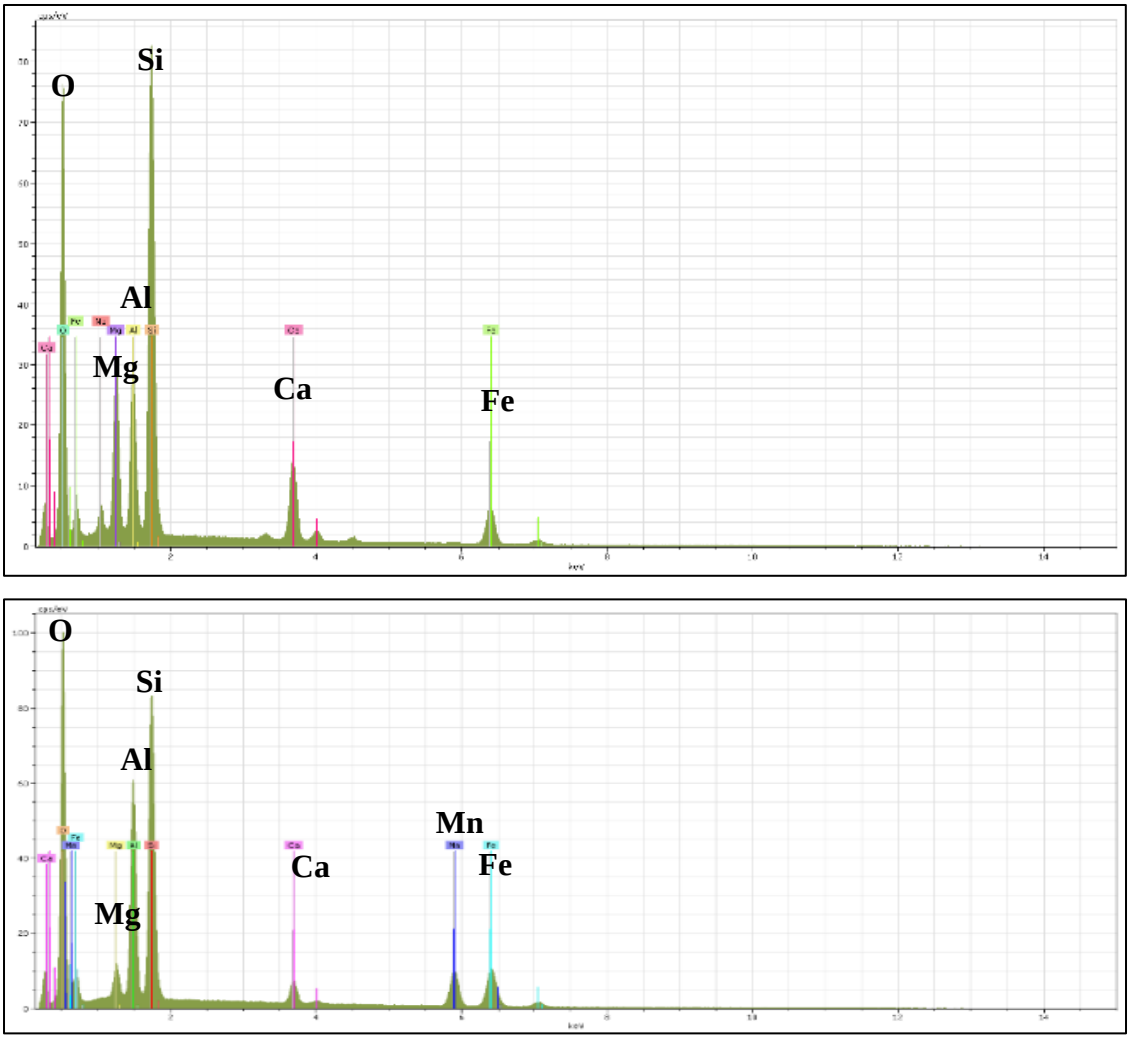

Fig. 6.2 Examples of EDS spectrum of mineral grains from polished sections of the Dupi Tila Formation. Top- pyrope garnet (Sample- CW, fraction B) and bottom- tourmaline (sample- SS-11, fraction C).

6.5.1 GARNET

Garnets are one of the most abundant minerals in all samples of the Dupi Tila Formation. A total of 22 garnet grains were analyzed (see Appendix B, Fig. 6.3), and calculated end members were plotted in Figures 6.4 through 6.7. The four end-members calculated are almandine, pyrope, grossular and spessartine, of which almandine is dominant. The average almandine content in garnet grains is 50.0% with a maximum of 79.0%. Other types of garnets are- Pyrope (average 10.0%, max. 26.0%), grossular (average 27.0%, max. 69.0%), and spessartine (average 13.0%, max. 61.0%).

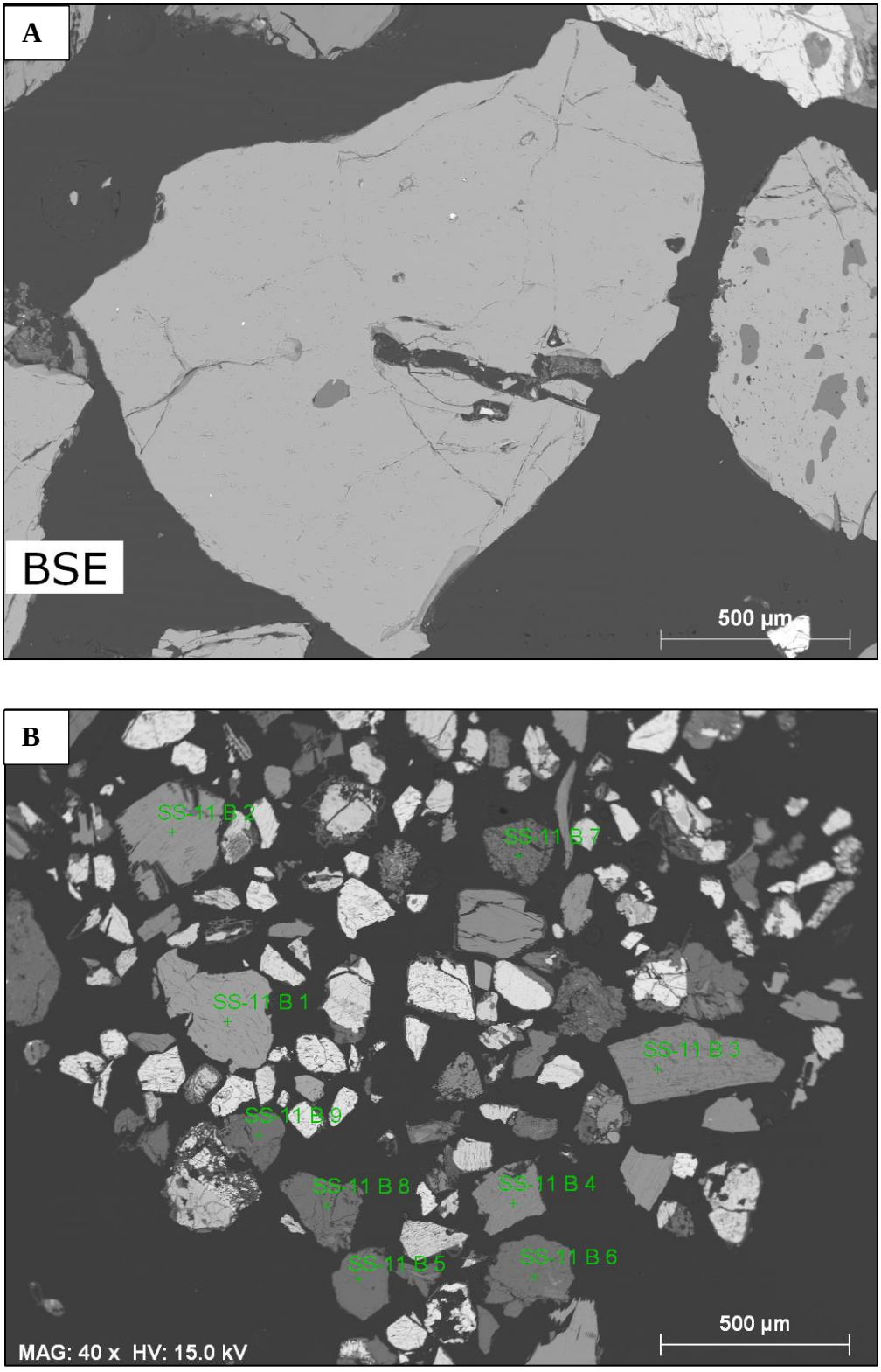

Fig. 6.3 A- Representative BSE photomicrographs of garnet grains in polished section (Sample KS-2, Fraction-B, WDS), B- EDS of individual grains from multiple-depth carbon-coated thin sections (Sample KS-2, Fraction D).

According to the (Sp+Gro)-Py-Alm plot (Fig. 6.4), almost all the garnets are rich in almandine except for a few samples from Lalmai hills and Stable Platform. The (Py+Alm)-Gro-Sp plot (Fig. 6.5) shows that most of the grains are high in pyrope+almandine, especially the Sylhet Trough and Sitapahar anticline samples. The (Alm+Sp)-Py-Gro plot (Fig. 6.6) shows that most garnets from the Stable Platform, Sitapahar anticline, and Lalmai hills fall in field I, which indicates garnets with almandine and grossular including <10% pyrope content. Samples from Sylhet Trough fall in fields II and III, which indicates garnets with almandine and pyrope including <10% grossular content and granets with pyrope and grossular including >10%, respectively. The Sp-Alm-Py plot indicates that most of the garnets are derived from amphibolite and granulite facies rocks (Fig. 6.7). However, all the samples from the Stable Platform were sourced from pegmatite and low-grade metamorphic facies.

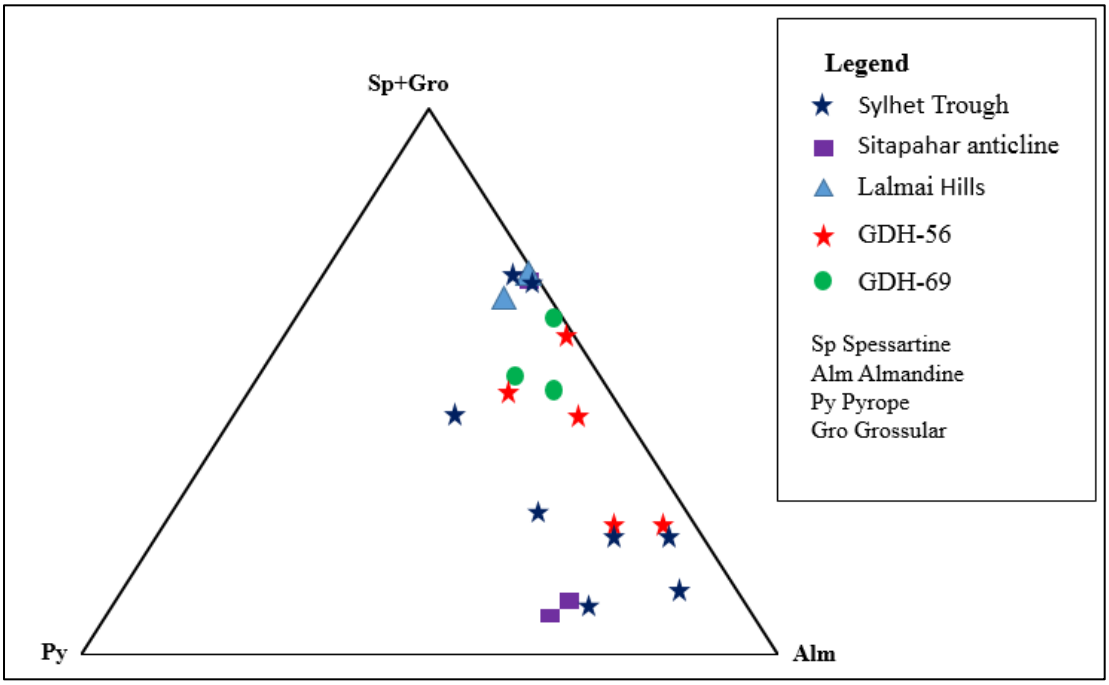

Fig. 6.4 Chemical compositions from garnets from Dupi Tila Formation samples from various parts of the Bengal basin plotted on (Sp+Gro)-Py-Alm (adapted from Nanayama, 1997).

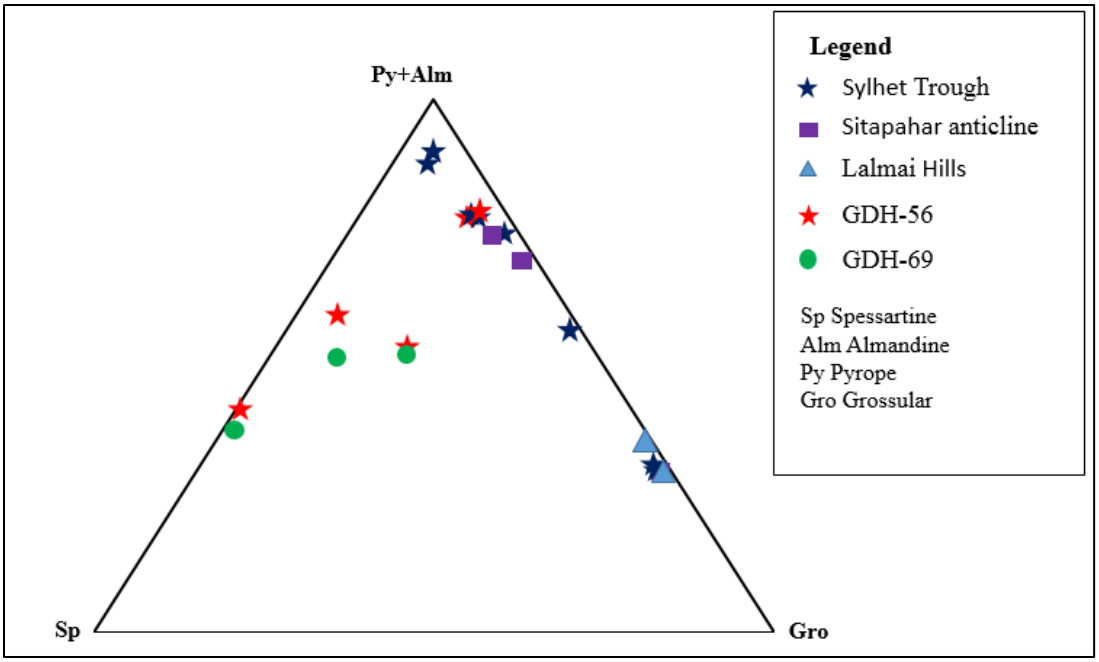

Fig. 6.5 Chemical compositions from garnets from Dupi Tila Formation samples from various parts of the Bengal basin plotted on (Py+Alm)-Gro-Sp (adapted from Nanayama, 1997).

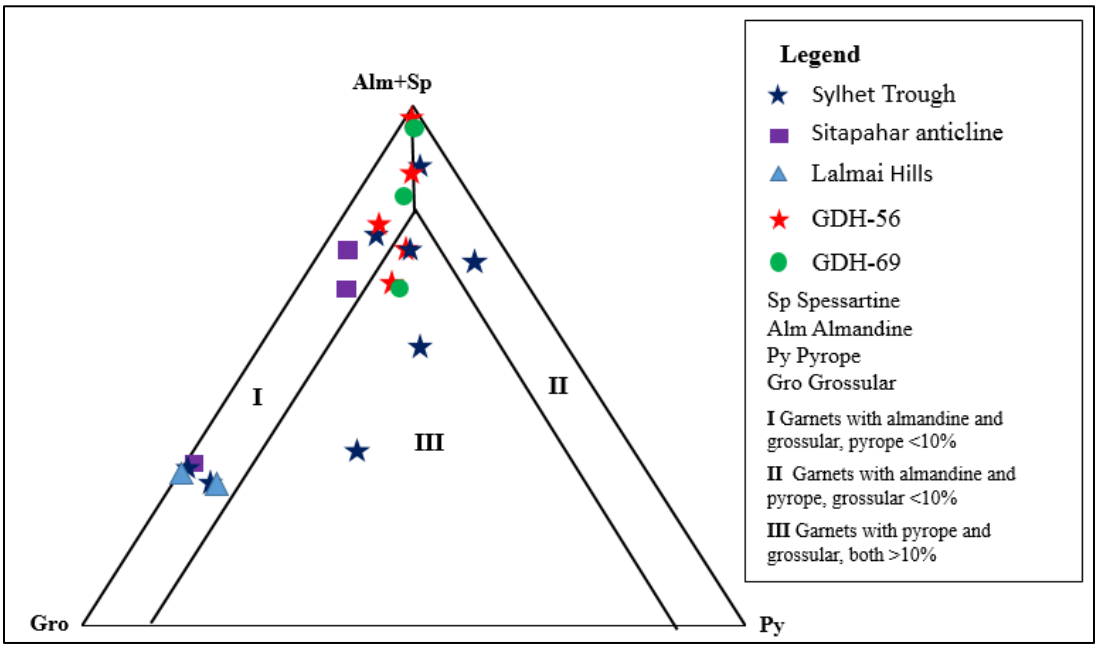

Fig. 6.6 Chemical compositions of garnets from Dupi Tila Formation samples from various parts of the Bengal basin plotted on (Alm+Sp)-Py-Gro (adapted from Nanayama, 1997).

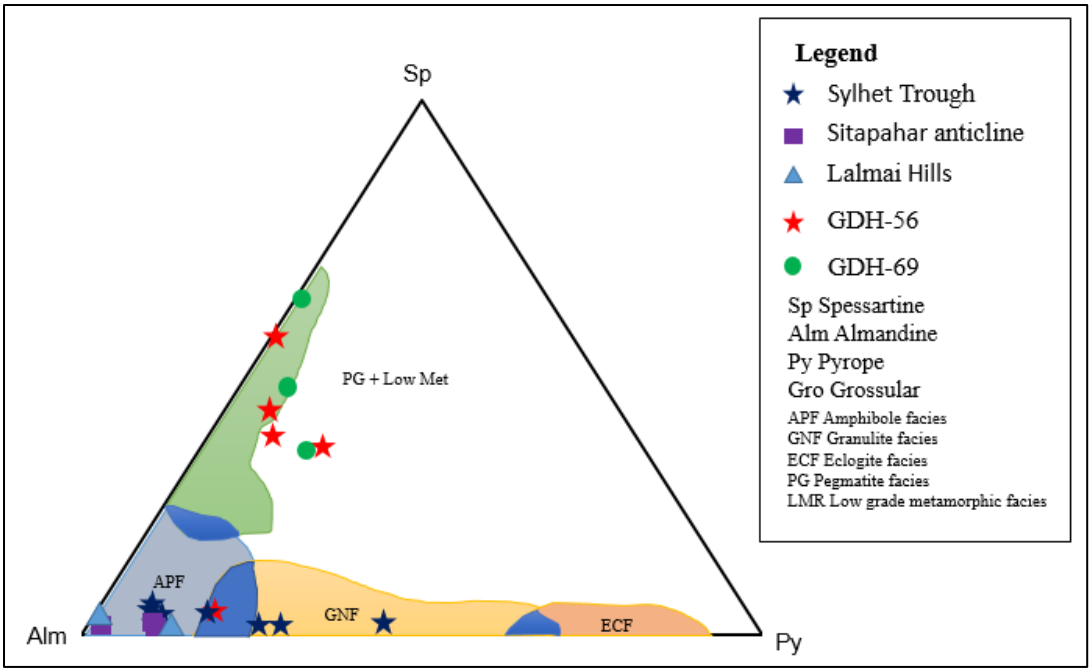

Fig. 6.7 Chemical composition of garnets from Dupi Tila Formation samples from various parts of the Bengal basin plotted on Alm-Py-Sp (adapted from Nanayama, 1997).

6.5.2 TOURMALINE

Tourmaline is very complex in terms of its chemical structure and is usually considered in terms of end-members. A complete solid solution exists between the two end-member series schorl-elbaite and schorl-dravite, although there is a large miscibility gap between elbaite and dravite. Hence, tourmalines are usually described depending on their position in the schorl-elbaite series or in the schorl-dravite series.

A total of 16 tourmaline grains were analyzed (see Appendix C, Fig. 6.8). Tourmalines were plotted on Al-$Al_{50}Fe_{50}$(tot)-$Al_{50}Mg_{50}$ (Fig. 6.9) and Ca-Fe(tot)-Mg (Fig. 6.10) diagrams. The Al-$Al_{50}Fe_{50}$(tot)-$Al_{50}Mg_{50}$ plot shows that all the tourmalines fall within the field indicating metapelites coexisting with an Al saturating phase.

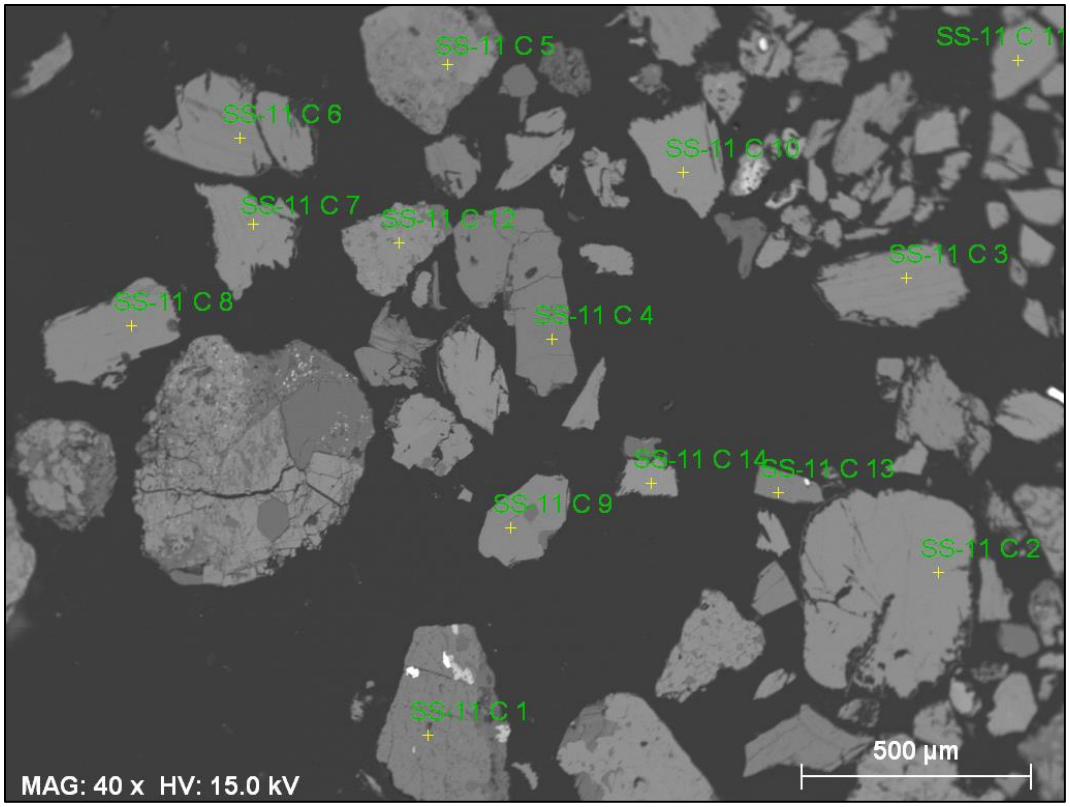

Fig. 6.8 Representative BSE photomicrographs of tourmaline grains in polished section (Sample- SS-11, Fraction-C).

According to the Ca-Fe(tot)-Mg plot (Fig. 6.9), tourmaline grains fall into four fields corresponding to (1) Li-rich granitoids pegmatites and aplites, (2) Li-poor granitoids pegmatites and aplites, (3) Ca-rich metapelites, metapsammites, and calc-silicate rocks, and (4) Ca-poor metapelites, metapsammites, and calc-silicate rocks. A few samples from Sitapahar anticline and Lalmai hills fall into the Li-rich granitoids pegmatites and aplites field. Most of the Stable Platform tourmalines fall into the Ca-poor metapelites, metapsammites, and calc-silicate rocks field. Sylhet Trough samples fall mainly into the Li-poor granitoids pegmatites and aplites field.

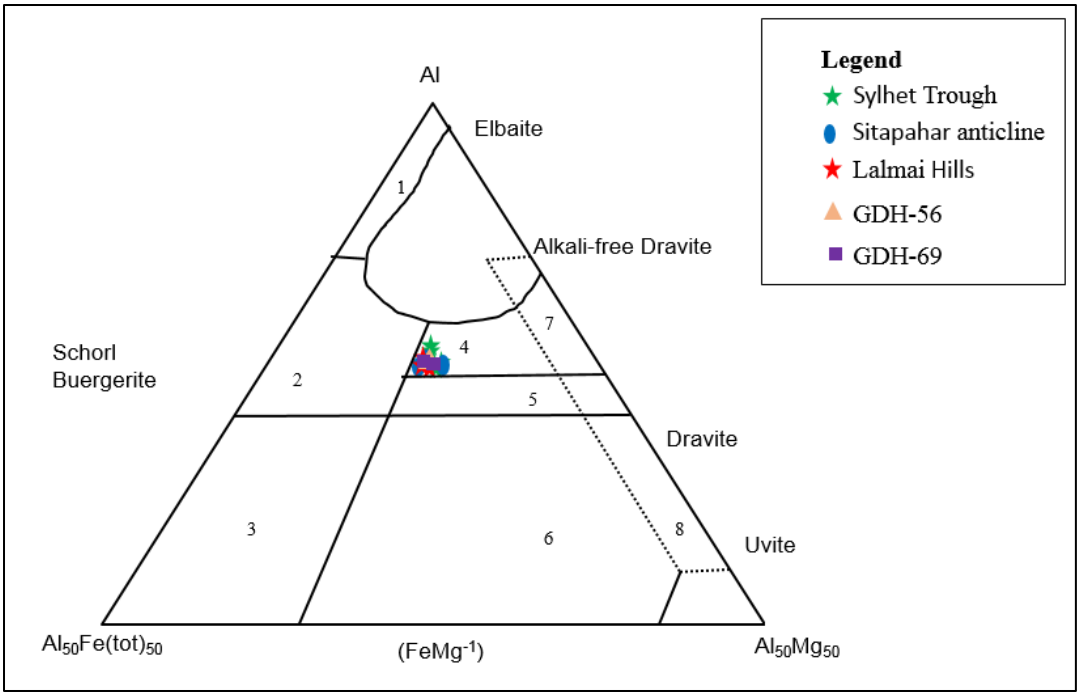

Fig. 6.9 Al-Fe (tot)-Mg plot (in molecular proportion) of tourmalines from Dupi Tila Formation samples from various parts of the Bengal basin. Fe (tot) represents the total iron in the tourmaline. Several end members are plotted for reference. Numbered fields correspond to the following rock types: (1) Li-rich granitoid, pegmatites, and aplites, (2) Li-poor granitoids and associated pegmatites and aplites, (3) Fe^{3+}-rich quartz-tourmaline rocks (hydrothermally altered granites), (4) Metapelites coexisting with an Al saturating phase, (5) Metapelites without an Al-saturating phase, (6) Fe^{3+}-rich quartz-tourmaline rocks, calc-silicate rocks, and metapelites, (7) Low-Ca meta-ultramafics and Cr and V-rich metasediments, and (8) Metacarbonates and meta-pyroxenites (adapted after Henry and Guidotti, 1985).

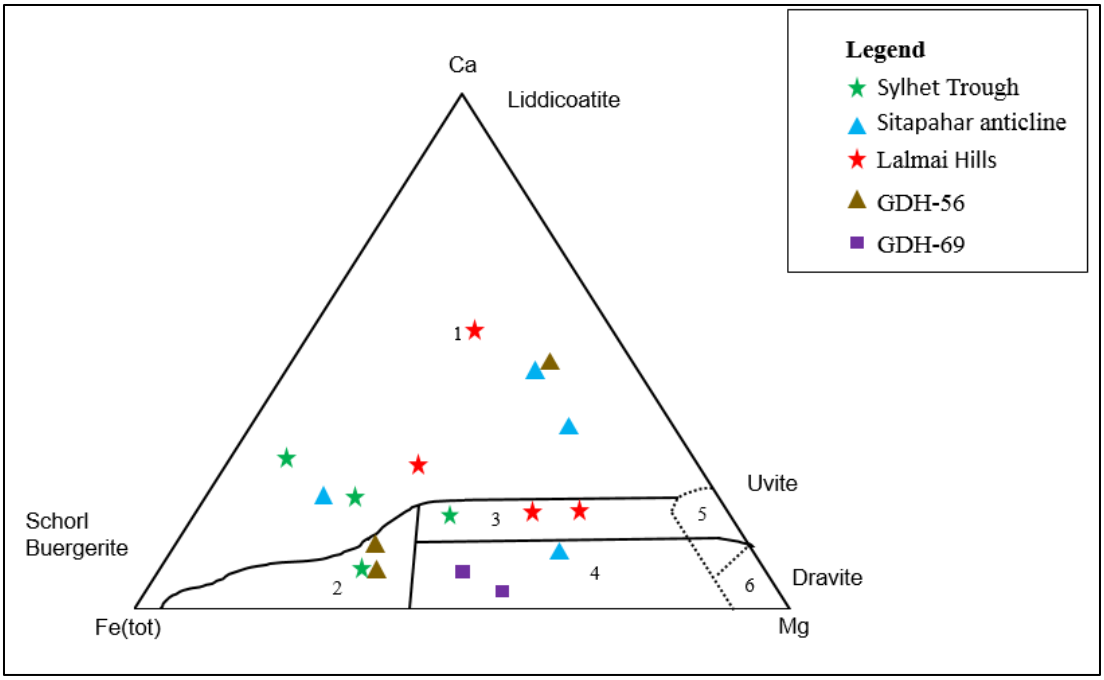

Fig. 6.10 Ca-Fe (tot)-Mg plot (in molecular proportion) for tourmalines from Dupi Tila Formation samples from various parts of the Bengal basin. Several end members are plotted for reference. The numbered fields correspond to the following rock types: (1) Li-rich granitoid pegmatites and aplites, (2) Li-poor granitoids and associated pegmatites and aplites, (3) Ca-rich metapelites and calc-silicate rocks, (4) Ca-poor metapelites and quartz-tourmaline rocks, (5) Metacarbonates, and (6) Meta-ultramafics (adapted after Henry and Guidotti, 1985).

6.5.3 EPIDOTE GROUP MINERALS

Twenty-nine grains from samples of detrital epidote-group minerals (SS-11, KS-2, KS-4, CCS, CWSaLDT, NWD, and NWR) were analyzed (see Appendix D). They are mostly of the epidote-clinozoisite series, with a subordinate amount of zoisite (Fig. 6.11). They have a wide compositional variability, indicated by a $Fe^{3+}/(Al+Fe^{3+})$ range from 0.023 to 0.085, with an average of about 0.525. Epidote recrystallized at low temperatures has a small compositional range, with $Fe^{3+}/ (Al+Fe^{3+})$ around 0.33 (Dollase, 1971; Liou, 1973), and its stability field enlarges toward the aluminous end as the temperature increases (Miyashiro and Seki, 1958; Nakajima et al., 1977). The epidotes from the Dupi Tila Formation from different parts of the Bengal basin are derived from relatively high-grade metamorphic rocks of the epidote-amphibolite facies.

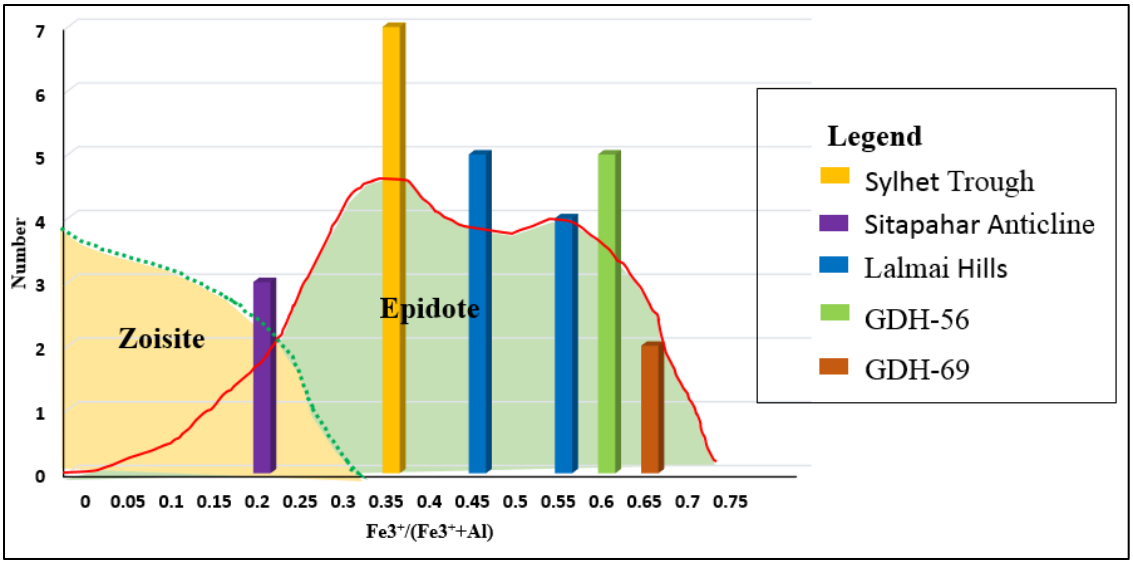

Fig. 6.11 Fe^{3+}/ (Al+Fe^{3+}) ratios in epidote-group minerals from Dupi Tila Formation samples from various parts of the Bengal basin (adapted from Nanayama, 1997). Fields are after Enami and Banno (1980). Shaded areas are representing zones of zoisite and epidote minerals.

6.5.4 CHLORITOID

Chloritoid is a common mineral phase in low- to medium-grade metapelites of various pressure conditions (Deer et al., 1992). Variations in the chemical composition of chloritoid are generally defined by variations in the abundance of Fe, Mg, and Mn (Morton, 1991). Chloritoid from low- to medium-pressure metapelites are usually rich in Fe and Mn, whereas chloritoid from high-pressure blueschist facies metapelites is rich in Fe and Mg (Chopin and Schreyer, 1983). Three (3) chloritoid grains were analyzed (see Appendix E). The Mn-Mg-Fe plot indicates that Sylhet Trough, Sitapahar anticline and Lalmai hills samples came from high-pressure blueschist metamorphic facies (Fig. 6.12).

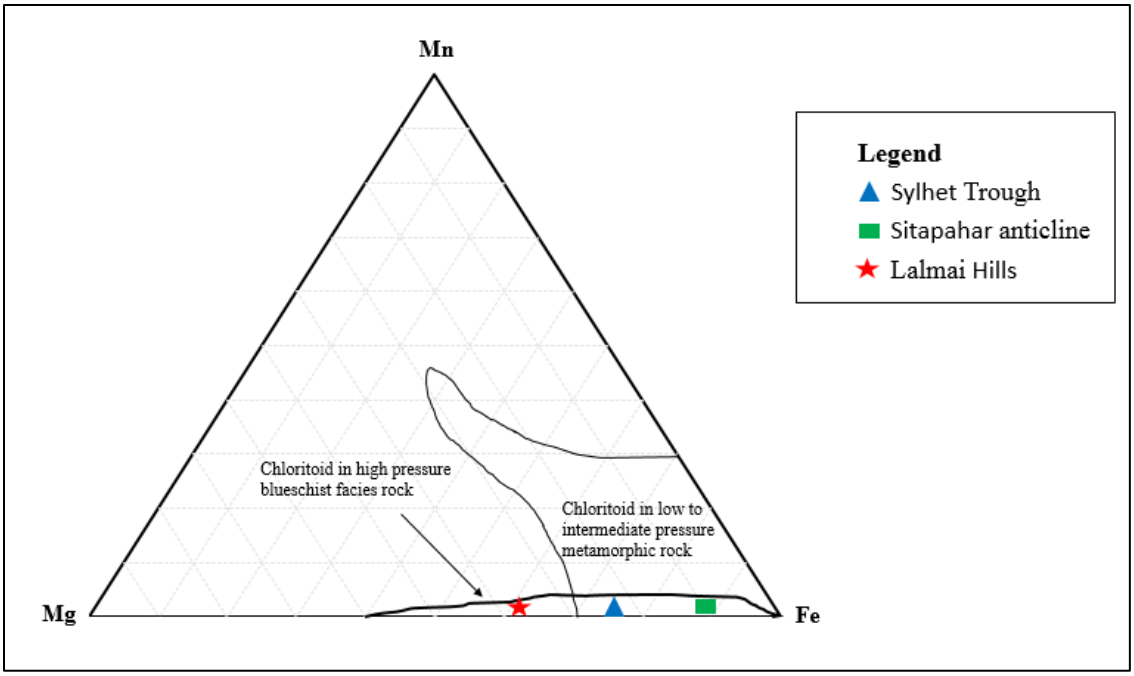

Fig. 6.12 Chemical composition of chloritoid from the Dupi Tila (adapted from Chopin and Schreyer, 1983).

6.5.5 ILMENITE

Ilmenite ($FeTiO_3$) (Fig. 6.13) is a very stable heavy mineral (Morton and Hallsworth, 1999) and is an important component of heavy-mineral placer deposits commonly associated with leucoxene and rutile (TiO_2). Ilmenite can occur in a wide variety of igneous rocks, both intrusive and extrusive, as well as pegmatites and other vein rocks, and even some metamorphic rocks, especially gneiss (Ramdohr, 1980). Ilmenite element contents were found to be useful as provenance indicators for the coastal sediments of the southeastern United States (Darby 1984; Darby et al. 1985; Darby and Tsang, 1987) because ilmenite composition varies depending on its source-rock paragenesis (Hutton 1950; Buddington and Lindsley 1964). Costal areas of the Bengal basin are similar to the southeastern United States (Graham et al., 1976), and Lalmai hills are located close to the coast line of the Bay of Bengal (Fig. 2.1).

Eight (8) ilmenite grains were analyzed (see Appendix F) from Lalmai hills sample (CWSaLDT). The amount of titanium, plotted in Fig. 6.14, indicates an average 30%

titanium oxides in these samples. The data set is insufficient to establish criteria for recognition of source-rock types of ilmenite-bearing rocks in the study area.

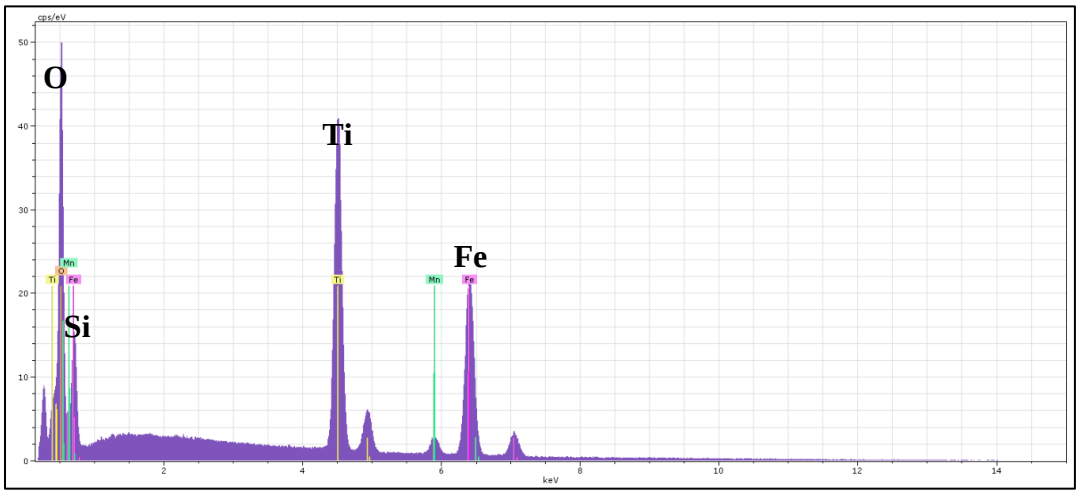

Fig. 6.13 Sample EDS spectrum of ilmenite grain from polished section of Dupi Tila Formation (Sample CW, fraction B).

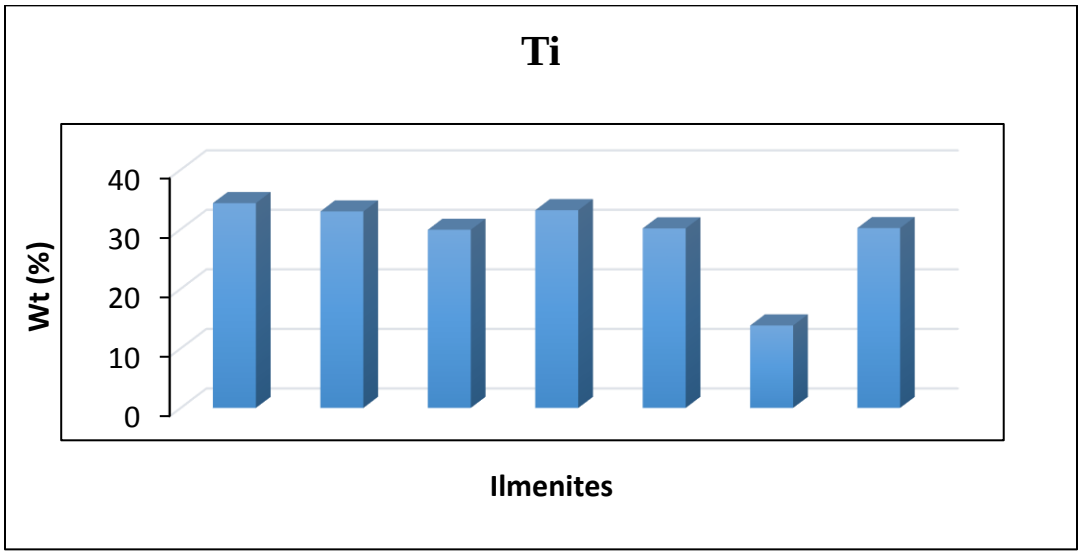

Fig. 6.14 Wt. Percentage of titanium oxides of ilmenites from Lalmai hills sample (Sample CW, fraction B and D).

6.6 PROVENANCE

Garnets are characteristic minerals of metamorphic rocks but also can be found in some igneous rocks (Deer et al., 1992). Four (4) different garnet species have been identified from the studied samples based on major oxide content. These are almandine,

pyrope, grossular, and spessartine. All studied grains are almandine rich. Garnet compositions suggest derivation of sediments from mixed source terranes. Most of the plots indicate a source of garnets from amphibolite, granulite, and eclogite facies rocks.

Compositional analyses of tourmaline suggest that metapelites coexisting with an Al saturating phase are the probable source rocks for these minerals (Fig 6.10). The Ca-Fe (tot)-Mg plot shows that most of the grains came from Li-bearing granitoids pegmatites and aplites, Li-poor granitoids pegmatites and aplites, Ca-rich metapelites, metapsammites, and calc-silicate rocks, and Ca-poor metapelites, metapsammites, and calc-silicate rocks (Fig 6.11).

The epidotes from the Dupi Tila Formation from different parts of the Bengal basin are derived from relatively high-grade metamorphic rocks of epidote-amphibolite facies. The Mn-Mg-Fe plot for chloritoid suggests that samples from the Sylhet Trough, Sitapahar anticline and Lalmai hills came from high-pressure blueschist metamorphic facies.

Chapter 7: WHOLE ROCK GEOCHEMISTRY

7.1 INTRODUCTION

Whole rock geochemical analyses are important tools to study provenance of terrigenous sedimentary rocks because they can provide information about rock types, tectonic settings, and weathering history of the source rocks. Recent developments in the field of sedimentary geochemistry highlight that chemical composition of the clastic sedimentary rocks is a function of a complex interplay of several variables, including the nature of the source rocks, source area weathering, and diagenesis (McLennan et al., 1993; McLennan et al., 2003). However, plate-tectonic processes impart a distinctive geochemical signature to sediments in two separate ways. Different tectonic environments have distinctive provenance characteristics. Therefore, clastic sedimentary rocks have been used to determine provenance and identify ancient tectonic settings (Bhatia, 1983; McLennan et al., 1993). Sedimentary basins may be assigned to the following tectonic settings: (1) oceanic island arcs, (2) continental island arcs, (3) active continental margins, and (4) passive continental margins (Bhatia and Crook, 1986).

Roser and Korsch (1988) used discriminant function analysis of major elements (TiO_2, Al_2O_3, Fe_2O_3 tot., MgO, CaO, and Na_2O) to discriminate four different provenance groups: (1) mafic detritus, (2) intermediate, dominantly andesite detritus, (3) felsic plutonic and volcanic detritus, and (4) recycled-mature polycyclic quartzose detritus from sandstones and mudstones. Major element geochemistry and mineralogy of siliciclastic rocks (Taylor and McLennan, 1985) is strongly affected by chemical weathering (Fedo et al., 1996). The characteristics of detrital sediments greatly depend on various geological processes involved in four major environments/settings encountered during the sediment's entire path of denudation from the source to deposition and burial (Sageman

and Lyons, 2003). These are: 1) the source area, where climate and tectonic setting might influence weathering and erosion of bed rock; 2) the transportation route, where different factors can modify the textural and compositional properties of sediments; 3) the depositional site, where different physical, chemical, and biological processes constrain the amount of sediment accumulation; and 4) the burial history during which diagenesis may further alter sediment characteristics. Plotting Al_2O_3-($CaO+Na_2O$)-K_2O relationships in ternary diagrams provides important information about weathering processes, sedimentary sorting, and identifying certain post-depositional processes. The potential influence exerted on sediment geochemistry by weathering, detrital sorting, and diagenesis/metamorphism are reasonably well understood. Trace element ratios of immobile elements normally reflect source-rock composition rather than the sedimentary processes (Taylor and McLennan, 1985).

7.2 RESULTS AND INTERPRETATIONS

Major, trace, and rare earth element compositions of Dupi Tila mudrock samples (SS-W, Sylhet Trough; BS-10, Garo hills; CWSal, Lalmai hills; NWD-56, Stable Platform; and KS-8, KS-9, KS-10, KS-11, KS-12, KS-13, Sitapahar anticline) from different parts of the Bengal basin are presented in Appendix F.

7.2.1 MAJOR ELEMENTS

Dupi Tila samples exhibit variations in major oxide (e.g., SiO_2, Al_2O_3, Fe_2O_3, MgO, and K_2O) concentrations from place to place. Silica (SiO_2) is abundant in all samples, ranging from 54-84% in different parts of the Bengal basin (Fig. 7.1). Samples from the northwest Stable Platform have the highest concentrations of silica. Concentrations of Al_2O_3 is highest in Garo hills regions. Fe_2O_3 and K_2O_3 concentrations are are low in samples from all sites.

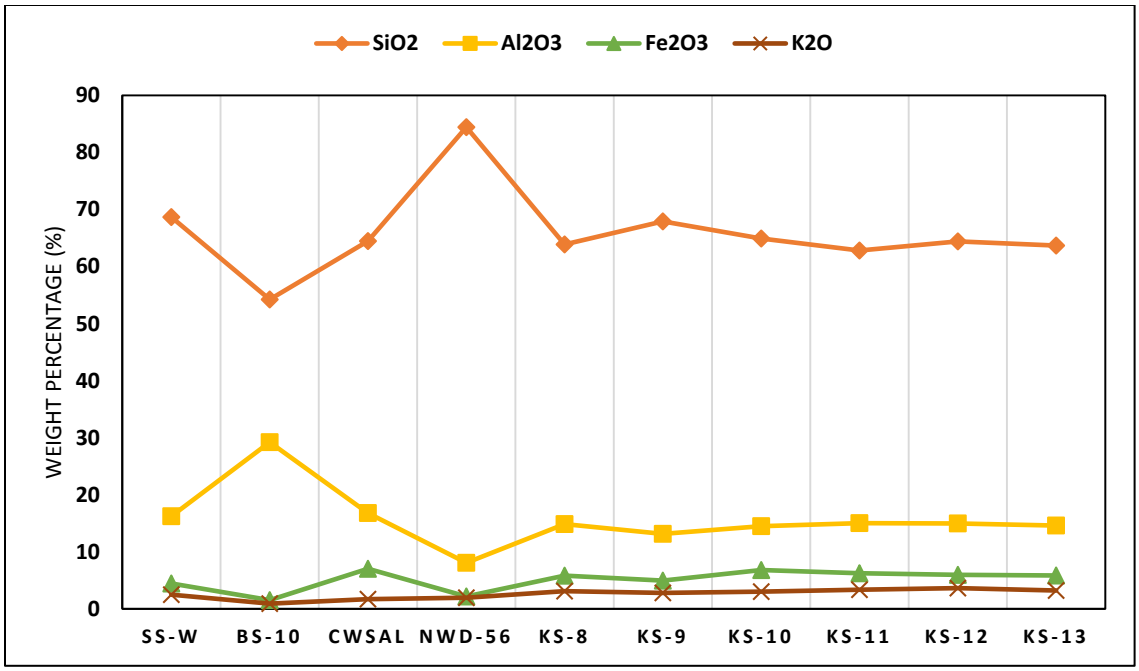

Fig. 7.1 Weight percentages of major oxides in Dupi Tila Formation samples from various parts of the Bengal basin.

Concentrations of other oxides (MgO, Cao, Na_2O, TiO_2, P_2O_5, MnO, and Cr_2O_3) are shown in the figure 7.2. The abundance of MgO, CaO, and Na_2O are relatively high in sediments from the Sitapahar anticline. Samples from the Garo hills, Sylhet Trough, and Lalmai hills have higher TiO_2 concentrations. Concentrations of P_2O_5, MnO, and Cr_2O_3 are very low in all samples. Concentration of CaO is very low in samples from Sylhet Trough, Garo hills, and Lalmai hills (< 0.5%).

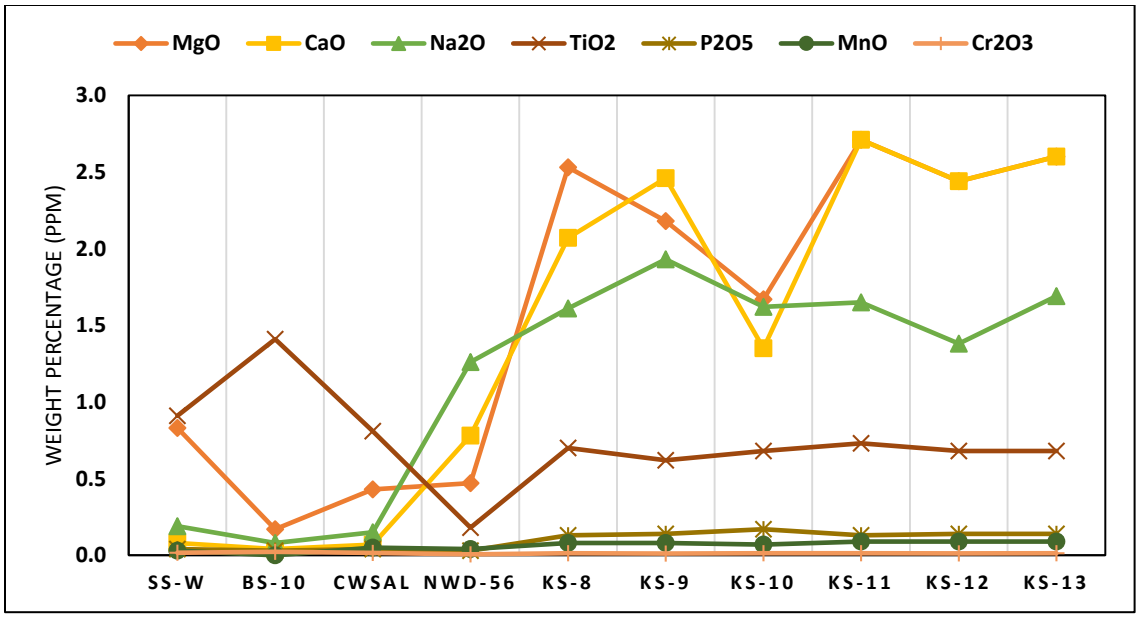

Fig. 7.2 Concentrations (ppm) of major oxides in the Dupi Tila Formation from various parts of the Bengal basin.

Ratios of some oxides can be useful in provenance interpretation (Rahman and Suzuki, 2007). However, some major oxides (e.g., CaO) can be depleted during the weathering process, and hence, major oxides should not be used alone to evaluate provenance. Rather, analyses should be accompanied by conventional petrographic studies and other geochemical analyses.

Harker's variograms of TiO_2, Al_2O_3, Fe_2O_3, MgO, Na_2O, and CaO do not show any linear correlation with SiO_2 content (Fig. 7.3). This is may be due to variations in the source terranes for these sediments.

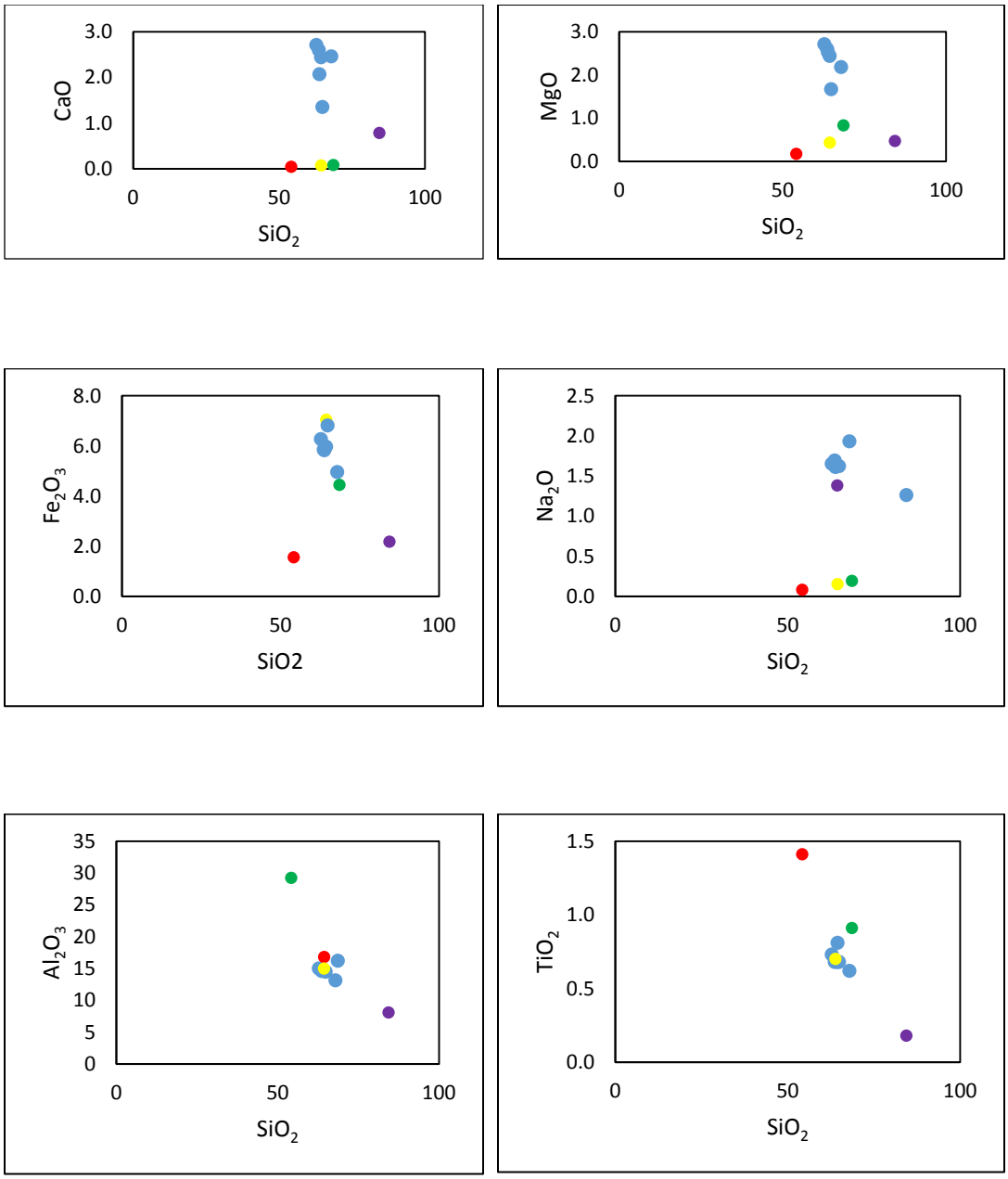

Fig. 7.3 Harker variograms of major element concentrations in samples from Dupi Tila Formation (green- Sylhet Trough, red- Garo hills, yellow- Lalmai hills, purple- Stable Platform, and blue- Sitapahar anticline).

The ratio of K_2O and Al_2O_3 (Fig. 7.4) can be used as an indicator of the original composition of the Dupi Tila Formation. K_2O/Al_2O_3 ratios are markedly different for clay minerals and mudrocks. K_2O/Al_2O_3 ratios range from 0-0.3 for clay minerals and from 0.3-0.9 for feldspars (Cox et al., 1995). Illite has a value of 0.28 (Lee, 2000). The ratios of K_2O/Al_2O_3 in samples from the study area suggest that they contain clay minerals.

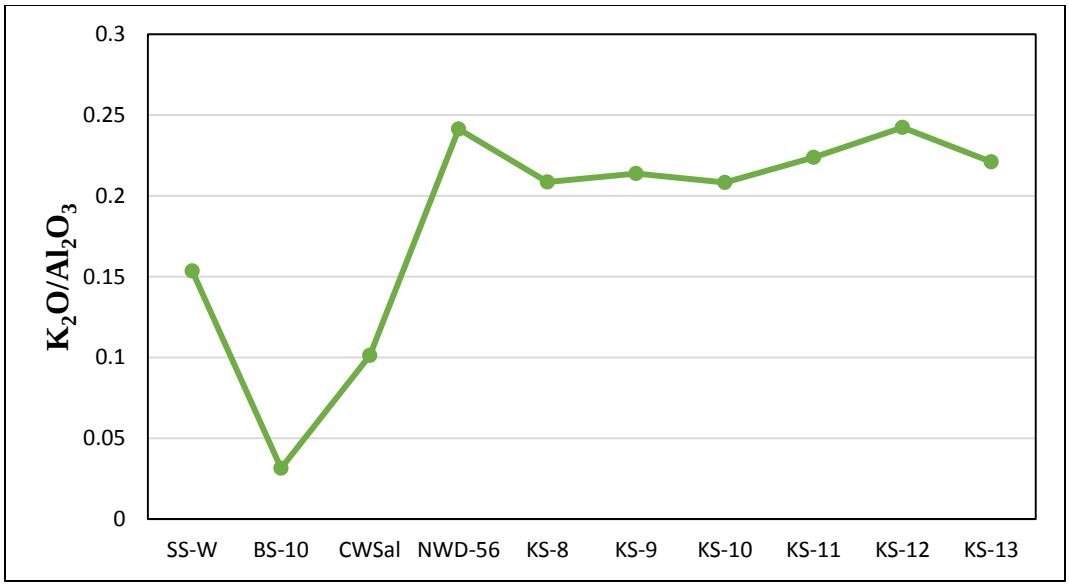

Fig. 7.4 Variations in K_2O/Al_2O_3 ratios for Dupi Tila samples from study area.

7.2.2 TRACE AND RARE EARTH ELEMENTS

Dupi Tila sediment samples from the study area exhibit variation in trace and rare earth element (e.g., Ba, Zr, Ni, Sr, Y, Nb, Sc, Th, and La) concentrations from place to place. All trace elements and rare earth elements are presented and described below.

Trace element data show high concentrations of Ba in Sitapahar anticline area and low concentrations in the Garo hills area (Fig. 7.5)

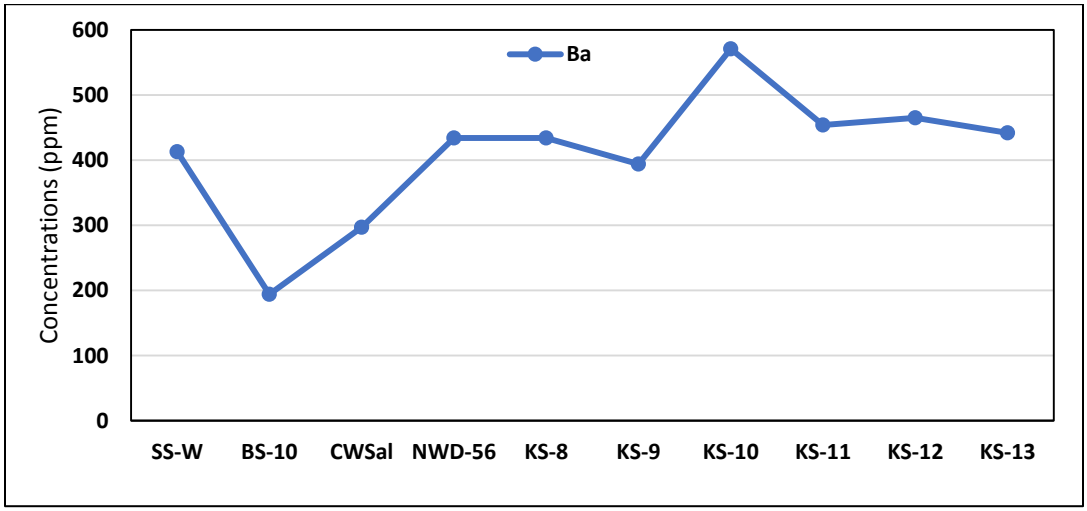

Fig. 7.5 Concentrations (ppm) of barium in Dupi Tila Formation samples from various parts of the Bengal basin.

Zirconium concentrations (Fig. 7.6) are also variable from place to place. Sediments from the Garo hills, Lalmai hills and Sylhet Trough have high Zr contents, whereas sediments from the Stable Platform study have the lowest amount of Zr concentrations.

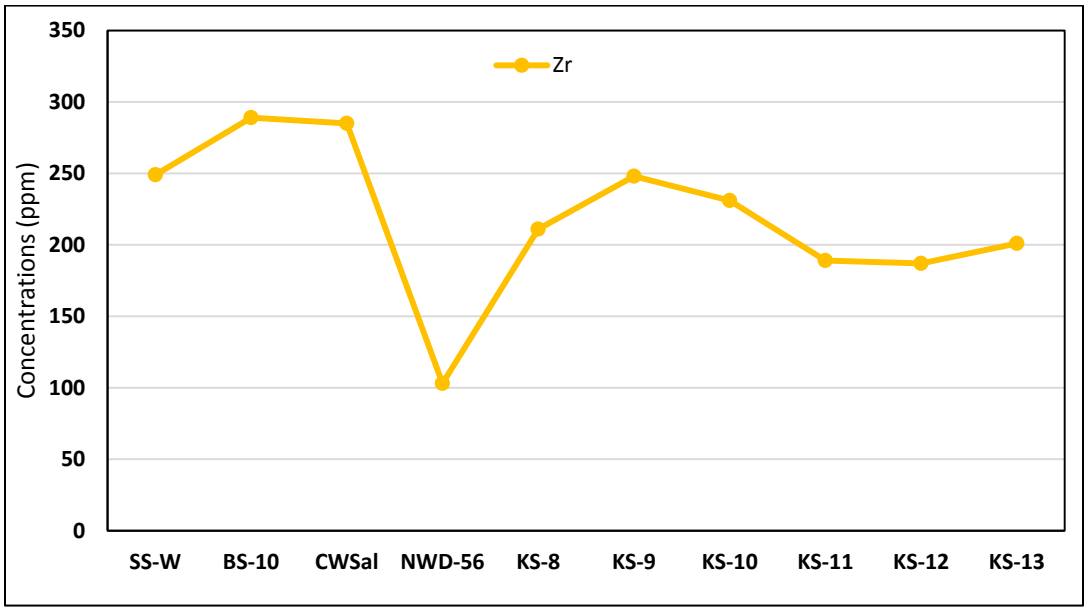

Fig. 7.6 Concentrations (ppm) of zirconium in the Dupi Tila Formation samples from various part of the Bengal basin.

The abundance of rare earth elements is not uniform in all study areas (Fig. 7.7). The distribution of strontium (Sr) is high in Sitapahar anticline area. Ni, Y, Nb, and Sc concentrations exhibit a similar trend in all areas. The Stable platform samples have low rare earth elements concentrations compared to the other areas. A negative correlation is observed between Zr and Sr.

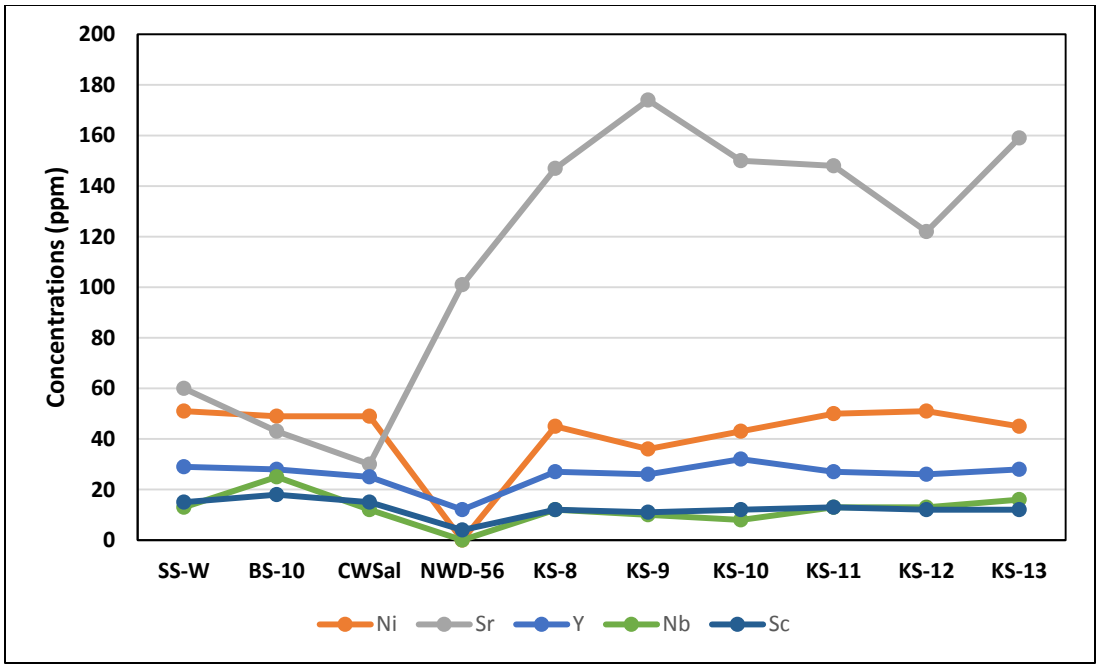

Fig. 7.7 Concentrations (ppm) of trace elements in the Dupi Tila samples from various parts of the Bengal basin.

7.3 WEATHERING AND DIAGENESIS

Weathering and diagenesis in source terranes can be estimated based on chemical composition of sediments. The A-CN-K (Al_2O_3 – $CaO+Na_2O$-K_2O) plot in Figure 7.8 shows that most samples fall on the Al_2O_3 - K_2O line close to the Al_2O_3 end member, indicating highly weathered source terranes. Samples from the Stable platform and Sitapahar anticline fall into the average granite field, whereas those from the Sylhet Trough, Lalmai hills and Garo hills fall into the illite and kaolinite-chlorite fields. This suggests that weathering in source regions for the latter three areas was more intense weathering than in the Sitapahar anticline and Stable Platform source areas.

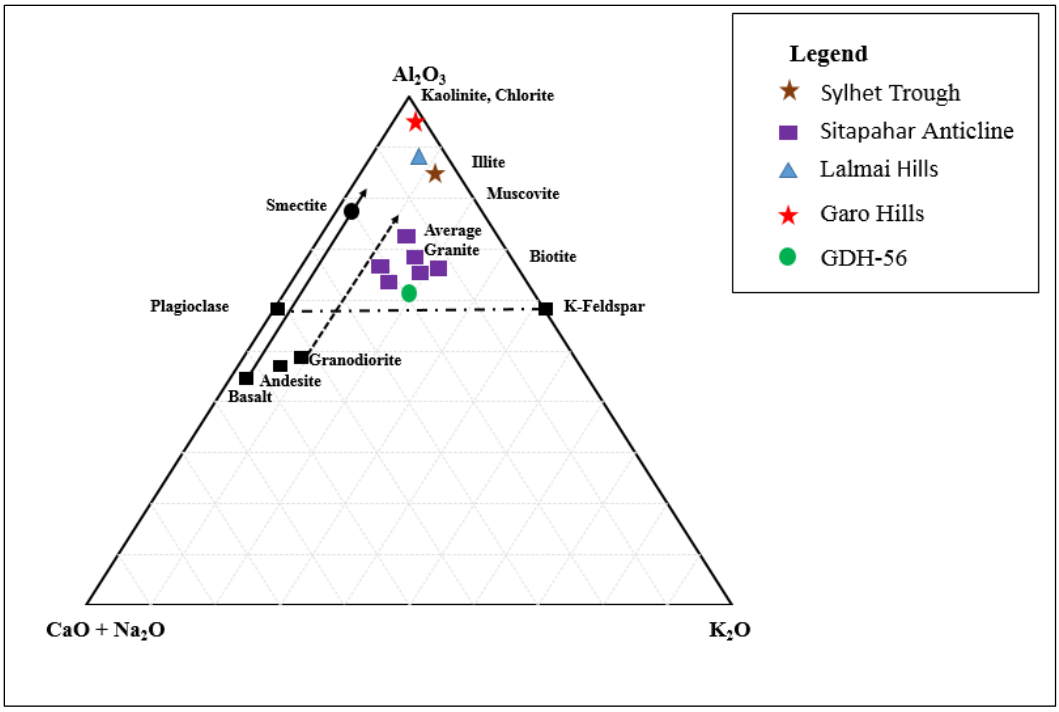

Figure 7.8 Ternary plots of A-CN-K of Dupi Tila samples from various regions of the Bengal basin (adapted from Nesbitt and Young, 1982, and Soreghan and Soreghan, 2007).

Several studies (Nesbitt and Young, 1982; Soreghan and Soreghan, 2007 and many others) reported that the chemical index of alteration (CIA) accurately reflects the intensity of weathering of source rocks of varied geological ages (Table 10). Low CIA values (50% to 60%) indicate relatively unweathered rocks, whereas intermediate (60% to 80%) and higher (80% to 100%) CIA values indicate moderate to extreme weathering conditions (Nesbitt and Young, 1984). This index is calculated using the equation:

$$CIA = Al_2O_3 / (Al_2O_3 + CaO + Na_2O + K_2O)$$

CIA values (Fig. 7.9) for all Sitapahar anticline samples indicate intermediate weathering. In contrast, for all other area samples, CIA reflect high weathering intensity.

Table 10. Ratios of select oxides and CIA (Chemical alteration index).

Sites	Log(SiO_2/Al_2O_3)	Log(Fe_2O_3/K_2O)	CIA (%)
SS-W	0.63	0.22	93.65
BS-10	0.27	0.25	99.02
CWSal	0.58	0.22	96.27
NWD-56	1.02	0.62	76.30
KS-8	0.62	0.05	70.53
KS-9	0.63	0.27	66.67
KS-10	0.71	0.24	75.76
KS-11	0.65	0.35	67.98
KS-12	0.62	0.27	70.53
KS-13	0.63	0.21	67.95

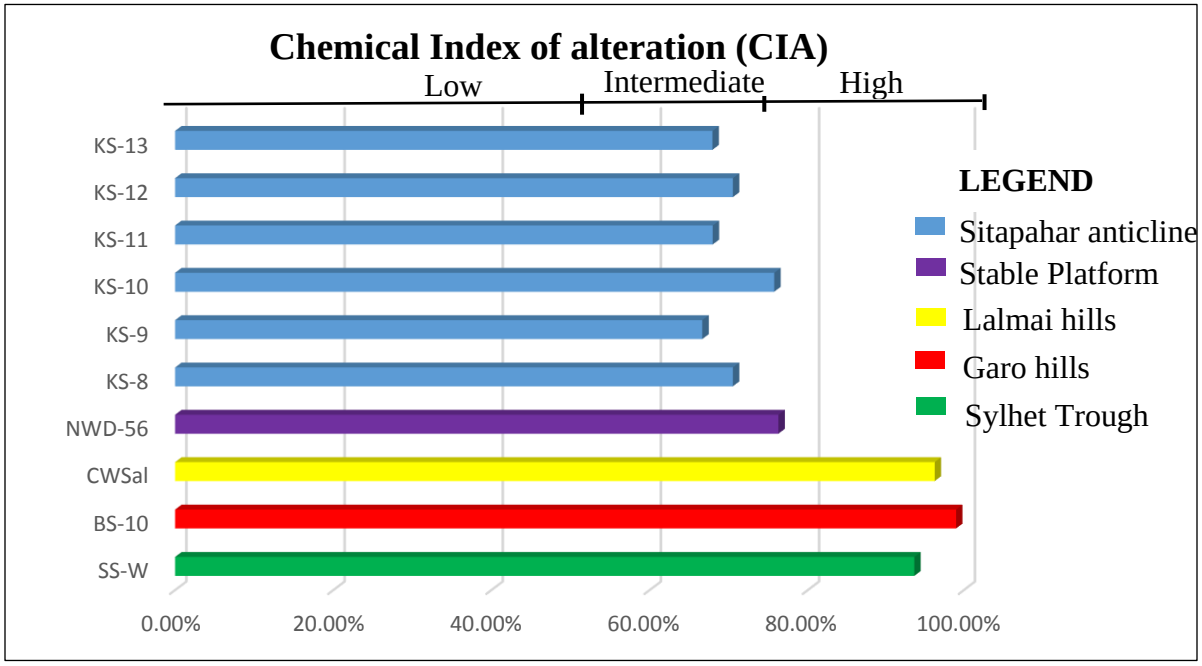

Fig. 7.9 CIA values of Dupi Tila Formation from different parts of the Bengal basin, Bangladesh (adepted from Nesbitt and Young, 1982, and Soreghan and Soreghan, 2007).

7.4 TECTONIC SETTINGS

Various chemical and petrographic (mineralogical) approaches can be used to determine provenance from bulk samples. Von Eynatten et al. (2003) concluded that bulk chemical analyses, including trace elements, are more effective than the study of heavy minerals, largely because identification and counting of heavy minerals required skill and

was time-consuming. In contrast, rock chemistry is a consequence of the mineralogical composition of a rock, so that petrographic studies are intrinsically more informative than bulk rock chemistry.

Sandstones from specific tectonic regimes possess characteristic chemical compositions. SiO_2 content and K_2O/Na_2O ratios have been utilized by several workers (e.g., Roser and Korsch, 1986; Sitaula, 2009) to discriminate tectonic settings of the source area. The SiO_2 vs K_2O/Na_2O plot for all studied samples in figure 7.10 reflects an active continental provenance. No samples shows Island Arc or Passive Margin provenances.

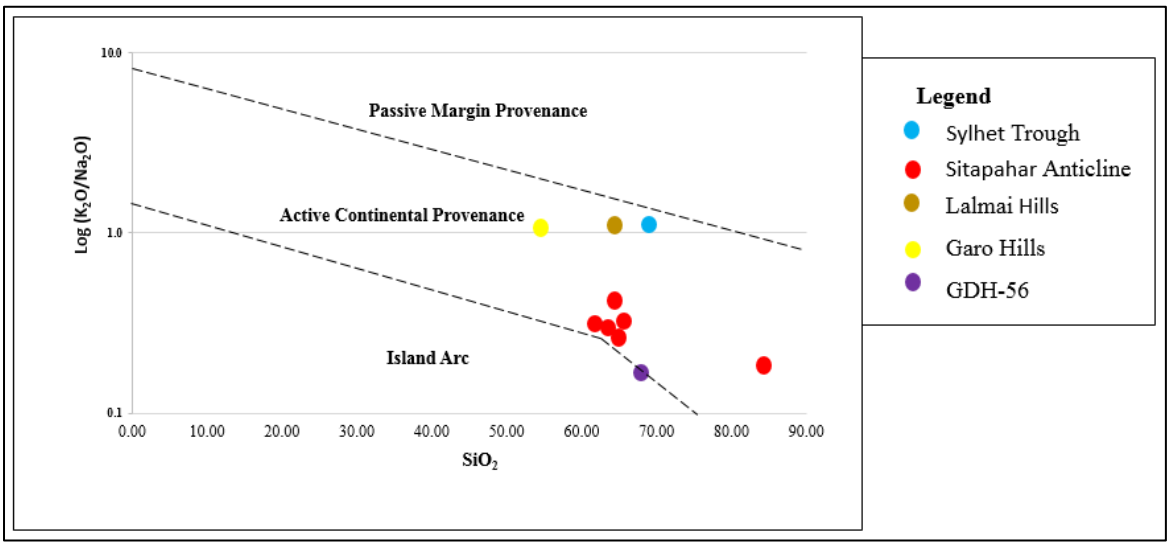

Figure 7.10 Dupi Tila samples plotted in the tectonic discrimination diagram (SiO_2 vs K_2O/Na_2O) of Roser and Korsch (1986).

According to Bhatia and Crook (1986), trace element plots of La-Th-Sc can be useful in the evaluation of tectonic settings of source areas. The La-Th-Sc plot in Figure 7.11

shows that all of the Dupi Tila samples fall in a continental island arc field.

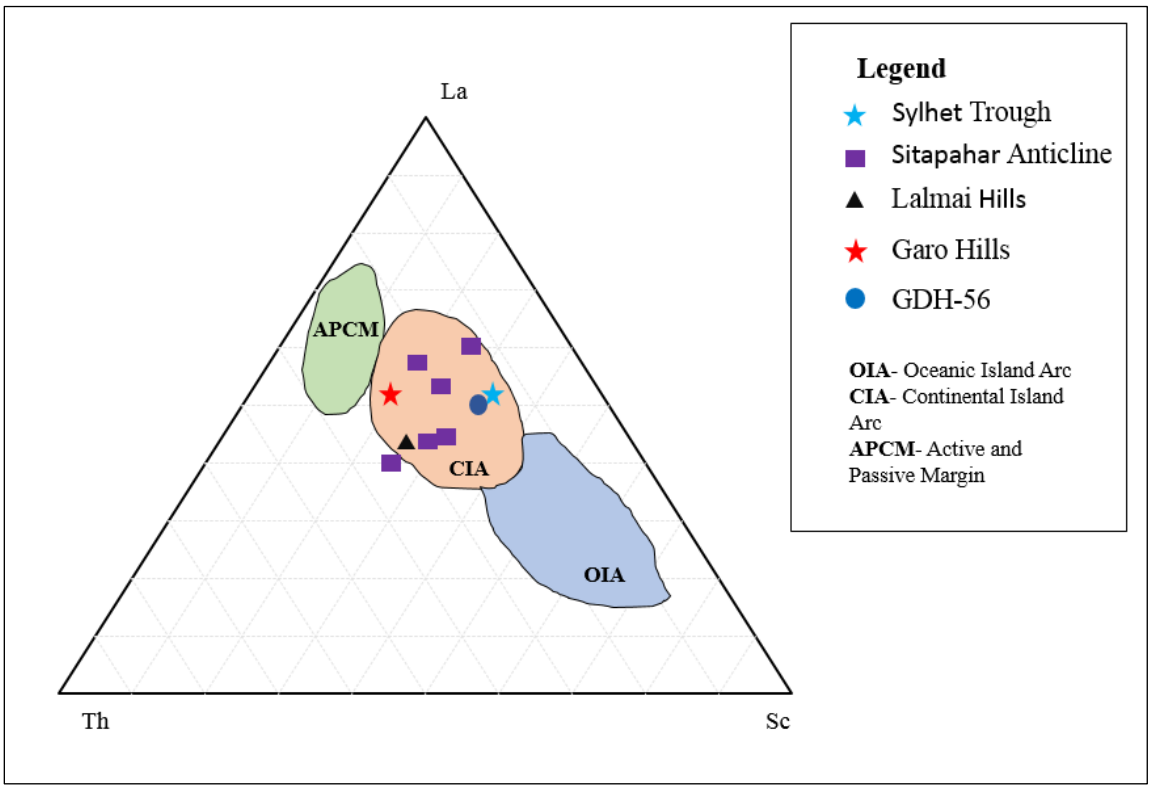

Figure 7.11 Dupi Tila samples from different regions of the Bengal basin plotted in La-Th-Sc ternary diagram. Tectonic fields are taken from Bhatia and Crook (1986).

Due to their immobility, TiO_2 and the trace element Zr can be used to discriminate among igneous source-rock types (Hayashi et al., 1997). The TiO_2 vs Zr plot in Figure 7.12 indicates felsic source rocks for most studied samples. However, the Dupi Tila samples from the Garo hills predominantly fall into the intermediate igneous rock field.

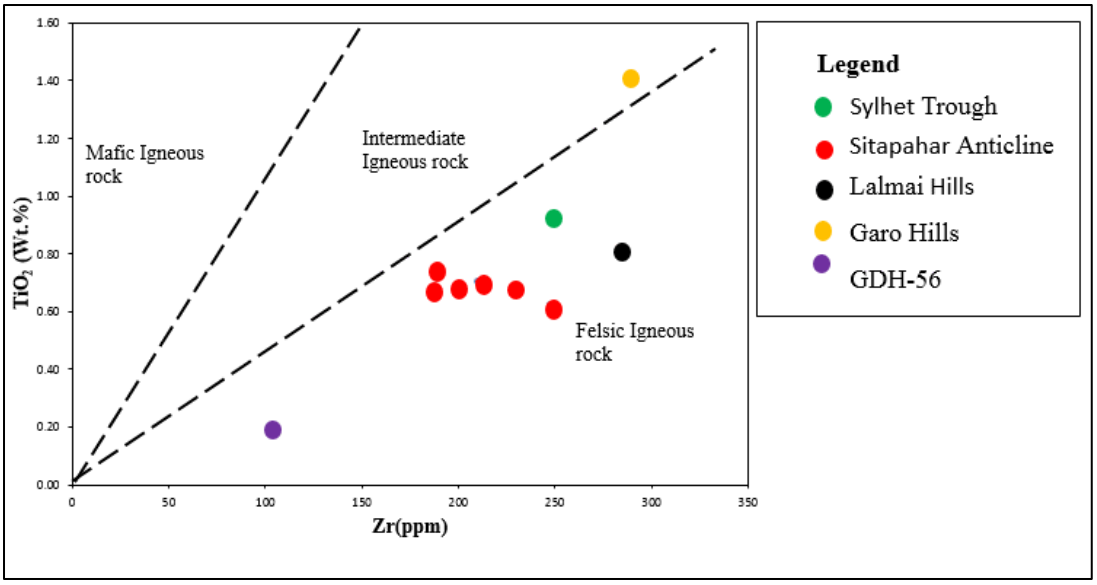

Figure 7.12 TiO_2 vs Zr plots of Dupi Tila samples from various regions of the Bengal basin. Fields are taken from Hayashi et al. (1997).

Chapter 8: DISCUSSION

8.1 PROVENANCE

Sandstone petrographic studies, heavy mineral analyses, sandstone chemistry, and bulk rock chemistry of mudrocks depict an orogenic detrital history for Dupi Tila Formation. Modal analyses of the sandstones of the Dupi Tila Formation from the Sitapahar anticline ($Qt_{64}F_{10}L_{27}$), Garo hills ($Qt_{88}F_{2}L_{10}$), Northwest Stable Platform ($Qt_{87}F_{6}L_{7}$), Sylhet Trough ($Qt_{66}F_{9}L_{25}$) and Lalmai hills ($Qt_{64}F_{6}L_{30}$) indicate that the sandstones were derived from orogenic provenances. The distribution of sedimentary and metamorphic lithic fragments in the provenance field indicate a source of low- to intermediate-grade metamorphic terrains. The heavy mineral analyses supports the Dupi Tila Formation has an orogenic source. The relative abundance of aluminosilicates and ultrastable minerals in the Dupi Tila Formation throughout the Bengal basin reflect unroofing of deeper crustal levels. Garnet, tourmaline, epidote and chloritoid chemistry also supports derivation from a low- to high-grade metamorphic facies rocks. Finally, the chemical indices of alteration from the bulk rock chemistry of Dupi Tila mudrocks reflect an active continental provenance of felsic rocks.

The Pliocene-Pleistocene Dupi Tila Formation is most likely derived from the Himalayas and the Indo-Burman ranges. Based on modal compositional analyses of all the samples, a nearby source is suggested. Possible sources also include the Mikir hills, and Mishmi hills to the northeast. The Shillong Plateau, which was uplifted during Pliocene time along the northern margin of the Bengal basin (Johnson and Nur Alam, 1991), may have provided detritus proximal to the uplift and contributed sand especially rich in sedimentary lithic fragments eroded from cover units.

The Dupi Tila Formation has more untwinned potassium feldspars than plagioclase, suggesting a plutonic source and/or an increase in mechanical weathering relative to chemical weathering in the source areas (Uddin and Lundberg, 1998b). The presence of andalusite from heavy mineral analyses also supports magmatic pluton and Miocene leucogranite in central-east Himalaya (Visona et al., 2012). Miocene leucogranites of the High Himalayan Crystalline terrane (France-Lanord et al., 1993) may have been a key source of the feldspars (Harrison et al., 1997; and many others). Mountain building in the eastern Himalaya and Indo-Burman ranges was significant and the orogenic fronts were presumably encroaching on the basin from the north and east by the Pliocene-Pleistocene (Uddin and Lundberg, 1998b). Orthopyroxenes, especially abundant hypersthene, further suggest unroofing, including that of ophiolitic rocks.

Based on sandstone modal analyses and heavy mineral study, i.e., the Garo hills samples show distinct deviation from samples from other localities. They contain more quartz, fewer lithic fragments, and different heavy mineral assemblages. It is possible that the Garo hills samples are not derived from the Dupi Tila Formation, but instead are older.

8.2 COMPARISON WITH THE UPPER SIWALIK

Neogene Siwalik sediments have been well studied along the strike of the Himalayas; e.g., in the western Himalayan foreland basin (i.e., Opdyke et al., 1982; Johnson et al., 1985; Critelli et al., 1994), in Nepal (Tamrakar and Syangbo, 2014), in Darjeeling (Kundu and Mukul, 2011), near the eastern syntaxis of the Himalayas (i.e., Chirouze et al., 2011), and the Upper Irrawaddy Formation in Myanmar (Licht et al., 2014). However, comparison of detrital history of Dupi Tila Formation with equivalent Upper Siwalik Formation has not yet been carried out in the Bengal basin.

The Dupi Tila sediment shows fining upward sequences, whereas the Upper Siwalik sediments are coarsening upward and relatively proximal to the orogenic belt. Both the Upper Siwalik and Dupi Tila Formation sourced from the deeper part of the orogenic system. Like the Upper Siwaliks, the sandstone modal composition and detrital heavy

mineral suites reflect that the sources of the Dupi Tila Formation are orogenic, and most likely located in the eastern Himalayas and Indo-Burman ranges.

Sediments of the Siwalik and Dupi Tila sediments formations fall into similar field on the ternary diagrams (Fig. 8.1-8.3). On the Q_tFL diagram, samples fall dominantly in the "recycled orogenic" field. On Q_mFL_t diagram, samples fall dominantly in the "transitional recycled" field. Q_mPK plots shows the predominance of quartz and plagioclase feldspars.

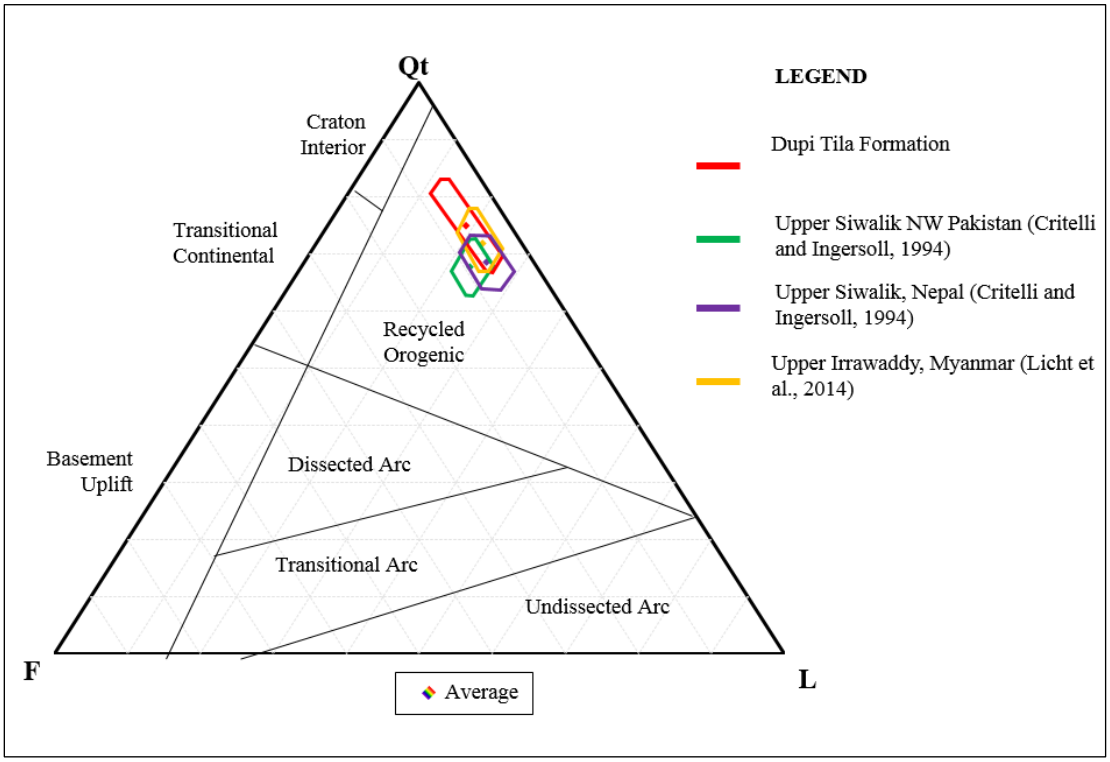

Fig. 8.1 QtFL plot of the Dupi Tila Formation of the Bengal basin (mean from all sites), and Upper Siwalik from northwest Pakistan, Upper Siwalik, Nepal (data from Ingersoll and Critelli, 1994), and Upper Irrawaddy, Myanmar (data from Licht et al., 2014) showing mean and standard deviation polygons (provenance fields are taken from Dickinson, 1985).

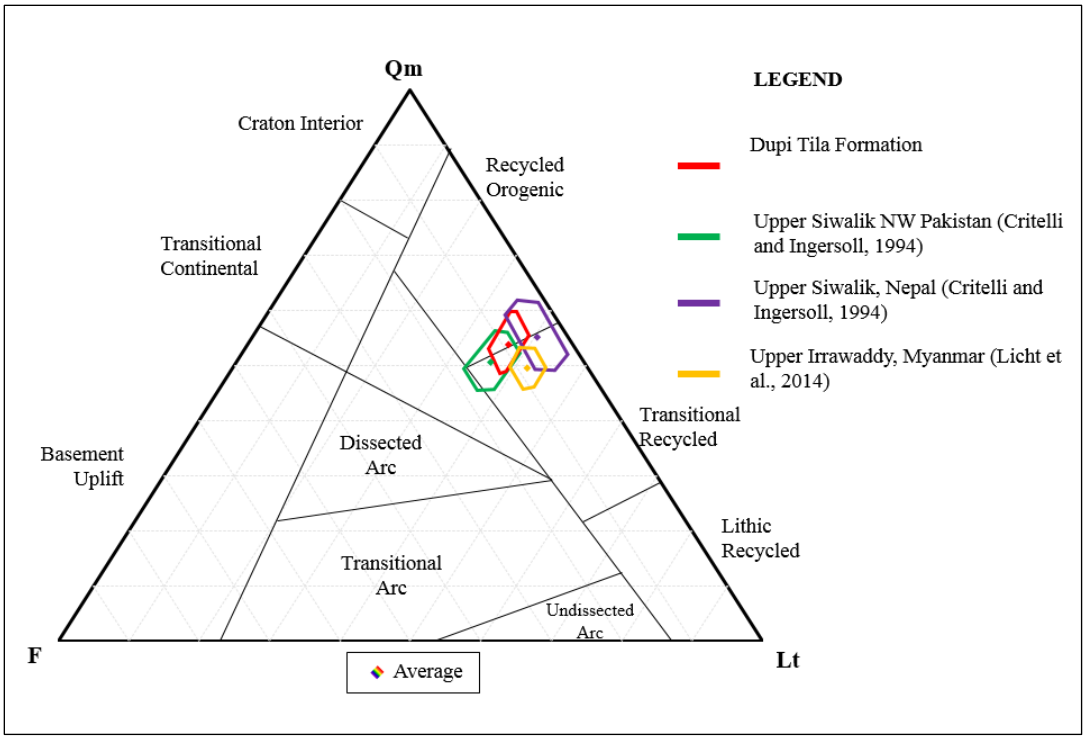

Fig. 8.2 QmFLt plot of the Dupi Tila Formation of the Bengal basin (mean from all sites), and Upper Siwalik from northwest Pakistan, Upper Siwalik, Nepal (data from Ingersoll and Critelli, 1994), and Upper Irrawaddy, Myanmar (data from Licht et al., 2014) showing mean and standard deviation polygons (provenance fields are taken from Dickinson, 1985).

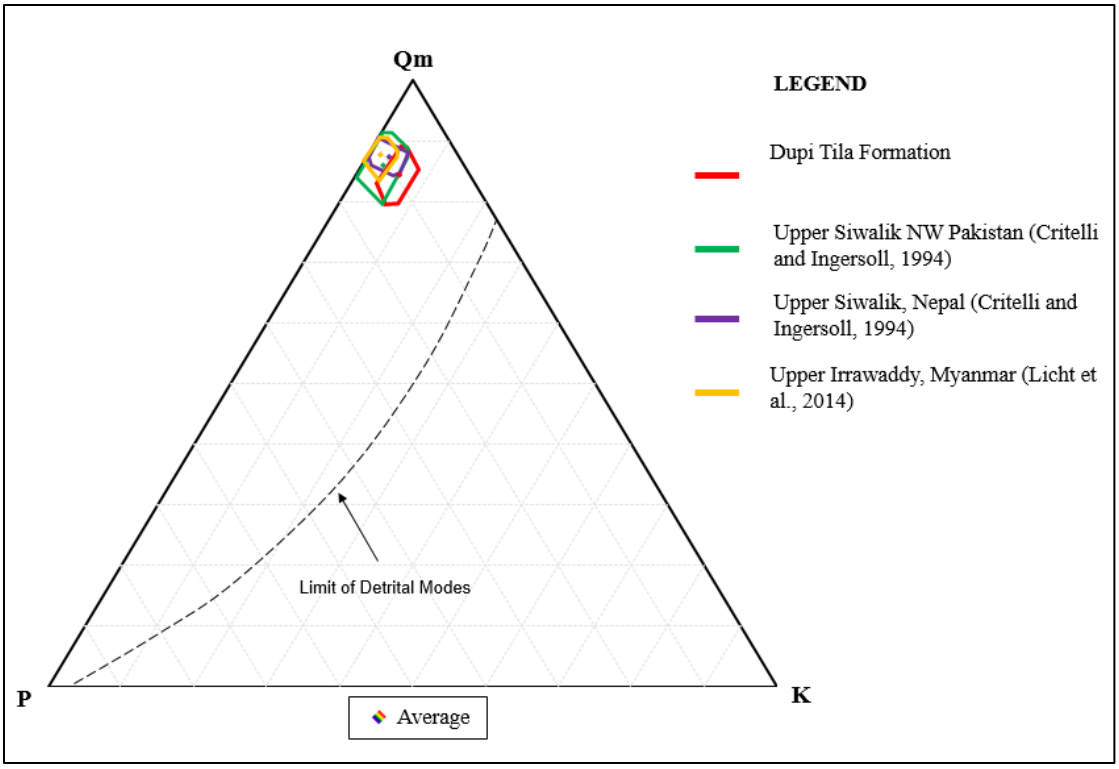

Fig. 8.3 QmPK plot of the Dupi Tila Formation of the Bengal basin (mean from all sites), and Upper Siwalik from northwest Pakistan, Upper Siwalik, Nepal (data from Ingersoll and Critelli, 1994), and Upper Irrawaddy, Myanmar (data from Licht et al., 2014) showing mean and standard deviation polygons.

The Dupi Tila Formation from different parts of the Bengal basin also compare favorably (Fig. 8.4) with those of the Upper Siwalik of the northwestern Himalaya (Chaudrhri, 1972; Gill, 1984) with respect to heavy mineral assemblages. Both units are characterized by high abundances of sillimanite, staurolite, ZTR, garnet, andalusite, epidote-group minerals, and kyanite minerals. Sillimanite is the index mineral for both of the formations.

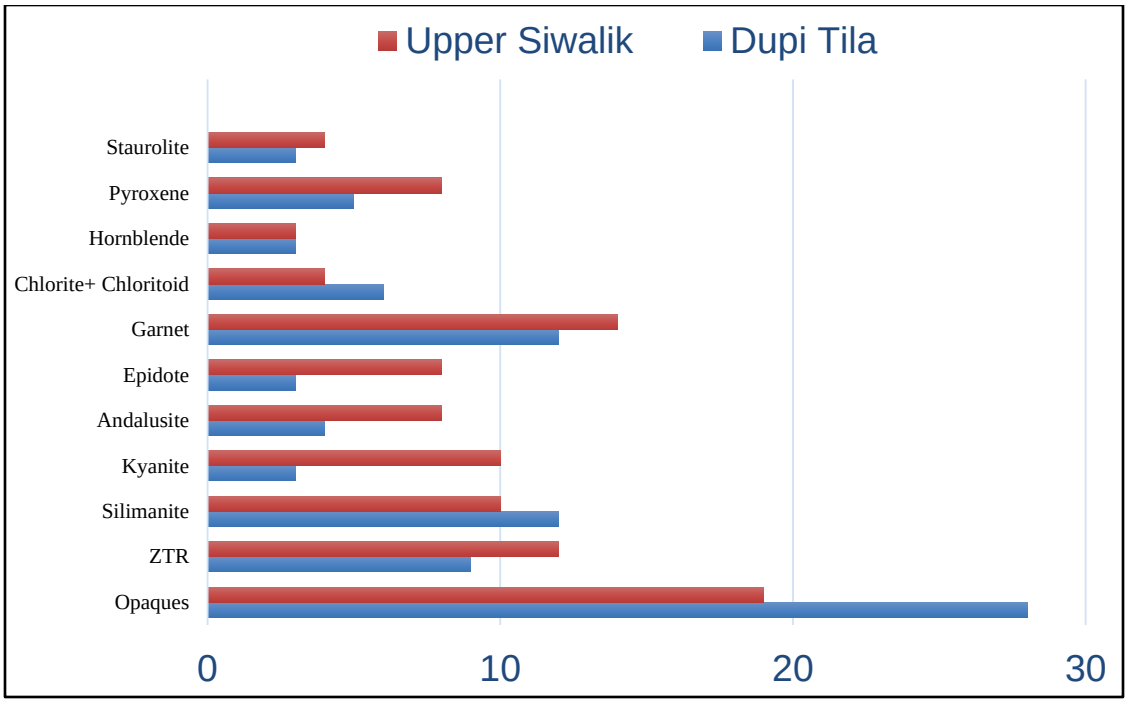

Fig. 8.4 Average heavy mineral frequency of distribution of Upper Siwaliks of the northwestern Himalaya (Chaudhri, 1972; Gill, 1984) and Dupi Tila Formation from several parts of the Bengal basin (ZTR- Zircon-Tourmaline-Rutile).

8.3 COMPARISON WITH OLDER BENGAL BASIN SANDSTONE UNITS

Data obtained from modal analysis in previous studies of the Eocene Cherra and Kopili Formations (Uddin and Lundberg, 1998b), Oligocene Barail Formation (Rahman, 2008), Early Miocene Bhuban Formation (Uddin and Lundberg, 1998b), Middle Miocene Boka Bil Formation (Uddin and Lundberg, 1998b), Late Miocene Tipam Sandstone (Rahman, 2008) are plotted along with the Dupi Tila data in figures 8.5-8.8. QtFL and QmFLt plots indicate that older formations are relatively more quartzose and feldspathic (Fig. 8.5, 8.6). Although the Eocene sandstones are completely non-orogenic, however, Oligocene and younger units including the Dupi Tila Formation, seem to have a 'recycled orogenic' source. The Miocene units also are more feldspathic compared to the Dupi Tila Formation, which suggest a change in sediment dispersal in the Bengal basin. In QmPK monocrystalline plot, the Dupi Tila sediments resemble that of Middle Miocene Bhuban Formation (Fig. 8.7).

The $LsLm_1Lm_2$ plots clearly show a temporal change in relative abundance of lithic fragment types that reflects the progressive unroofing of the orogenic source regions. Lithic fragments in Eocene sandstones are mostly sedimentary, reflecting supracrustal sources whereas metamorphic lithic fragments, particularly intermediate- to higher-grade types, become increasingly more abundant through time, reflecting unroofing to deeper crustal levels (Fig. 8.8).

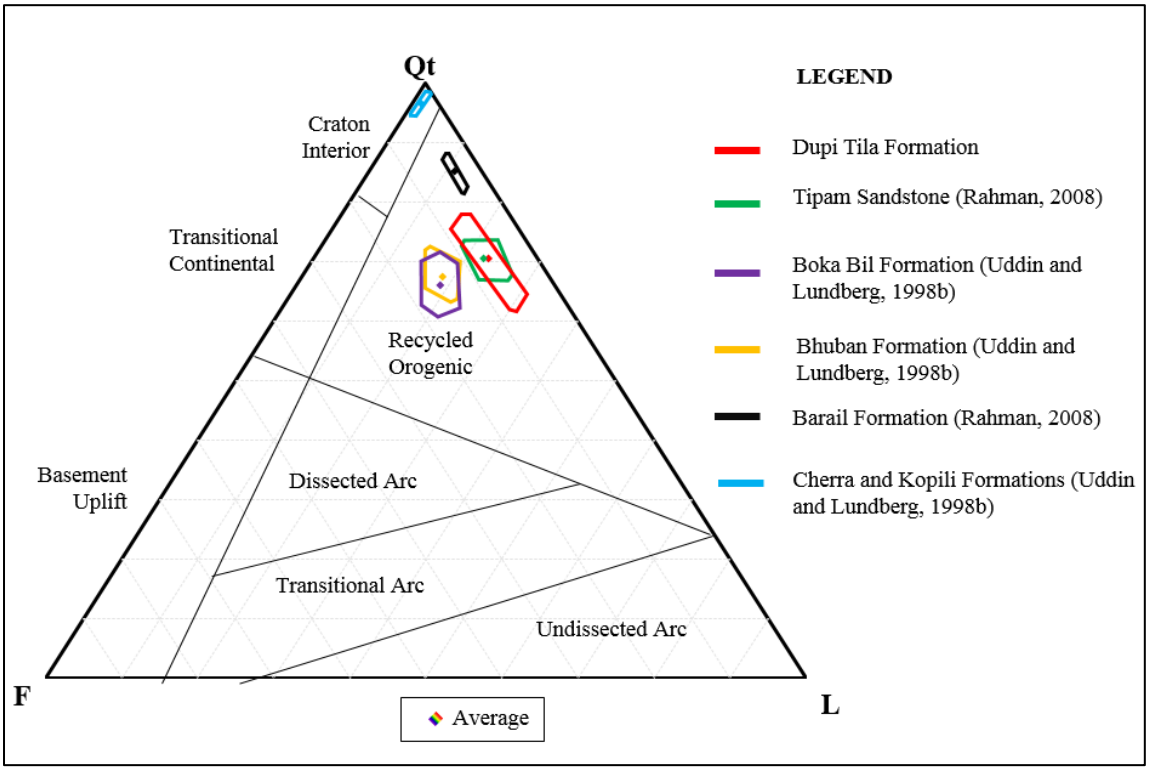

Fig. 8.5 QtFL plots of different formations from Bengal basin stratigraphy showing distribution of sandstones modes within a well defined compositional field. Provenance fields are taken from Dickinson (1985). Data source- Eocene Cherra and Kopili Formations (Uddin and Lundberg, 1998b), Oligocene Barail Formation (Rahman, 2008), Early Miocene Bhuban Formation (Uddin and Lundberg, 1998b), Middle Miocene Boka Bil Formation (Uddin and Lundberg, 1998b), and Late Miocene Tipam Sandstone (Rahman, 2008).

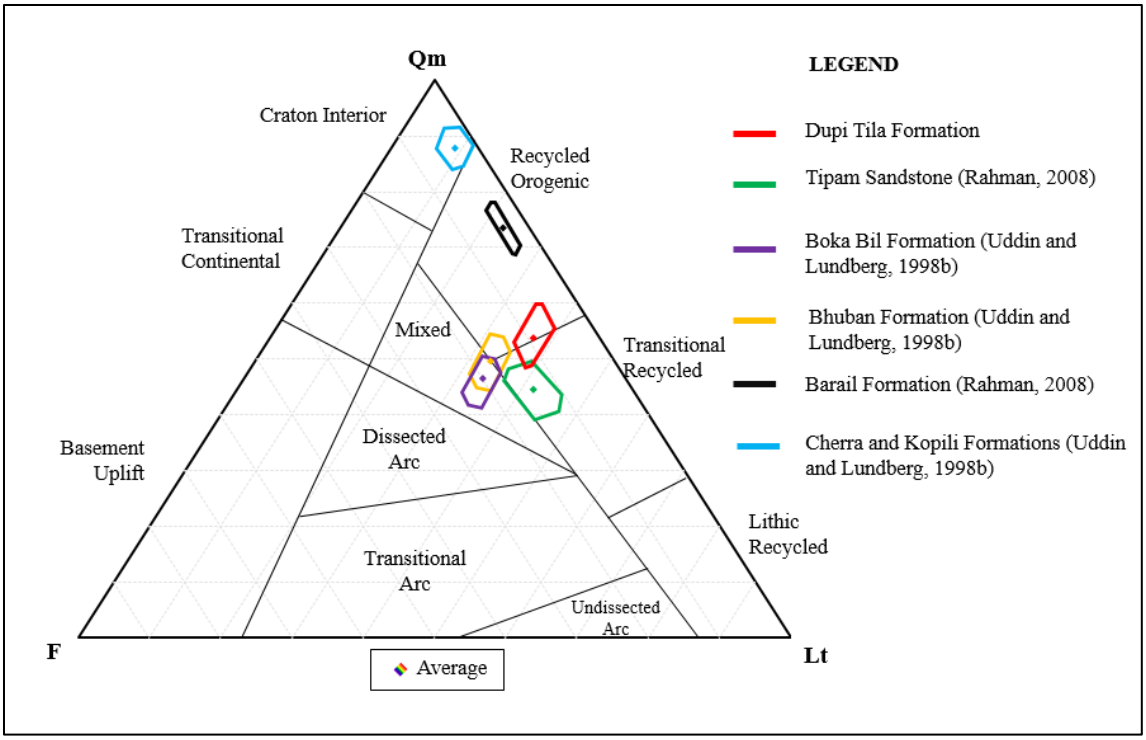

Fig. 8.6 QmFLt plot of different formations from Bengal basin stratigraphy showing distribution of sandstones modes within a well defined compositional field. Provenance fields are taken from Dickinson (1985). Data source- Eocene Cherra and Kopili Formations (Uddin and Lundberg, 1998b), Oligocene Barail Formation (Rahman, 2008), Early Miocene Bhuban Formation (Uddin and Lundberg, 1998b), Middle Miocene Boka Bil Formation (Uddin and Lundberg, 1998b), and Late Miocene Tipam Sandstone (Rahman, 2008).

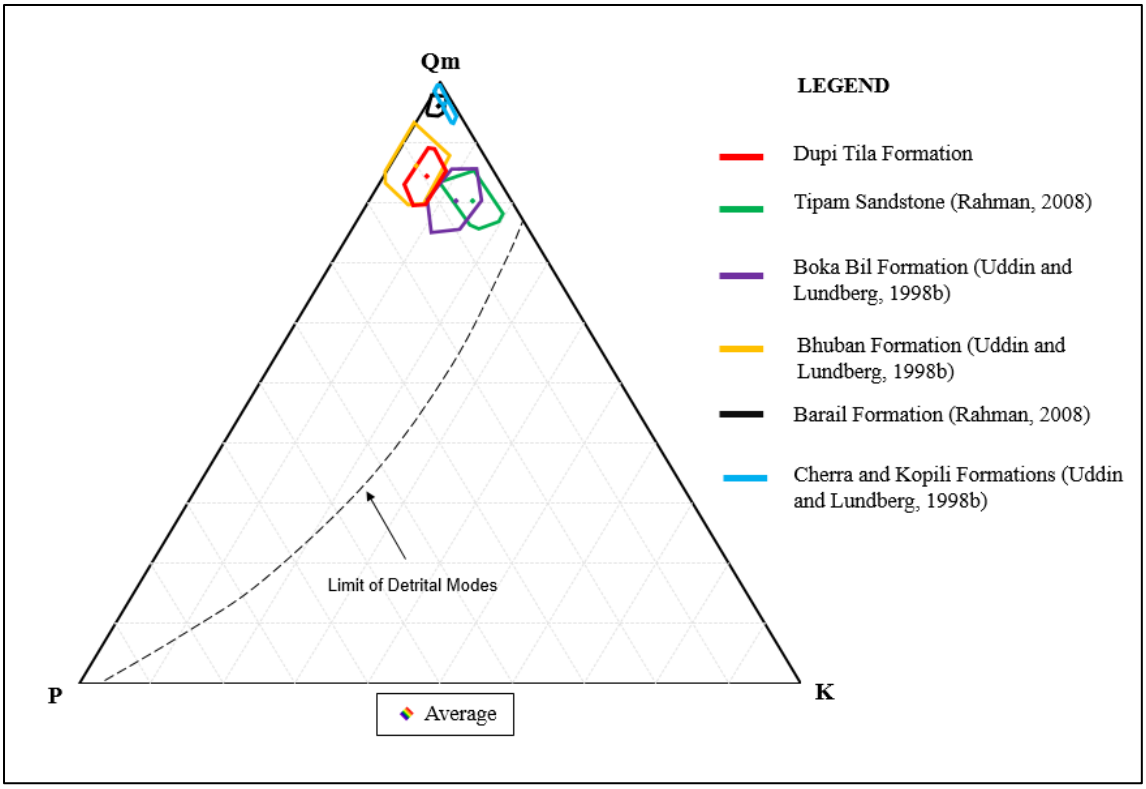

Fig. 8.7 QmPK plot of different formations from Bengal basin stratigraphy showing distribution of sandstones modes. Data source- Eocene Cherra and Kopili Formations (Uddin and Lundberg, 1998b), Oligocene Barail Formation (Rahman, 2008), Early Miocene Bhuban Formation (Uddin and Lundberg, 1998b), Middle Miocene Boka Bil Formation (Uddin and Lundberg, 1998b), and Late Miocene Tipam Sandstone (Rahman, 2008).

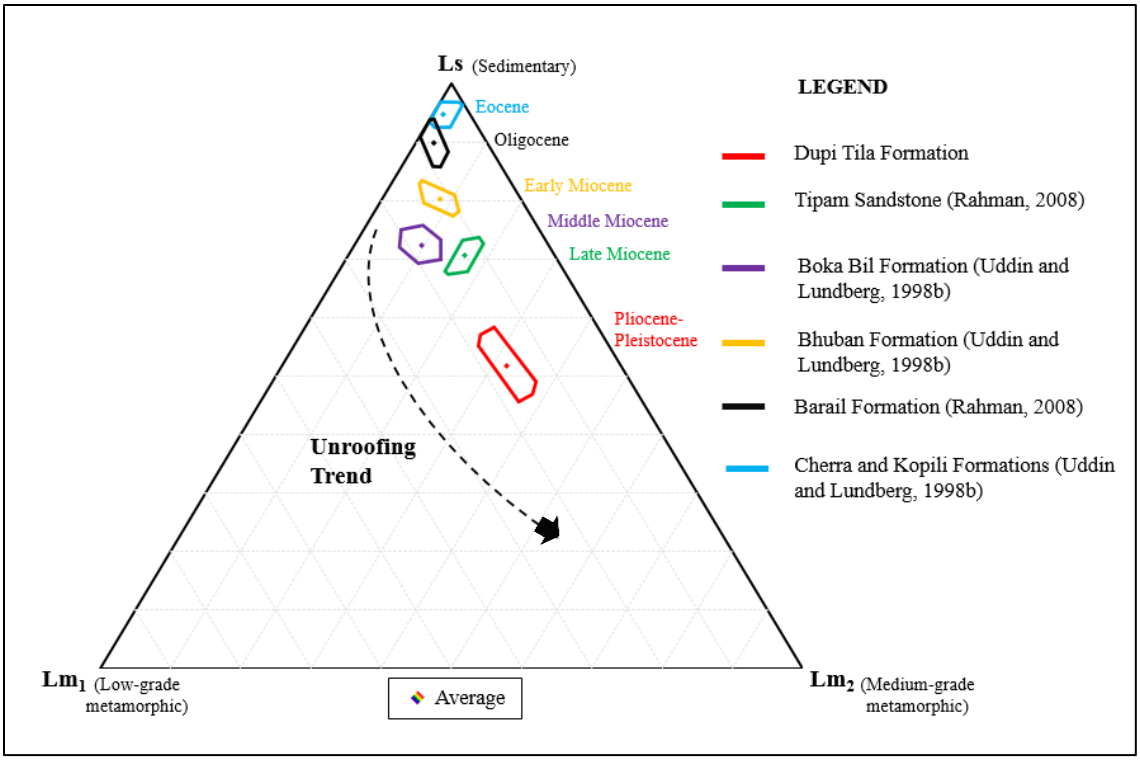

Fig. 8.8 $LsLm_1Lm_2$ plot of different formations from the Bengal basin stratigraphy showing variation of lithic fragments within a well defined compositional field adapted from Dorsey (1988). Data source- Eocene Cherra and Kopili Formations (Uddin and Lundberg, 1998b), Oligocene Barail Formation (Rahman, 2008), Early Miocene Bhuban Formation (Uddin and Lundberg, 1998b), Middle Miocene Boka Bil Formation (Uddin and Lundberg, 1998b), and Late Miocene Tipam Sandstone (Rahman, 2008).

8.4 PALEOCLIMATE IN THE SOURCE

The chemical indices of alteration (CIA) derived from analyses of Dupi Tila mudrocks indicate a moderate to intense weathering in the source terranes. This is consistent with inferences that can be drawn from sandstone petrography. A bivariant log-log plot of the ratios of polycrystalline quartz to feldspar plus rock fragments versus total quartz to feldspar plus rock fragments (Fig. 8.9) indicates that all Dupi Tila samples were derived from humid to semi-humid source areas, wherein weathering would be significant.

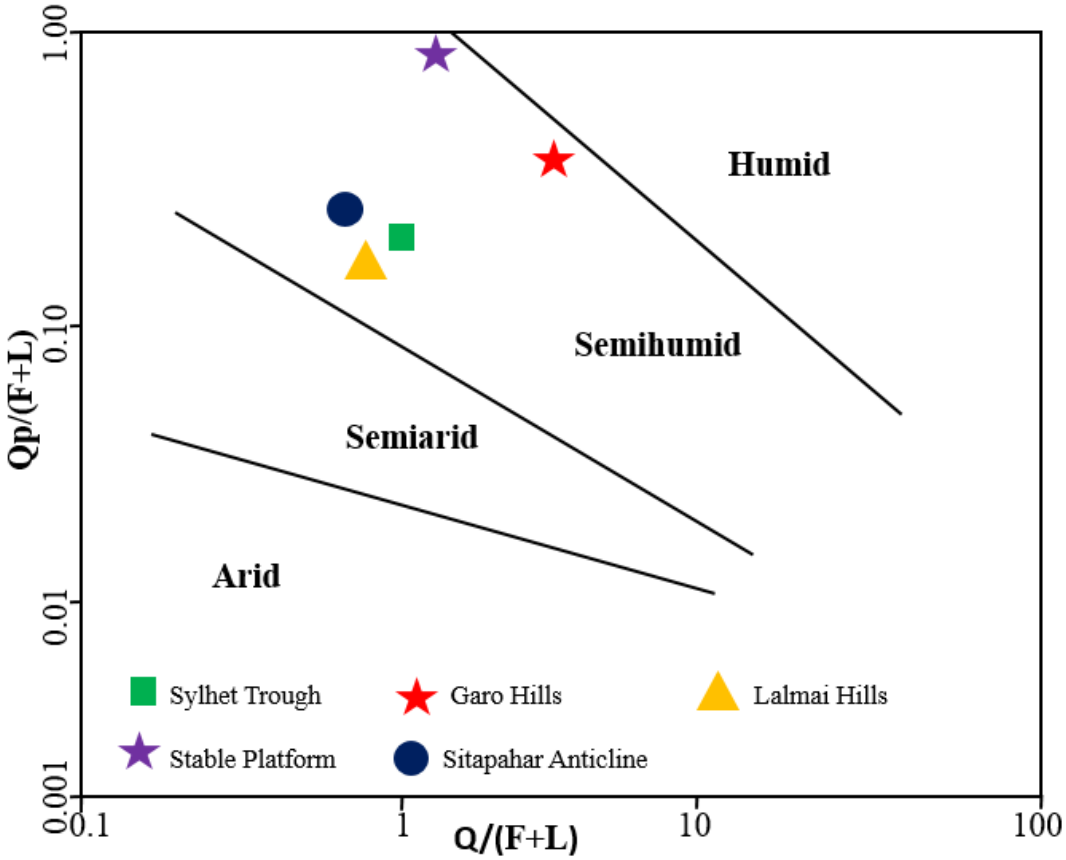

Fig. 8.9 Qp/(F+L) vs Q/(F+L) plot of source-area climatic regimes based on Suttner and Dutta (1986).

8.5 PALEOTECTONIC SETTING

The modal composition of sandstones from the present study area reflects the changes in detrital history and hinterland tectonics. The quartzose composition, paucity of unstable grains (e.g., lithic fragments and feldspar), and high ZTR indices of sandstone from the Dupi Tila Formation suggest proximity to an orogenic system. The Himalaya and Indo-Burma Ranges probably supplied sediments in the study area during the Pliocene-Pleistocene.

During the Miocene, the study area received sediments continuously from orogenic sources as revealed from previously reported sandstone compositional data (Uddin and Lundberg, 2004; Uddin et al., 2010). The depositional lobe, which formed in upper Assam during the Eocene, prograded south-southwestward through the study area and western part of Indo-Burma Ranges (Fig. 8.10A, Mandal, 2009).

During Pliocene time, sediment continued to be delivered from the orogenic belts into an actively prograding Bengal foreland basin. The Shillong Plateau, which was uplifted in the Pliocene along the northern margin of the Bengal basin, may have provided another source for detritus proximal to the uplift (Fig. 8.10B, C; Johnson and Nur Alam, 1991). Due to continuous crustal shortening, the Indo-Burman Ranges became a structural high towards the end of the Miocene-Pliocene and may have become a source of detritus in the Bengal basin. This is indicated by the presence of pyroxenes in the Dupi Tila sandstones. Due to the uplift of the Shillong Plateau, the paleo-Brahmaputra shifted its course from east to west (Fig. 8.10D, Uddin and Lundberg, 1999). Due to the presence of Mn-rich garnet (spessartine) in the Dupi Tila Formation, it can be concluded that, not only there is sediment contribution from orogeny, but the Rajmahal traps might also have contributed to the Bengal basin.

Similarly, paleo-Ganges sedimentary fluxes came from the western side of the Bengal basin (Stable Platform) as evidenced by the Tista fan depositing at northwestern end of the Bengal basin (Fig. 8.10C, Reimann, 1993).

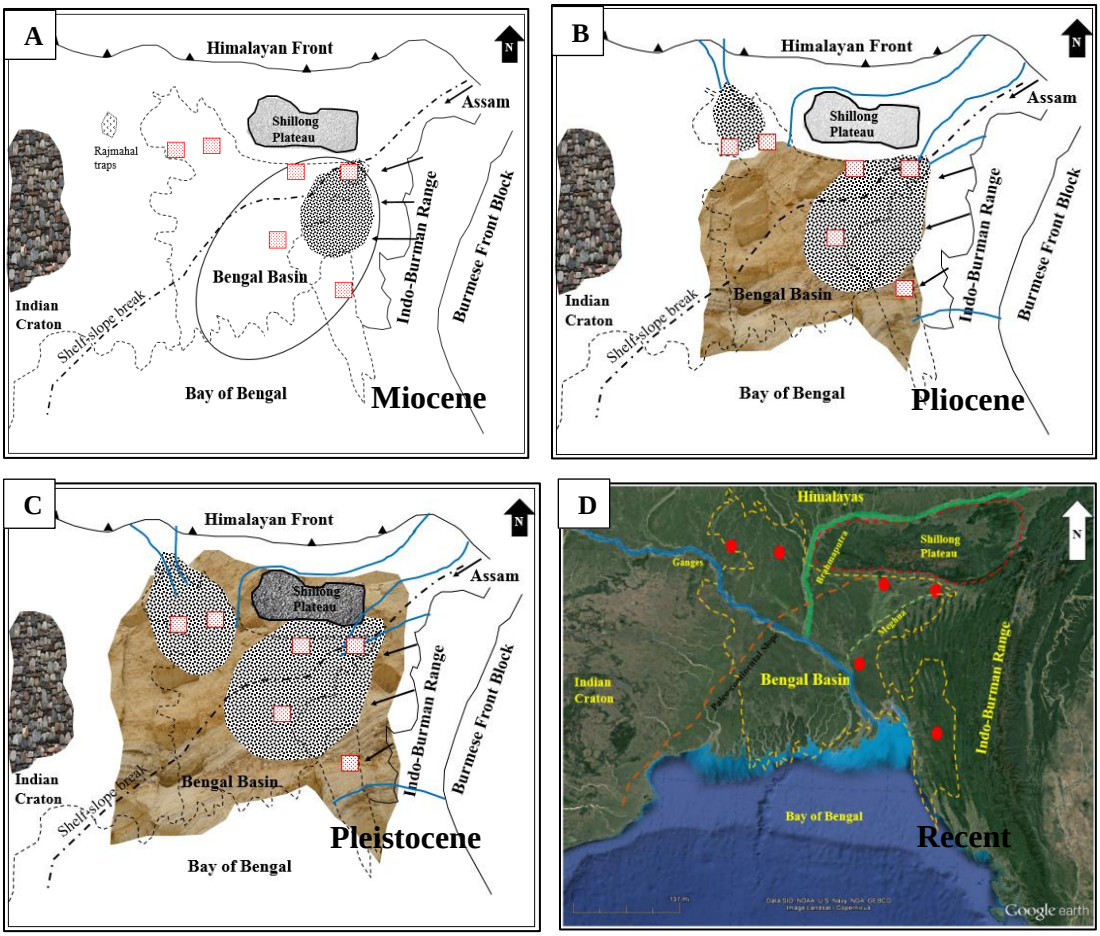

Fig. 8.10 Paleogeographic reconstruction Maps of the study area (in red box) with reference to the Bengal basin. Dotted textures are the deposition lobe prograding basinward with time and progressive move of depocenters. Brown shaded areas are the extent of deposits of the Dupi Tila Formation. Blue lines are rivers. The Shlillong Plateau uplifted during the Pliocene (A- Miocene, after Mandal, 2009, B- Pliocene, C- Pleistocene, and D-Recent, Google Earth).

Chapter 9: CONCLUSIONS

Based on sandstone modal composition, heavy mineral assemblages, electron probe analyses and whole rock chemistry of mudrocks, the following inferences can be drawn from this study:

1. The Dupi Tila sediments of the Bengal basin are orogenic. Clastic sediments were derived from the exhumation of the Himalayas and Indo-Burman Ranges.

2. Sandstone compositions indicate that sediments of the Dupi Tila Formation are predominantly comprised of monocrystalline quartz, polycrystalline quartz, plagioclase feldspar, orthoclase feldspar and metamorphic (primarily Lm_2) and sedimentary lithic fragments.Volcanic lithic fragments are absent. Their compositions indicate that Dupi Tila sediments were derived from low- to intermediate-grade metamorphic and granitoid terranes.

3. The presence of sillimanite (fibrolites), kyanite, andalusite, staurolite, and ZTR minerals suggest that the sediments were sourced from the low- to high-grade metamorphic rocks.

4. The abundance of almandine garnet indicates amphibole and granulite facies provenances. The presence of Mn-rich garnets in the Stable platform samples indicate sediments were partly sourced from the Rajmahal volcanic trap. Tourmaline chemistry suggests that sediments were sourced from Al-saturated metapelites, clac-silicates, metasammites, Li –bearing pegmatites, granitoid pegmatites, and aplites. Epidote compositions indicate derivation from relatively high-grade metamorphic rocks of epidote-amphibolite facies. Chloritoid chemistry suggests a source from high-pressure blueschist metamorphic facies.

5. Bulk sediment chemistry data indicate that the sediments were sourced from felsic igneous rocks (i.e., average granitoid terranes) in an active continental provenance. The chemical indices of alteration indicate intense weathering in the source terranes.

6. Sandstone modal studies indicate that the Upper Siwalik sediments from the northwest Pakistan, Nepal, and Upper Irrawaddy Formation from Myanmar are very similar to those of the Dupi Tila Formation. Sillimanite is the index mineral for both the Upper Siwaliks and Dupi Tila Formation.

7. When compared with sandstones of older Cenozoic sequences of the Bengal basin, the sedimentary and metamorphic lithic fragments of the Dupi Tila Formation strongly show a progressive unroofing of the Himalayas and Inro-Burman ranges.

8. Modal compositions and heavy mineral distributions suggest the Dupi Tila sediments form the Garo hills are different than other Dupi Tila sequences of the basin. This calls into question the true stratigraphic position of the Dupi Tila at Garo hills.

REFERENCES

Alam, A.K.M. M., Xie, S., and Chowdhury, S.Q., 2009. Clay Mineralogy and Diagenesis of Shale: A Case Study from the Mio-Pliocene Tipam and Dupi Tila Shales of Bandarban Anticline, Bandarban Hill Tracts, Bangladesh: Journal of Applied Sciences, v. 9, p. 2770-2777.

Alam, M., Alam, M.M., Curray, J.R., Chowdhury, M.L.R., and Gani, M.R., 2003. An overview of the sedimentary geology of the Bengal basin in relation to the regional tectonic framework and basin-fill history: Sedimentary Geology, v. 155, p. 179–208.

Alam, M.I., 2011. Petrofacies and Paleotectonic Evolution of Permo-Carboniferous Gondwanan Sequences of the Bengal basin, Bangladesh [unpublished M.S. Thesis]: Auburn University, Auburn, AL, 134 p.

Amano, K., and Taira, A., 1992. Two-phase uplift of Higher Himalayas since 17 Ma: Geology, v. 20, p. 391-394.

Auden, J. B., 1935. Traverses in the Himalaya: Record of Geological Survey of India, v. 69, p. 123–169.

Bakhtine, M.I., 1966. Major tectonic features of Pakistan, Part II, The eastern province: Science and Industry, v. 4, p. 89-100.

Bhatia, M., 1983. Plate tectonics and geochemical composition of sandstones: Journal of Geology, v. 91, p. 611-627.

Bhatia, M. R., and Crook, K. A. W., 1986. Trace element characteristics of greywacke and tectonic setting discrimination of sedimentary basins: Contributions to Mineralogy and Petrology, v. 92, p. 181-193.

Blatt, H., 1967. Provenance determinations and recycling of sediments: Journal of Sedimentary Research, v. 37.

Basu, A., 1976. Petrology of Holocene fluvial sand derived from plutonic source rocks: implications to paleoclimatic interpretation: Journal of Sedimentary Research, v. 46.

Basu, A., Young, S. W., Suttner, L. J., James, W. C., and Mach, G. H., 1975. Reevaluation of the use of undulatory extinction and polycrystallinity in detrital quartz for provenance interpretation: Journal of Sedimentary Petrology, v. 45, p. 873-882.

Bateman, R.M., and Catt, J.A., 1985. Modification of heavy mineral assemblages in English coversands by acid pedochemical weathering: Catena, v. 12, p. 1-21.

Bilham, R., and England, P., 2001. Plateau 'pop-up' in the great 1897 Assam earthquake: Nature, v. 410, p. 806-809.

Buddington, A. F., AND Lindsley, D. H., 1964. Iron-titanium oxide minerals and synthetic equivalents: Journal of Petrology, v. 5, p. 310-357.

Burbank, D. W., Beck, R. A., and Mulder, T., 1996. The Himalayan Foreland Basin: In the Tectonic evolution of Asia: Cambridge University Press, p. 149-188.

Catlos, E.J., Harrison, T.M., Manning, C.E., Grove, M., Rai, S.M., and Hubbard, M.S., 2002. Records of the evolution of the Himalayan orogen from in situ Th-Pb ion microprobe dating of Monazite: Eastern Nepal and western Garhwal: Journal of Asian Earth Sciences, v. 20, p. 459-479.

Cerveny, P.F., 1986. Uplift and Erosion of the Himalaya over the past 18 Million years: Evidence from fission track dating of detrital zircons and heavy mineral analysis: unpublished M.S. thesis, Dartmouth College, 198 p.

Chaudhri, R.S., 1972. Heavy minerals from the Siwalik formations of the northwestern Himalayas: Sedimentary Petrology, v. 8, p. 77-82.

Chirouze, F., Dupont-Nivet, G., Huyghe, P., Van der Beek, P., Chakraborti, T., Bernet, M., and Erens, V., 2011. Magnetostratigraphy of the Neogene Siwalik Group in the far eastern Himalaya: Kameng section, Arunachal Pradesh, India: Asian Earth Sciences, v. 44, p. 117-135.

Chowdhury, N.U.Md.K., 2014. Paleogeographic reconstruction of part of Eastern Gondganaland: Paterofacies and Detrital Geochronologic study of Permo-Carboniferous Gondwanan Sequences of India and Bangladesh: M.S. Thesis (unpublished), 169 p.

Chopin, C., and Schreyer, P., 1983. A unique magnesiochloritoid-bearing, highpressure assemblage from the Monte Rosa, Western Alps: petrologic and 40Ar-39Ar radiometric study: Contribution of Mineral Petrology v. 87, p. 388-398.

Clark, M.K., and Bilham, R., 2008. Miocene rise of the Shillong Plateau and the beginning of the end for the Eastern Himalaya: Earth and Platetary Science Letters, v. 269, p. 337-351.

Cox, R., Lowe, D. R., and Cullers, R. L., 1995. The influence of sediment recycling and basement composition on evolution of mudrock chemistry in the southwestern United States: Geochimica et Cosmochimica Acta, v. 59, no. 4, p. 2919-2940.

Critelli, S., and Ingersoll, R.V., 1994. Sandstone Petrology and Provenance of the Siwalik Group (NW Pakistan and WS Nepal): Journal of Sedimentary Research, v. 64, p. 815-823.

Curray, J.R., 1991. Geological history of the Bengal geosyncline: Journal of Association of Exploration of Geophysicist XII, v. 12, p. 209-219.

Curray, J.R., and Moore, D.G., 1974. Sedimentary and tectonic processes of the Bengal deep-sea fan and geosyncline: in Burk, C.A., and Drake, C.L., eds., The Geology of Continental Margins: New York, Springer-Verlag, p. 617-628.

Curray, J. R., Moore, D. G., Lawver, L. A., Emmel, F. J., Taitt, R. W., Henry, M., and Kieckhefer, R., 1979. Tectonics of the Andaman Sea and Burma, in Watkins, J.S., Montadert, L., and Dickinson, P., eds., Geological and geophysical investigations of continental margins: American Association of Petroleum Geologists, Memoir 29, p. 189-198.

Darby, D. A., 1984. Trace elements in ilmenite: a way to discriminate provenance or age in coastal sands: Geological Society America Bulletin, v. 95, p. 1208-1218.

Darby, D. A., Tsang, Y. W., and Council Ill, E. A., 1985. Detrital ilmenite composition: implications for coastal sand sources and dispersal pathways: Geological Society of America Abstract Program, v. 17, p. 559.

Darby, D.A., Tsang, Y.W., 1987. Variation in ilmenite element composition within and among drainage basins: implications for provenance: Journal of Sedimentary Petrology, v. 57, p. 831–838.

DeCelles, P.G., Gehrels, G.E., Quade, J., Ojha, T.P., Kapp, P.A., and Upreti, B.N., 1998. Neogene foreland basin deposits, erosional unroofing, and the kinematic history of the Himalayan fold-thrust belt, western Nepal: Geological Society of America Bulletin, v. 110, p. 2-21.

DeCelles, P.G., Robinson, D.M., Quade, J., Ojha, T.P., Garzione, C.N., Copeland, P., and Upreti, B.N., 2001. Stratigraphy, structure, and tectonic evolution of the Himalayan fold-thrust belt in western Nepal: Tectonics, v. 20, p. 487-509.

Decelles, P.G., Gehrels, G.E., Najman, Y., Martin, A.J., Carter, A., and Garzanti, E., 2004. Detrital Geochronology and geochemistry of Cretaceous-early Miocene strata of Nepal: implications for timing and diachroneity of initial Himalayan orogenesis: Earth and Planetary Science Letters, v. 277, p. 313-330.

Deer, W.A., Howie, R.A., and Zussman, J., 1992. Rock-Forming Minerals (2nd ed.): London, Longman Scientific Technical, Harlow, United Kingdom, 696 p.

Dickinson, W.R., 1970. Interpreting detrital modes of greywacke and arkose: Journal of Sedimentary Petrology, v. 40, p. 695-707.

Dickinson, W.R., and Suczek, C.A., 1979. Plate tectonics and sandstone compositions: American Association of Petroleum Geologist Bulletin, v. 63, p. 2164-2182.

Dickinson, W.R., 1982. Composition of sandstones in Circum-Pacific subduction complexes and fore-arc basins: American Association of Petroleum Geologists Bulletin, v. 66, p. 121-137.

Dickinson, W.R., 1985. Interpreting provenance relations from detrital modes of sandstone, in Zuffa, G.G., ed., Reading Provenance from Aranites: Dordecht, The Netherlands, Riedel, v. 148, p. 333-361.

Dollase, W.A., 1971. Refinement of the crystal structures of epidote, allanite and hancockite: American Mineralogist, v. 56, p. 447-464.

Dorsey, R. J., 1988. Provenance evolution and unroofing history of a modern arc continent collision: Evidence from petrography of Plio-Pleistocene sandstones, eastern Taiwan: Journal of Sedimentary Petrology, v. 58, p. 208-218.

Dryden, A.L., and Dryden, C., 1946. Comparative rates of weathering of some common heavy minerals: Journal of Sedimentary Petrology, v. 16, p. 91-96.

Enami, M., and Banno, S., 1980. Zoisite-clinozoisite relations in low- to medium-grade high-pressure metamorphic rocks and their implications: Mineralogical Magazine, v. 43, p. 1005-1013.

Evans, P., 1964. Tertiary succession in Assam: Transactions of Mineralogical and Geological Institute of India, v. 27, p. 155-260.

Fedo, C. M., Nesbitt, H. W., and Young, G. M., 1996. Unraveling the effects of metasomatism in sedimentary rocks and paleosols, with implications for paleoweathering conditions and provenance: Geology, v. 23, p. 921-924.

France-Lanord, C., Derry, L. and Michard, A., 1993. Evolution of the Himalaya since Miocene time: Isotopic and sedimentologic evidence from the Bengal Fan, in Himalayan Tectonics, edited by P. J. Treloar and M. Searle: Geological Soc. Spec. Publ., v. 74, p. 603–621.

Freise, F.W., 1931. Untersuchung von Mineralen auf Ab-nutzbarkeit bei Verfrachtung im Wasser: Tschermaks Mineralogy of Petrology, v. 41, p. 1-7

Gani, M.R., Alam, M. M., 2002. Fluvial facies architecture in small-scale river systems in the Upper Dupi Tila Formation, northeast Bengal basin, Bangladesh: Journal of Asian Earth Sciences, v. 24, p. 225-236.

Gansser, A., 1964. Geology of the Himalayas: Interscience, London, 289 p.

Garzanti, E., Critelli, S., and Ingersoll, R. V., 1996. Paleogeographic and paleotectonic evolution of the Himalayan range as reflected by detrital modes of Tertiary sandstones and modern sands (Indus transect, India and Pakistan): Geological Society of America Bulletin, v. 24, p. 631–642.

Garzanti, E., Vezzoli, G., Ando, S., Lave, J., Attal, M., France-Lanord, C., and Decelles, P., 2007. Quantifying sand provenance and erosion (Marsyandi River, Nepal Himalaya): Earth and Planetary Sciences Letters, v. 258, p. 500-515.

Gill, G.T.S., 1984. Heavy mineral assemblage of the Siwalik Group exposed between the rivers Ghaggar and Markanda, northwestern Himalaya. In: Srivastava, R.A.K. (Ed.), Sedimentary Geology of the Himalaya: Current Trends in Geology, v. 5, p. 223–234.

Graham, S.A., Ingersoll, R.V., and Dickinson, W.R., 1976. Common provenance for lithic grains in Carboniferous sandstones from Ouachita Mountains and black Warrior Basin: Journal of Sedimentary Petrology, v. 46, p. 620-632.

Grimm, W.D., 1973. Stepwise heavy mineral weathering in the residual quartz gravel, Bavarian Molasse (Germany): Contribution to Sedimentology, v. 1, p 103-125.

Harrison, T.M., Ryerson, F.J., Le Fort, P., Yin, A., Lovera, O.M., Catlos, E.J., 1997. A Late Miocene-Pliocene origin for central Himalayan inverted metamorphism: Earth and Planetary Sciences Letters, v. 146, p. 1-8.

Hayashi, K. I., H.Fujisawa, Holland, H. D., and H.Ohmoto, 1997. Geochemistry of 1.9 Ga sedimentary rocks from northeastern Labrador, Canada: Geochimica et Cosmochimica Acta, v. 61, p. 4115–4137.

Henry, D. J., and Dutrow, B. L., 1992. Tourmaline in a low grade clastic metasedimentary rocks: an example of the petrogenetic potential of tourmaline: Contributions to Mineralogy and Petrology, v. 112, p. 203-218.

Henry, D. J., and Guidotti, C. V., 1985. Tourmaline in the staurolite grade metapelites of NW Maine: a petrogenetic indicator mineral: American Mineralogist, v. 70, p. 1-15.

Hess, H.H., 1966. Notes on Operation of Frantz Isodynamic Magnetic Separator, Princeton University: User manual guide, 6 p.

Hiller, K., and Elahi, M., 1984. Structural development and hydrocarbon entrapment in the Surma Basin, Bangladesh (northwest Indo–Burman Fold belt): Proceedings of 4th Offshore Southeast Asia Conference, Singapore, p. 6-50 – 6-63.

Hiller, K., and Elahi, M., 1988. Structural growth and hydrocarbon entrapment in the Surma basin, Bangladesh: Wagner, H.C., (Ed), Petroleum Resources in China and Related Subjects, Circum-Pacific Council Energy Mineral Resources Earth Science Series, v. 10, p. 657-669.

Hodges, K.V., Hames, W.E., Olszewski, W., Burchfiel, B.C., Royden, L.H., and Chen, Z., 1994. Thermobarometric and 40Ar/39Ar geochronologic constraints on Eohimalayan metamorphism in the Dinggye area, Southern Tibet: Contributions to Mineralogy and Petrology, v. 117, p. 151–163.

Hodges, K.V., 2000. Tectonics of the Himalaya and southern Tibet from two perspectives: Geological Society of America Bulletin, v. 112, p. 324-350.

Holtrop, J.F., and Keizer, J., 1970. Some aspects of stratigraphy and correlation of the Surma Basin wells, East Pakistan: New York, United Nations, ECAFE Mineral Resources Development Series no. 36, p. 143-155.

Hossain, M.S., 2009. Overpressure in the eastern Bengal basin, Bangladesh, and its relation to compressional tectonics [unpublished M.S. Thesis], Auburn University, Auburn, AL, 119 p.

Hubert, J.F., 1962. A zircon-tourmaline-rutile maturity index and the interdependence of the composition of heavy mineral assemblages with the gross composition and texture of sandstones: Journal of Sedimentary Research, v. 32.

Hutton, C.O., 1950. Studies of heavy detrital minerals: Geol. Soc. America Bull., v. 61, p. 635-716.

Imam, B., 2005. Energy Resources of Bangladesh: University Grants Commission of Bangladesh, Dhaka, 132 p.

Imam, M. B., and Hussain, M., 2002. A review of hydrocarbon habitats in Bangladesh: Journal of Petroleum Geology, v. 25, p. 31–52.

Ingersoll, R.V., Bullard, T.F., Ford, R.L., Grimm, J.P., Pickle, J.D., and Sares, S.W., 1984. The effect of grain size on detrital modes: A test of the Gazzi-Dickinson point-counting method: Journal of Sedimentary Petrology, v. 54, p. 103-116.

Ingersoll, R.V., and Busby, C., 1995. Tectonics of sedimentary basins: Blackwell science.

Ingersoll, R.V., and Suezek, C.A., 1979. Petrology and Provenance of Neogene sand from Nicobar and Bengal fans, DSDP sites 211 and 218: Journal of Sedimentary Research, v. 49, p. 1217-1228.

Jahan, S., Uddin, A., Savrda, S., and Pashin, J., 2017. Petroleum source-rock evaluation of upper Eocene Kopili Shale, Bengal basin, Bangladesh: International Journal of Coal Geology, v. 172, p. 71-79.

Johnson, M.J., 1993. The system controlling the composition of clastic sediments, in Geological Society of America Special Papers, Geological Society of America, p. 1–20.

Johnson, N.M., Stix, J. Tauxe, L., Cerveny, P.F., and Tahirkheli, R.A.K., 1985. Paleomagnetic chronology, fluvial processes, and tectonic implications of the Siwalik deposits near Chinji village, Pakistan: Journal of Geology, v. 93, p. 27–40.

Johnsson, M.J. 1990. Tectonic versus chemicalweathering controls on the composition of fluvial sands in tropical environments. Sedimentology, v. 37, p. 713–116.

Johnson, S.Y., and Nur Alam, A. M. N., 1991. Sedimentation and tectonics of the Sylhet Trough, Bangladesh: Geological Society of America Bulletin, v. 103, p. 1513-1527.

Johnsson, M.J. 1993. The system controlling the composition of clastic sediments. In: Processes controlling the composition of clastic sediments (Johnsson, M.J., and Basu, A. Eds.), Geological Society of America Special Papers, v. 284, p. 1–19.

Kayal, J.R., 2010. Himalayan tectonic model and the great earthquakes: an appraisal, Geomatics, Natural Hazards and Risk, 1:1, 51-67, DOI: 10.1080/19475701003625752

Kearey, P., and Vine, F.J., 1990. Global Tectonics: Blackwell Science limited, 2nd edition, 333 p.

Khan, F.H., 1991. Geology of Bangladesh, the University Press Limited, 207 p.

Khan, M.R., and Muminullah, M., 1980. Stratigraphy of Bangladesh, in petroleum and mineral resources of Bangladesh: Seminar and exhibition: Dhaka, Government of People's Republic of Bangladesh, p. 35-40.

Khan, M.R., and Muminullah, M., 1988. Stratigraphic lexicon of Bangladesh: Geological Survey of Bangladesh, Records, v. 5, p. 1-67.

Khandoker, R.A., 1989. Development of major tectonic elements of the Bengal basin: a plate tectonic appraisal: Bangladesh Journal of Scientific Research, v. 7, p. 221–232.

Krynine, P.D., 1946. The Tourmaline Group in sediments: Geology, v. 54, no. 2, p. 65-87.

Kumar, P., 2004. Provenance history of Cenozoic sediments near Digboi-Margherita area, eastern syntaxis of the Himalayas, Assam, northeast India (M.S. Thesis): Auburn University, Auburn, AL, 131 p.

Kundu, A., Matin, A., and Mukul, M., 2012. Depositional environment and provenance of Middle Siwalik sediments in Tista Valley, Darjiling District, Eastern Himalaya, India: Journal of Earth System Science, v. 121, p. 73-89.

Lee, Y. I., 2000. Provenace derived from the geochemistry of the Paleozoic-early Mesozoic mudrocks of the Pyeongan Supergroup, Korea: Sedimentary Geology, v. 149, p. 219-235.

Lee, T.Y., and Lawver, L., 1995. Cenozoic plate reconstruction of Southeast Asia: Tectonophysics, v. 251, p. 85-138.

Liou, J.G., 1973. Synthesis and stability relations of epidote, $Ca_2Al_2FeSiO_{12}$ (OH): Journal of Petrology, v. 14, p. 381-413.

Litcht, A., Reisberg, L., France-Lanord, C., Soe, A.N., and Jaeger, J.J., 2014. Cenozoic evolution of the central Myanmar drainage system: insights from sediment provenance in the Minbu Sub-Basin: Basin Research, p. 1-15.

Mack, G.H., 1984. Exceptions to the relationship between plate tectonics and sandstone composition: Journal of Sedimentary Petrology, v. 54, p. 212-220.

Mandal, S., 2009. Sedimentation and tectonics of the Lower Cenozoic sequences from southeast of Shillong Plateau, India: Provenance history of the Assam-Bengal system, Eastern Himalayas (M.S. Thesis): Auburn University, Auburn, AL, 136 p.

Mange, M.A., and Maurer, H.F.W., 1992. Heavy Minerals in color: London, Chapman & Hall, London, 147 p.

McDougall and McElhinny, 1970. The Rajmahal traps of India: K-Ar ages and palaeomahnetism: Earth and Planetary Science Letters, v. 9, p. 371-378.

McLennan, S. M., Barbara, B., Hemming, S. R., Hurowitz., J. A., lev, S. M., and McDaniel, D. K., 2003. The role of provenance and sedimentary processes in the geochemistry of sedimentary rocks. In Geochemistry of sediments and

sedimentary rocks: Evolutionary considerations to mineral deposit-forming environments, Geological Association of Canada, v.4, p. 7-38.

McLennan, S. M., Hemming, S., McDaniel, D. K., and Hanson, G. N., 1993. Geochemical approaches to sedimentation, provenance and tectonics. In Johnson, M. J., Basu, A., eds, processes controlling the composition of the clastic sediments: Geological Society of America., Boulder, Colorado, Special Paper, v. 284, p. 21-40.

Miyashiro, A., and Seki, Y., 1958. Enlargement of the composition field of epidote and piemontite with rising temperature: American Journal of Science, v., 256, p. 423-430.

Molnar, P., 1984. Structure and tectonics of the Himalaya: Constraints and implications of geophysical data: Annual Review of Earth and Planetary Sciences, v. 12, p. 489-518.

Molnar, P., and Tapponier, P., 1975. Cenozoic Tectonics of Asia: effects of a continental collision: Science, v. 189, p. 419-426.

Morgan, J.P. and McIntire, W.G., 1959. Quaternary Geology of the Bangal Basin, East Pakistan and India. Bull. Geol. Soc. Amer., v. 70, p.319-342.

Morton, A.C., 1984. Stability of detrital heavy minerals in Tertiary sandstones of the North Sea Basin: Clay Mineralogy, v. 19, p 287-308.

Morton, A.C., 1985. Heavy minerals in provenance studies: in G.G. Zuffa (editor), Provenance of Arenites: D. Reidel Publishing, Boston, p. 249-277.

Morton, A.C., 1986. Dissolution of apatite in North Sea Jurassic sandstone: Implications for the generation of secondary porosity: Clay Mineralogy, v. 21, p 711-733.

Morton, A.C., and Taylor, P.N., 1991. Geochemical studies of detrital heavy minerals and their application to provenance research: Geological Society, London, Special Publications, v. 57, p. 31–45.

Morton, A.C., and Hallsworth, C.R., 1999. Processes controlling the composition of heavy mineral assemblages in sandstones: Sedimentary Geology, v. 124, p. 3-30.

Morton, A., Hallsworth, C.R., and Chaltonb, B., 2004. Garnet compositions in Scottish and Norwegian basement terrains: a framework for interpretation of North Sea sandstone provenance: Marine and Petroleum Geology, v. 21, p. 393-410.

Morton, A.C., and Taylor, P.N., 1991. Geochemical and isotopic constraints on the nature and age of basement rocks from Rockall Bank, NE Atlantic: Journal of the Geological Society, London, v. 148, p. 630-634.

Murphy, R.W., 1971. Bangladesh enters the oil era: Oil and Gas Journal, v. 86, no. 9 p. 76-82.

Murphy, R.W., 1988. Stratigraphic revision of the Cretaceous-Tertiary sediments of the Shillong Plateau: Geological Survey of India Records, v. 107, p. 80-90.

Najman, Y., and Garzanti, E., 2000. Reconstructing early Himalayan tectonic evolution and paleogeography from Tertiary foreland basin sedimentary rocks, northern India: Geological Society of America Bulletin, v. 112, p. 951-952.

Nakajima, T., Banno, S., and Suzuki, T., 1977. Reactions leading to the disappearance of pumpellyite in low-grade metamorphic rocks of the sanbagawa metamorphic belt in central Shikoku, Japan: Journal of Petrology, v. 18, p. 263-284.

Nanayama, F., 1997. An electron microprobe study of the Amazon Fan: Proceedings of the Ocean Drilling Program, Scientific Results, v. 155, p. 147-168.

Nandi, K., 1967. Garnets as indices of progressive regional metamorphism: Mineralogical Magazine, v. 36, p. 89-93.

Najman, Y., Bickle, M., BouDagher-Fadel, M., Carter, A., Garzanti, E., Paul, M., Wijbrans, J., Willett, E., Oliver, G., Parrish, R., Akhter, S. H., Allen, R., Ando, S., Chisty, E., Reisberg, L., and e, G. V., 2008. The Paleogene record of Himalayan erosion: Bengal basin, Bangladesh: Earth and Planetary Science Letters, v. 273, p. 1-14.

Nesbitt, H.W., Fedo, C.M., and Young, G.M., 1997. Quartz and feldspar stability steady and non-steady state weathering, and petrogenesis of siliciclastic sands and muds: Journal of Geology, v. 105, p. 173-191.

Nesbitt, H.W., and Young, G.M., 1984. Prediction of some weathering trend of plutonic and volcanic rocks based on thermodynamic and kinetic considerations: Journal of Geology, v. 48, p. 1523-1534.

Opdyke, N.D., Johnson, N.M., Johnson, G.D., Linsay, E.H., and Tahirkheli, R.A.K., 1982. Paleomagnetism of the Middle Siwalik formations of northern Pakistan and rotation of the Salt Range Decollement: Palaeogeography, v. 37, p. 1–15.

Pettijohn, F. J., Potter, P. E., and Siever, R., 1987. Sand and Sandstone: Berlin, Springer-Verlag, 553 p.

Pickering, J.L., Goodbred, S.L., Beam, J.C., Ayers, J.C., Covey, A.K., Rajapara, H.M., and Singhvi, A.K., 2017. Terrace formation in the upper Bengal basin since the Middle Pleistocene: Brahmaputra fan delta construction during multiple highstands: Basin research, p. 1-18.

Rahman, M.W., 2008. Sedimentation and Tectonic evolution of Cenozoic sequence from Bengal and Assam foreland basin, Eastern Himalayas (unpublished M.S. Thesis): Auburn, Auburn University, 180 p.

Rahman, M. J. J., and Suzuki, S., 2007. Geochemistry of sandstones from the Miocene Surma Group, Bengal basin, Bangladesh: Implications for Provenance, tectonic setting and weathering: Geochemical Journal, v. 41, p. 415-428.

Reimann, K.U., 1993. Geology of Bangladesh, Borntraeger, Berlin, 154 p.

Ramdohr, P., 1980. Ore Minerals and Their Intergrowth (2nd ed.): New York, Pergamon Press, 1205 p.

Peavy, T., 2008, Provenance of lower Pennsylvanian Pottsville Formation, Cahaba synclinorium, Alabama [unpublished M.S. Thesis]: Auburn University, Auburn, AL, 106 p.

Pettijohn, F.J., 1941, Persistence of heavy minerals and geologic age: Journal of Geology, v. 49, p 610-625.

Pilgrim, G.E., 1913. The structure and correlation of the Simla rocks: Memoire of the Geological Survey of India, v. 53, 140 p.

Rajendran, C.P., Rajendran, K., Durah, B.P., Baruah, S. and Earnest, A., 2004. Interpreting the style of faulting and paleoseismicity associated with the 1897 Shillong, northeast India earthquake: Implications for regional tectonism: Tectonics, v. 23, TC4009, DOI 1029/2003 TC001605.

Roser, B. P., and Korsch, R. J., 1988. Provenance signatures of sandstone-mudstone suites determined using discriminant function analysis of major-element data: Chemical Geology, v. 67, p. 119-139.

Rowley, D.B., 1996. Age of initiation of collision between India and Asia: A review of stratigraphic data: Earth and Planetary Science Letters, v. 145, p. 1-13.

Roy, M.K., Ahmed, S.S., Bhattacharjee, T.K., Mahmud, S., Moniruzzaman, M., Haque, M.M., Saha, S., Molla, M.I., and Roy, P.C., 2012. Paleoenvironment of Depositional of the Dupi Tila Formation, Lalmai Hills, Comilla, Bandladesh, 2012: Journal of Geological Society of India, v. 80, p. 409-419.

Sageman, B.B., and Lyons, T.W., 2003. Geochemistry of fine-grained sediments and sedimentary rocks: volume 7. In F. Mackenzie (Ed.): Treatise on Geochemistry, v. 7, p. 115-158.

Salt, C.A., Alam, M.M., and Hossain, M.M., 1986. Bengal basin: current exploration of the hinge zone area of southwestern Bangladesh: Proceedings of 6th Offshore Southeast Asia Conference, Singapore, p. 55-57.

Sclater, J.G., and Fisher, R.L., 1974. Evolution of the east-central Indian Ocean, with emphasis on the tectonic setting of the Ninetyeast Ridge: AAPG bulletin, v. 85, p. 683-702.

Sengupta, S., Ray, K.K., Acharyya, S.K., and Smith, J.B.D., 1990. Nature of ophiolite occurrence along the eastern margin of the Indian plate and their tectonic significance: Geology, v. 18, p. 439-442.

Sifeta, K., Korch, R., and Kimura, J.I., 2005. Geochemistry, provenance, and tectonic setting of Neoproterozoic metavolcanic and metasedimentary units, Werri area, Northern Ethiopia: journal of African Earth Science, v. 41, p. 212-234.

Sitaula, R.P., 2009. Petrofacies and paleotectonic evolution of Gondwanan and post-Gondwanan sequences of Nepal (unpublished M.S. Thesis): Auburn, Auburn University, 186 p.

Soreghan, M. J., and Soreghan, G. S. L., 2007. Whole-rock geochmistry of upper Paleozoic loessite, western Pangaea: Implication for paleo-atmospheric circulation: Earth and Planetary Science Letters, v. 255, p. 117-132.

Suttner, L.J., 1974. Sedimentary Petrology Provinces: An evaluation, in Ross, C.A., ed., Paleogeographic Provinces and Provinciality: Society of Economic Paleontologists and Mineralogists, Special Publication, v. 21, p. 75-84.

Suttner, L.J., Basu A., and Mack, G.H. 1981. Climate and the origin of quartz arenite. Journal of Sedimentary Petrology, v. 51, p. 1235–1244.

Suttner, L.J., and Dutta, P.K. 1986. Alluvial sandstone composition and paleoclimate. 1. Framework mineralogy: Journal of Sedimentary Petrology, v. 56, p. 329–345.

Strut, B.A., 1962. The composition of garnets from pelitic schists in relation to the grade of regional metamorphism: Journal of Petrology, v. 3, p. 181-191.

Tamrakar, N.K., and Syangbo, D.K. 2014. Petrography and provenance of the Siwalik Group sandstones from the Main Boundary Thrust region, Samari River area, Central Nepal, sub-Himalaya: Boletín de Geología, v. 36, p. 25-44.

Taylor, S. R., and McLennan, S. M., 1985. The continental crust: Its composition and evolution: Oxford, Blackwell Scientific Publication, 9-16 p.

Tripathi, C., 1986. Siwaliks of the Indian Subcontinent: Paleontological Society of India, v. 31, p. 1-8.

Tucker, M., 1988. Techniques in Sedimentology: Blackwell Scientific Publications, London, 395 p.

Uddin, A., 1987. A Geological Evaluation of the Hydrocarbon Potential of the Ganges/Bengal Delta of Bangladesh: M.S. Thesis, University of Hawaii, Honolulu, Hawaii, 167 p.

Uddin, A., Lundberg, N., 1998a. Unroofing history of the Eastern Himalaya and the Indo-Burman Ranges: Heavy mineral study of Cenozoic sediments from the Bengal basin, Bangladesh: Journal of Sedimentary Research, v. 68, p. 465-472.

Uddin, A., and Lundberg, N., 1998b. Cenozoic history of the Himalayan-Bengal system: Sand composition in the Bengal basin, Bangladesh: Geological Society of America Bulletin, v. 110, p. 497-472.

Uddin, A., and Lundberg, N., 1999. A paleo-Brahmaputra? Subsurface lithofacies analysis of Miocene deltaic sediments in the Himalayan-Bengal system, Bangladesh: Sedimentary Geology, v. 123, p. 239-254.

Uddin, A., Lundberg, N., 2004. Miocene sedimentation and subsidence during continent-continent collision, Bengal basin, Bangladesh: Sedimentary Geology, v. 164, p. 131-146.

Uddin, A., Kumar, P., and Sarma, J.N., 2007. Early orogenic history of the eastern Himalayas: Compositional studies of Paleogene sandstones from Assam, NE India: International Geology Review, v. 49, p. 798-810.

Uddin, A., Kumar, P., Sarma, J.N., and Akhter, S.H., 2009. Heavy-mineral constraints on provenance of Cenozoic sediments from the foreland basins of Assam, India and Bangladesh: Erosional history of the eastern Himalayas and the Indo-Burman ranges, in Mange, M.A., and Wright, D.T., eds., Heavy minerals in use, Developments in Sedimentology, Elsevier, Amsterdam, v. 58, p. 823-847.

Uddin, A., Hames, W.E., and Zahid, K.M., 2010. Laser 40Ar/39Ar age constraints on Miocene sequences from the Bengal basin: Implications for middle Miocene denudation of the eastern Himalayas: Journal of Geophysical Research, v. 115, B07416, doi: 10.1029/2009JB006401.

Visona, D., Carosi, R., Montomoli, C., Tiepolo, M., and Peruzzo, L., 2012. Miocene andalusite leucogranite in central-east Himalaya (Everest-Masang Kang area): Low-pressure melting during heating: Lithos, v. 144-145, p. 194-208.

Von Eynatten, H.; Barcelo´ -Vidal, C.; and PawlowskyGlahn, V. 2003. Composition and discrimination of sandstones: a statistical evaluation of different analytical methods: Journal of Sedimentary Research, v. 73, p. 47–57.

West, R.M. 1984. Siwalik faunas from Nepal: Paleoecologic and Paleoclimatic implications. In: The evolution of the East Asian environment Centre of Asian Studies. Vol. 2. (Whyte, R.O. Ed.). University of Hongkong, p. 724–744.

Worm, H.U., Ahmed, A.M.M., Ahmed, N.U., Islam, H.O., Huq, M.M., Hambach, U., Lietz, J., 1998. Large sedimentation rate in the Bengal delta: Magnetostratigraphic dating of Cenozoic sediments from northeastern Bangladesh: Geology, v. 26, p. 487-490.

Zaher, M.A., and Rahman, A., 1980, Prospects and investigations for minerals in the northern part of Bangladesh in Petroleum and Mineral Resources of Bangladesh, Seminar and Exhibition: Dhaka, Government of People's Republic of Bangladesh, p. 9-18.

Zahid, K. M., 2005. Provenance and basin tectonics of Oligocene-Miocene sequences of the Bengal basin, Bangladesh [Unpublished M.S. Thesis]: Auburn University, 142p.

APPENDICES

APPENDIX-A (Heavy mineral data from the Bengal basin)

Sample Code	Weight	Heavy Minerals Weight	Light Minerals Weight	Heavy Minerals weight percentage
KS-1	29.93	0.59	29.34	1.971266288
KS-2	31.27	2.35	28.92	7.515190278
KS-3	30.44	0.28	30.16	0.919842313
KS-4	32.29	0.79	31.5	2.446577888
KS-5	30.1	0.003	30.097	0.009966777
KS-6	30.8	0.17	30.63	0.551948052
SS-2	30.24	2.23	28.01	7.374338624
SS-3	29.51	0.22	29.29	0.745509997
SS-4	31.12	0.86	30.26	2.763496144
SS-5	31.01	0.43	30.58	1.386649468
SS-6	27.82	0.3	27.52	1.078360891
SS-7	31.01	0.063	30.947	0.203160271
SS-8	29.58	0.41	29.17	1.38607167
SS-9	29.78	0.013	29.767	0.043653459
SS-10	28.8	0.34	28.46	1.180555556
SS-11	29.2	0.73	28.47	2.5
BS-1	29.9	0.01	29.89	0.033444816
BS-5	31	0.098	30.902	0.316129032
BS-6	30.6	0.04	30.56	0.130718954
BS-8	26.7	0.021	26.679	0.078651685
NWD-1	27.9	0.26	27.64	0.931899642
NWD-3	30.2	0.76	29.44	2.516556291
NWR-2	30.8	0.2	30.6	0.649350649
NWR-3	20.4	0.04	20.36	0.196078431
CCS-2	30.7	0.087	30.613	0.283387622
CCS-3	30.01	0.057	29.953	0.189936688
CCS-4	31.01	0.11	30.9	0.354724282
CCHS-1	28	0.085	27.915	0.303571429
CWSalo	28.4	0.12	28.28	0.422535211
Cglau	27.06	0.11	26.95	0.406504065
CLSal-1	30.54	0.15	30.39	0.491159136
CWSal-1	29	0.045	28.955	0.155172414
CWSal-4	30.05	0.04	30.01	0.133111481
CWSalLDT-1	29.81	1.24	28.57	4.15967796
CRup-1	27.65	0.07	27.58	0.253164557

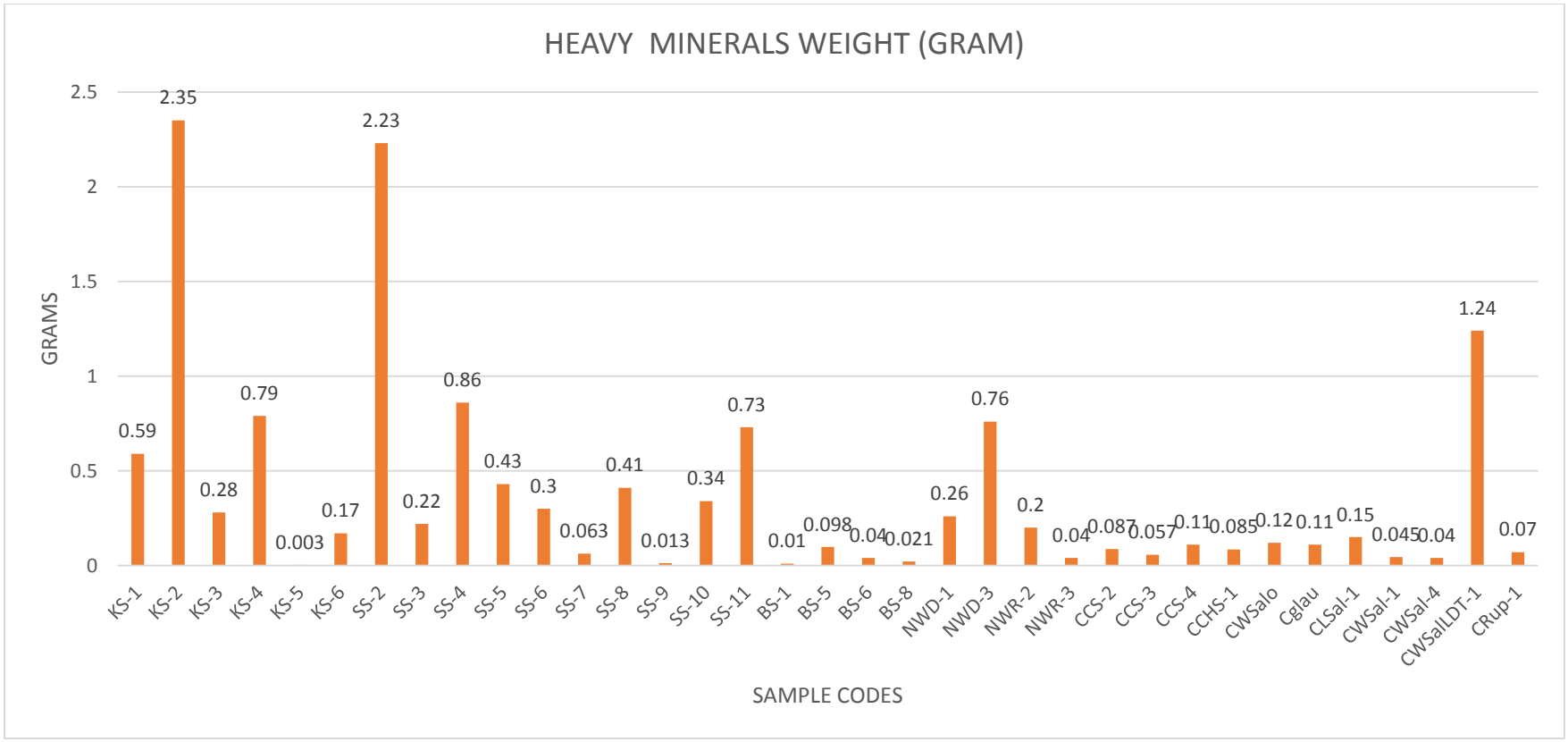
HEAVY MINERALS WEIGHT (GRAM)
GRAMS
SAMPLE CODES
2.5
2
1.5
1
0.5
0
0.59
2.35
0.28
0.79
0.003
0.17
2.23
0.22
0.86
0.43
0.3
0.063
0.41
0.013
0.34
0.73
0.01
0.098
0.04
0.021
0.26
0.76
0.2
0.04
0.087
0.057
0.11
0.085
0.12
0.11
0.15
0.045
0.04
1.24
0.07
KS-1
KS-2
KS-3
KS-4
KS-5
KS-6
SS-2
SS-3
SS-4
SS-5
SS-6
SS-7
SS-8
SS-9
SS-10
SS-11
BS-1
BS-5
BS-6
BS-8
NWD-1
NWD-3
NWR-2
NWR-3
CCS-2
CCS-3
CCS-4
CCHS-1
CWSalo
Cglau
CLSal-1
CWSal-1
CWSal-4
CWSalLDT-1
CRup-1

APPENDIX-B

Garnet data from the Bengal basin

		Lalmai Hills		Sitapahar Anticline			Stable Platform (GDH-56)				
	Standard	CCS-1	CCS-2	KS-1	KS-2	KS-3	NWD-1	NWD-2	NWD-3	NWD-4	NWD-5
SiO_2	36.70	36.49	38.54	36.06	36.50	38.11	36.65	34.55	31.93	36.29	36.36
TiO_2	0.75	0.00	0.00	0.00	0.00	0.00	0.00	0.00	0.00	0.00	0.00
Al_2O_3	21.40	22.12	21.10	21.11	20.00	22.25	20.11	19.41	18.88	20.62	20.21
FeO	29.90	13.43	12.80	30.40	30.00	13.39	18.52	24.37	20.55	33.23	30.86
MnO	1.14	0.40	0.50	1.53	0.55	0.45	13.45	17.31	28.62	1.58	3.00
MgO	0.90	0.00	1.50	2.64	2.00	0.00	3.69	1.77	0.00	1.60	3.29
CaO	9.02	23.96	22.18	8.25	10.50	24.23	7.56	2.57	0.00	6.66	6.25
Na_2O		0.00	0.00	0.00	0.00	0.00	0.00	0.00	0.00	0.00	0.00
K_2O		0.00	0.00	0.00	0.00	0.00	0.00	0.00	0.00	0.00	0.00
BaO		0.00	0.00	0.00	0.00	0.00	0.00	0.00	0.00	0.00	0.00
sum	99.81	96.40	96.62	99.99	99.55	98.43	99.98	99.98	99.98	99.98	99.97
Si	5.90	5.86	6.10	5.81	5.91	5.97	5.89	5.76	5.53	5.90	5.88
Ti	0.09	0.00	0.00	0.00	0.00	0.00	0.00	0.00	0.00	0.00	0.00
Al	4.05	4.19	3.94	4.01	3.82	4.11	3.81	3.82	3.85	3.95	3.85
Fe	4.02	1.81	1.70	4.10	4.06	1.76	2.49	3.40	2.97	4.52	4.17
Mn	0.16	0.05	0.07	0.21	0.08	0.06	1.83	2.45	4.20	0.22	0.41
Mg	0.22	0.00	0.35	0.63	0.48	0.00	0.88	0.44	0.00	0.39	0.79
Ca	1.55	4.13	3.76	1.42	1.82	4.07	1.30	0.46	0.00	1.16	1.08
Na	0.00	0.00	0.00	0.00	0.00	0.00	0.00	0.00	0.00	0.00	0.00
K	0.00	0.00	0.00	0.00	0.00	0.00	0.00	0.00	0.00	0.00	0.00
Ba	0.00	0.00	0.00	0.00	0.00	0.00	0.00	0.00	0.00	0.00	0.00

Total	15.98	16.04	15.93	16.18	16.18	15.97	16.21	16.33	16.55	16.13	16.19
IV	5.898	5.86	6.10	5.81	5.91	5.97	5.89	5.76	5.53	5.90	5.88
VIII	5.943	5.99	5.88	6.36	6.45	5.89	6.51	6.75	7.17	6.28	6.46
Alm	67.6%	30%	29%	64%	63%	30%	38%	50%	41%	72%	65%
Spe	2.6%	1%	1%	3%	1%	1%	28%	36%	59%	3%	6%
Pyr	3.6%	0%	6%	10%	7%	0%	14%	7%	0%	6%	12%
Grs	26.1%	69%	64%	22%	28%	69%	20%	7%	0%	18%	17%
Fe/(Fe+Mg)	95%	100%	83%	87%	89%	100%	74%	89%	100%	92%	84%

		Stable Platform (GDH-69)			Sylhet Trough								
	Standard	NWR-1	NWR-2	NWR-3	SS-1	SS-2	SS-3	SS-4	SS-5	SS-6	SS-7	SS-8	SS-9
SiO_2	36.70	36.66	36.50	33.94	36.29	36.36	35.30	37.02	37.03	35.53	38.56	38.06	38.47
TiO_2	0.75	0.00	0.00	0.00	0.00	0.00	0.00	0.00	0.00	0.00	0.00	0.00	0.00
Al_2O_3	21.40	19.11	20.42	17.88	20.62	20.21	19.58	21.01	22.07	22.07	23.50	23.06	20.56
FeO	29.90	18.52	19.37	17.56	33.23	30.87	35.88	25.89	31.65	31.65	11.83	13.67	15.52
MnO	1.14	13.45	17.31	28.62	1.58	3.00	3.68	0.30	0.80	0.80	0.50	0.35	0.73
MgO	0.90	3.69	1.77	0.00	1.61	3.29	2.10	6.00	6.21	6.21	0.85	0.00	7.28
CaO	9.02	7.56	3.57	0.50	6.66	6.11	1.40	8.38	2.03	2.03	23.26	23.21	15.79
Na_2O		0.00	0.00	0.00	0.00	0.00	0.00	0.00	0.00	0.00	0.00	0.00	0.00
K_2O		0.00	0.00	0.00	0.00	0.00	0.00	0.00	0.00	0.00	0.00	0.00	0.00
BaO		0.00	0.00	0.00	0.00	0.00	0.00	0.00	0.00	0.00	0.00	0.00	0.00
sum	99.81	98.99	98.94	98.50	99.99	99.84	97.94	98.60	99.79	98.29	98.50	98.35	98.35
Si	5.90	5.96	5.98	5.86	5.90	5.89	5.93	5.88	5.86	5.74	5.96	5.95	5.97
Ti	0.09	0.00	0.00	0.00	0.00	0.00	0.00	0.00	0.00	0.00	0.00	0.00	0.00
Al	4.05	3.66	3.94	3.64	3.95	3.86	3.87	3.94	4.12	4.20	4.28	4.25	3.76
Fe	4.02	2.52	2.66	2.54	4.52	4.18	5.04	3.44	4.19	4.27	1.53	1.79	2.01
Mn	0.16	1.85	2.40	4.19	0.22	0.41	0.52	0.04	0.11	0.11	0.07	0.05	0.10

Mg	0.22	0.89	0.43	0.00	0.39	0.79	0.53	1.42	1.46	1.49	0.20	0.00	1.68
Ca	1.55	1.32	0.63	0.09	1.16	1.06	0.25	1.43	0.34	0.35	3.85	3.89	2.63
Na	0.00	0.00	0.00	0.00	0.00	0.00	0.00	0.00	0.00	0.00	0.00	0.00	0.00
K	0.00	0.00	0.00	0.00	0.00	0.00	0.00	0.00	0.00	0.00	0.00	0.00	0.00
Ba	0.00	0.00	0.00	0.00	0.00	0.00	0.00	0.00	0.00	0.00	0.00	0.00	0.00
Total	15.98	16.21	16.05	16.32	16.13	16.19	16.14	16.15	16.08	16.16	15.89	15.92	16.15
IV	5.898	5.96	5.98	5.86	5.90	5.89	5.93	5.88	5.86	5.74	5.96	5.95	5.97
VIII	5.943	6.58	6.12	6.82	6.28	6.44	6.34	6.33	6.11	6.23	5.65	5.72	6.42
Alm	67.6%	38%	43%	37%	72%	65%	79%	54%	69%	69%	27%	31%	31%
Spe	2.6%	28%	39%	61%	3%	6%	8%	1%	2%	2%	1%	1%	1%
Pyr	3.6%	14%	7%	0%	6%	12%	8%	22%	24%	24%	3%	0%	26%
Grs	26.1%	20%	10%	1%	18%	16%	4%	23%	6%	6%	68%	68%	41%
Fe/(Fe+Mg)	95%	74%	86%	100%	92%	84%	91%	71%	74%	74%	89%	100%	54%

*'Standard' presents an almandine microprobe analysis from Deer et al., 1992, for reference.
Cations are calculated on the basis of 24 oxygen per formula unit.
See thesis text for further details of standardization and analysis.

APPENDIX-C

Tourmaline data from the Bengal basin

		Lalmai hills			Sylhet Trough				Sitapahar anticline				Stable Platform				
Sample No.	Standard	CCS-1	CCS-2	CCS-3	SS-1	SS-2	SS-3	SS-4	KS-1	KS-2	KS-3	KS-4	NWD-1	NWD-2	NWD-3	NWR-1	NWR-2
SiO_2	33.78	37.63	35.55	38.37	36.51	40.96	36.2	35.23	43.32	37.18	36.63	42.56	40.42	37.62	39.21	35.75	38.06
TiO_2	0.41	1.5	0.2	0.22	0.41	0.14	0.13	0.88	1.2	0.04	0.26	0.56	0.22	0.43	0.23	0.56	1.2
Al_2O_3	33.8	32.42	26.41	29.23	41.78	40.48	41.78	31.56	32.56	42.18	34.48	31.26	39.35	41.62	40.48	39.61	38.6
MgO	0.74	7.72	4.2	1.56	2.3	0.25	2.41	7.12	2.19	8.09	5.72	6.59	3.64	2.1	0.34	6.53	4.19
FeO	15.11	10.33	8.51	13.74	8.5	6.64	8.7	9.98	9.45	6.53	9.33	3.89	2.21	6.65	5.91	10.23	6.32
CaO	0.74	4.88	15.2	5.5	1.75	2.81	2.8	5.2	3.6	2.41	3.36	6.5	3.9	0.68	2.68	3.5	0.63
MnO	0.21	1.23	0.25	1.2	0.67	1.05	2.08	1.11	0.25	0.61	1.62	0.74	0.73	0.56	0.68	0.61	0.39
K_2O	0.11	0.78	0.11	0.56	0.42	0.09	0.31	0.56	0.44	0.56	0.3	0.65	0.34	0.42	0.08	0.38	0.32
Na_2O	0.13	0.01	1.48	0.76	0.62	0.98	0.14	0.01	2.61	0.23	0.06	0.01	0.56	0.23	0.63	0.08	1.75
Cr_2O_3	0.03	0	0	0	0.01	0	0.01	0.01	0	0	0.58	0.21	0.31	0.08	0	0.06	0.32
Ca		0.81	2.63	0.98	0.3	0.48	0.48	0.9	0.61	0.39	1.38	1.11	0.67	0.12	0.47	0.57	0.11
Mg		1.78	1.01	0.39	0.55	0.06	0.57	1.72	0.52	1.81	1.26	1.56	0.87	0.51	0.08	1.49	1
Fe (tot)		1.34	1.15	1.91	1.14	0.89	1.15	1.35	1.25	0.82	45.44	0.52	0.3	0.91	0.81	1.31	0.84
Al		44.18	45.15	45.45	47.46	48.49	47.39	44.35	46.51	45.95	27.08	45.92	48.11	47.88	48.61	45.54	47.02
Al50Fe(tot)50		27.08	27.74	30.26	27.16	27.07	27.19	27.15	28.2	25.5	27.48	24.99	25.02	26.65	26.82	26.94	26.24
Al50Mg50		28.74	27.12	24.26	25.38	24.44	25.42	28.5	25.3	28.55		29.09	26.87	25.47	24.56	27.52	26.74
Total		100	100	100	100	100	100	100	100	100	100	100	100	100	100	100	100

*'Standard' presents in a tourmaline microprobe analysis from Deer et al., 1992, for reference.
See thesis text for further details of standardization and analysis.

APPENDIX-D

Epidote data from the Bengal basin

Epidote data for Lalmai Hills					
Element	CCS-1	CCS-2	CCS-3	CCS-4	CCS-5
Silicon	17.5601	15.53323	17.288	15.88339	17.38774
Aluminium	13.86715	10.29227	12.67098	10.48007	14.9123
Oxygen	40.98024	38.90383	39.44371	40.31211	40.38996
Iron	8.004678	10.85665	7.835737	9.91188	2.996941
Calcium	17.45194	17.83147	17.41497	17.32808	18.05376
Epidote data for Sitapahar Anticline					
Element	KS-1	KS-2	KS-3		
Silicon	16.80519	17.05278	16.60791		
Aluminium	12.3194	8.376464	13.62979		
Oxygen	39.78069	36.7531	40.5128		
Iron	8.036875	16.40844	6.908249		
Calcium	17.09463	0	17.35836		
Epidote data for Stable Platform					
Element	NWR-1	NWR-2	NWR-3	NWR-4	
Silicon	17.29955	13.10643	16.92263	16.52433	
Aluminium	14.09981	17.09388	12.39552	12.65241	
Oxygen	40.56636	40.44721	39.5147	38.9124	
Iron	4.662273	7.739702	8.121765	7.174781	
Calcium	17.48324	17.7766	17.23921	16.97445	
Epidote data for Sylhet Trough					
Element	SS-1	SS-2	SS-3	SS-4	SS-5
Silicon	15.45946	16.55207	21.12624	17.01255	17.20785
Aluminium	10.22208	13.03681	6.639434	9.658089	13.14791
Oxygen	36.62465	39.1711	41.68457	38.87775	40.41496
Iron	9.864275	6.267363	9.727766	8.317692	6.733154
Calcium	17.76774	17.33803	9.061077	21.34564	18.00046

APPENDIX-E

Chloritoid data from the Bengal basin

Chloritoid data for Lalmai Hills	
Element	CCS-1
Aluminium	16.63475
Silicon	15.45702
Oxygen	36.47793
Iron	14.21078
Chloritoid data for Sitapahar Anticline	
Element	KS-1
Aluminium	20.87102
Silicon	10.98217
Oxygen	38.14222
Iron	21.04884
Chloritoid data for Sylhet Trough	
Element	SS-1
Aluminium	28.53829
Silicon	12.95162
Oxygen	43.20288
Iron	10.69117

APPENDIX-F

Ilmenite data from the Bengal basin

Ilmenite data for Lalmai Hills								
Element	CCS-1	CCS-2	CCS-3	CCS-4	CCS-5	CCS-6	CCS-7	CCS-8
Titanium	34.42735	32.99818	29.92272	38.44565	33.2146	30.15069	13.83822	30.00657
Iron	36.80911	37.33192	40.99616	26.14245	37.22756	31.23147	58.65482	39.20253
Oxygen	33.86176	33.50979	32.13699	37.11207	33.33066	39.86943	31.69085	33.92924
Manganese	1.545613	0.696833	0.758106	0	1.152257	1.570935	0	3.021121

APPENDIX-G

Whole rock chemistry data from the Bengal basin

Sample Sites	**SiO2**	**Al2O3**	**Fe2O3**	**MgO**	**CaO**	**Na2O**	**K2O**	**TiO2**	**P2O5**	**MnO**	**Cr2O3**	**Ba**	**Ni**	**Sr**	**Zr**	**Y**	**Sc**	**Th**	**Nb**	**La**	**Sum**
	%	**%**	**%**	**%**	**%**	**%**	**%**	**%**	**%**	**%**	**%**	**ppm**	**ppm**	**ppm**	**ppm**	**ppm**	**ppm**	**ppm**	**ppm**		**%**
	0.01	**0.01**	**0.04**	**0.01**	**0.01**	**0.01**	**0.01**	**0.01**	**0.01**	**0.01**	**0.002**	**5**	**20**	**2**	**5**	**3**	**15**	**5**	**1**	**1**	**0.01**
NWD-56	84.42	8.08	2.17	0.47	0.78	1.26	1.95	0.18	0.03	0.04	0.006	434	<20	101	103	12	18	15	25	29	100.01
KS-10	64.90	14.50	6.81	1.67	1.35	1.62	3.02	0.68	0.17	0.07	0.013	571	43	150	231	32	15	25	12	28	99.96
SS-W	68.66	16.22	4.44	0.83	0.08	0.19	2.49	0.91	0.04	0.03	0.017	413	51	60	249	29	4	20	<5	25	99.96
KS-8	63.87	14.86	5.82	2.53	2.07	1.61	3.10	0.70	0.13	0.08	0.013	434	45	147	211	27	12	25	12	12	99.94
CWSal	64.47	16.79	7.04	0.43	0.07	0.15	1.70	0.81	0.04	0.05	0.015	297	49	30	285	25	11	25	10	27	99.97
BS-10	54.22	29.22	1.55	0.17	0.04	0.08	0.92	1.41	0.03	<0.01	0.023	194	49	43	289	28	12	15	8	26	99.97
KS-13	63.66	14.61	5.85	2.60	2.40	1.69	3.23	0.68	0.14	0.09	0.013	442	45	159	201	28	13	10	13	32	99.95
KS-12	64.41	14.98	5.96	2.44	1.24	1.38	3.63	0.68	0.14	0.09	0.012	465	51	122	187	26	12	25	13	27	99.94
KS-11	62.81	15.01	6.26	2.71	2.20	1.65	3.36	0.73	0.13	0.09	0.013	454	50	148	189	27	12	25	16	26	99.94
KS-9	67.92	13.14	4.95	2.18	2.46	1.93	2.81	0.62	0.14	0.08	0.011	394	36	174	248	26	11	30	13	28	99.95